Design of Fractionally Spaced Equalizers

by

Azzedine Zerguine

A Thesis Presented to the

FACULTY OF THE COLLEGE OF GRADUATE STUDIES

KING FAHD UNIVERSITY OF PETROLEUM & MINERALS

DHAHRAN, SAUDI ARABIA

In Partial Fulfillment of the
Requirements for the Degree of

MASTER OF SCIENCE

In

ELECTRICAL ENGINEERING

January, 1990

INFORMATION TO USERS

This manuscript has been reproduced from the microfilm master. UMI films the text directly from the original or copy submitted. Thus, some thesis and dissertation copies are in typewriter face, while others may be from any type of computer printer.

The quality of this reproduction is dependent upon the quality of the copy submitted. Broken or indistinct print, colored or poor quality illustrations and photographs, print bleedthrough, substandard margins, and improper alignment can adversely affect reproduction.

In the unlikely event that the author did not send UMI a complete manuscript and there are missing pages, these will be noted. Also, if unauthorized copyright material had to be removed, a note will indicate the deletion.

Oversize materials (e.g., maps, drawings, charts) are reproduced by sectioning the original, beginning at the upper left-hand corner and continuing from left to right in equal sections with small overlaps. Each original is also photographed in one exposure and is included in reduced form at the back of the book.

Photographs included in the original manuscript have been reproduced xerographically in this copy. Higher quality 6" x 9" black and white photographic prints are available for any photographs or illustrations appearing in this copy for an additional charge. Contact UMI directly to order.

UMI

A Bell & Howell Information Company
300 North Zeeb Road, Ann Arbor MI 48106-1346 USA
313/761-4700 800/521-0600

DESIGN OF FRACTIONALLY SPACED EQUALIZERS

BY

Azzedine Zerguine

A Thesis Presented to the

FACULTY OF THE COLLEGE OF GRADUATE STUDIES

KING FAHD UNIVERSITY OF PETROLEUM & MINERALS

DHAHRAN, SAUDI ARABIA

In Partial Fulfillment of the
Requirements for the Degree of

MASTER OF SCIENCE

In

ELECTRICAL ENGINEERING

JANUARY 1990

KING FAHD UNIVERSITY OF PETROLEUM AND MINERALS
DHAHRAN, SAUDI ARABIA

COLLEGE OF GRADUATE STUDIES

This thesis, written by ***AZZEDINE ZERGUINE*** under the direction of his Thesis Advisor and approved by his Thesis Committee, has been presented to and accepted by the Dean of the College of Graduate Studies, in partial fulfillment of the requirements for the degree of ***MASTER OF SCIENCE*** in ***ELECTRICAL ENGINEERING.***

THESIS COMMITEE

Chairman

Co-chairman

Member

Department Chairman

Dean, College of Graduate Studies

College of Graduate Studies
Office of the Dean

To My Parents,

To My Wife and My Daughters Dalila and Asma

ACKNOWLEDGEMENT

Acknowledgement is due to *King Fahd University of Petroleum and Minerals* for support of this research.

I would like to express my deep appreciation to *Dr. Essam E. Hassan* my thesis advisor, for his patient guidance and his generous support for this research, and also I would like to express my gratefulness to *Dr. Mohamed S. EL-Hennawey* my thesis co-advisor for his valuable suggestions, as well as *Dr. Maamar Bettayeb* for his helpful remarks.

Special thanks are to *Dr. Ali Cherid*, *Mr. Choukri Ahmed Belhadj* and *Mr. Tharwat Al-Jamaan* for their assistance in producing this work in a nice form, and many others for the memorable days we shared together.

Finally, I would like to send my sincere gratitude to *My Wife* whose constant encouragement made the completion of this work possible.

خلاصة

عنوان الدراسة : تصميم المسويات جزئية التباعد

اسم الطالب : عز الدين زرقين

التخصص : هندسة كهربائية

تاريخ الدرجة : يناير ١٩٩٠م

تعتمد الفكرة الاساسية للمسويات في الاتصالات الرقمية على تعويض الخصائص غير المرغوب فيها لقنوات الاتصال وذلك باستخدام ترشيحات إضافية . وفي هذه الحالة يعتبر المسوى أو (المعادل) عبارة عن مرشح ذاتي الانضباط بحيث يتم الاتصال الرقمي السريع على الوجه الامثل عبر قنوات بطيئة التغيير ومحدودة الحزمة والتي تعتبر استجابتها النبضية مجهولة لدى المستقبل .

ولعل اهم المسويات انتشاراً هي المسويات المتزامنة ونظيرتها المسويات جزئية التباعد حيث يكون الزمن بين معاملات المرشح في النوع الأول مساوية لزمن الرمز بينما يكون في النوع الثاني أقل منه .

وتتفوق المسويات جزئية التباعد على المسويات المتزامنة من حيث قدرتها على التغلب على مشاكل التداخل الطيفي وعدم اعتمادها بشكل مؤثر على طور أخذ العينات الرمزية . وعلى الجانب الاخر إذا افترضنا أن هذين النوعين لهما نفس مجر الزمن فإن المسويات جزئية التباعد تتطلب عدداً من العمليات الحسابية يفوق بنسبة كبيرة نظيره المطلوب لتنفيذ المسويات المتزامنة . وذلك يتطلب بالطبع زيادة في قدرة الحاسب المصغر والمستخدم في بناء المستقبل حيث يؤول ذلك إلى زيادة في سعر التكلفة ويعتبر ذلك من اهم عيوب المسويات جزئية التباعد .

وقد تم في هذه الرسالة عرض اقتراح لتنفيذ نوع جديد من المسويات يتطلب عمليات حسابية بعدد يتوسط تلك المطلوبة في كل من النوعين السابقين من المسويات بحيث يكون قادراً على التغلب على معظم مشاكل المسويات المتزامنة ولو بشكل جزئي.

وقد أجريت دراسات لتحديد أداء فاعلية المسوي المقترح وذلك بإجراء محاكاة للأنظمة باستخدام الحاسب الآلي وشملت الدراسات نماذج من تضمين سعة النبضة وكذلك تضمين السعة التربيعية ، وقد أظهرت نتائج البحث ايجابيات أداء المسوي المقترح .

درجة الماجستير في العلوم

جامعة الملك فهد للبترول والمعادن

الظهران ، المملكة العربية السعودية

يناير ١٩٩٠م

ABSTRACT

Title : **DESIGN OF FRACTIONALLY SPACED EQUALIZERS**

By : **Azzedine Zerguine**

Major Field : **Electrical Engineering**

Date : **January 1990**

The main idea of equalization is simply to compensate for nonideal characteristics by additional filtering. An equalizer is, then, an adaptive filter that is capable of high-speed digital signaling over slowly varying, band limited channels whose impulse responses are unknown at the receiver.

Among the most widely used equalizers are the synchronous equalizer and the fractionally-spaced equalizer. In the synchronous equalizer the tap coefficients are spaced at the reciprocal of the symbol rate. While in a fractionally-spaced equalizer, on the other hand, the tap coefficients are spaced closer than the reciprocal of the symbol rate.

The fractionally-spaced equalizer is superior to the synchronous equalizer, and this is in its ability to be not affected by aliasing problems and independent of the sampler phase. However, for a given time span NT, a synchronous equalizer will need N tap coefficients, while (2N) tap coefficients are needed for a fractionally-spaced equalizer with tap spacing T/2. This will result in a great amount of computations needed to update the tap coefficients every symbol period, an important drawback of the fractionally-spaced equalizer.

In this thesis, we introduce an idea where a compromise between performance and complexity, for both equalizers, is presented. The idea consists of setting some of the tap coefficients of a fractionally-spaced equalizer, with tap spacing T/2, to zero. The zero tap coefficients are neither updated nor entered in the computational process, thus leading to simplified algorithms.

The study was carried out through simulation for PAM and QAM systems. Simulation results show the validity of the proposed equalizer.

MASTER OF SCIENCE

KING FAHD UNIVERSITY OF PETROLEUM AND MINERALS
DHAHRAN, SAUDI ARABIA

January 1990

CONTENTS

LIST OF TABLES

Table

LIST OF FIGURES

Figure

LIST OF SYMBOLS

A	Correlation matrix
a_n	Information sequence
b	Crosscorrelation vector
C	Sampled impulse response of the equalizer
$\mathbf{C}_{op}$	Optimum tap coefficients
D_m	Mean-square distortion
D_p	Peak distortion
FSE	Fractionally-spaced equalizer
FSK	Frequency shift keying
G	Gradient vector
H	Sampled impulse response of the channel
h(t)	Channel impulse response
ISI	Intersymbol interference
J	Performance index of the MSE criterion
J_{min}	Minimum MSE
LMS	Least mean square
MSE	Mean square error
n(t)	Additive Gaussian noise
PAM	Pulse amplitude modulation
PSK	Phase shift keying

QAM	Quadrature amplitude modulation
R	Received vector
r(nT)	Received sampled signal
r(t)	Received signal
SNR	Signal to noise ratio
T	Symbol period
TDL	Tapped-delay line
Δ	Step size
λ	Eigenvalue of the correlation matrix

CHAPTER I

INTRODUCTION

In this introductory chapter, first, Nyquist's first criterion is presented as well as the transversal filter. After this, a review on the literature followed by the statement of the problem are treated. Finally, the proposed scheme is presented.

1.1 GENERAL

In efficient digital communication systems the effect of each symbol transmitted over time dispersive channel extends beyond the time interval used to represent that symbol. The distortion caused by the resulting overlap is called Intersymbol Interference (ISI). This distortion is one of the major obstacles to reliable high-speed data transmission over low-background-noise channels of limited bandwidth [1], [2].

All pulse-modulation systems, including frequency-shift keying (FSK), phase shift keying (PSK), and quadrature amplitude modulation (QAM),

give rise to intersymbol interference.

A baseband pulse-amplitude (PAM) system can be used to describe the effects of ISI. Figure 1.1 shows a model of such a PAM communication system. Its impulse response, h(t), takes care of both the transmitter filter and the channel impulse responses. An information sequence $\{a_n\}$ is transmitted at every symbol period T. At the output of the assumed linear channel, the total transmitted signal is

$$r_1(t) = \sum_{j=-\infty}^{\infty} a_j h(t-jT) \tag{1.1}$$

Noise is added to the signal at the output of the channel. The noise process n(t) is assumed to be stationary and zero mean Gaussian. From the above discussion it follows that the total received signal is

$$r(t) = \sum_{j=-\infty}^{\infty} a_j h(t-jT) + n(t) \tag{1.2}$$

If the received signal is sampled at instant mT, we get

$$r(mT) = a_m h(0) + \sum_{j \neq m} a_j h(mT-jT) + n(mT) \tag{1.3}$$

The second term on the right hand side of equation (1.3) represents the ISI term, while the first term and the last term are the desired signal used to identify the transmitted signal and the additive noise, respectively.

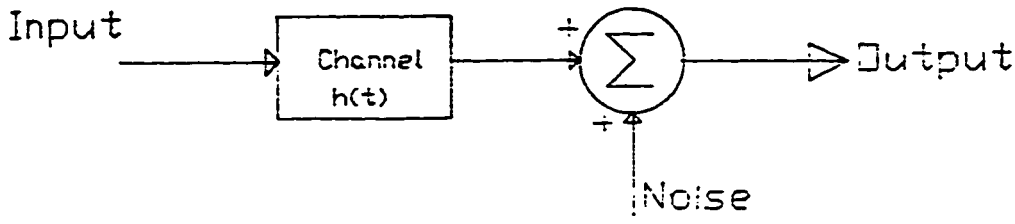

Figure 1.1 Baseband PAM communication system.

1.1.1 Intersymbol interference and Nyquist's first criterion

The ISI term is zero if h(iT) is zero for all i other than zero; that is the impulse response has zero crossings at symbol times. When this condition is satisfied, the impulse response is said to satisfy Nyquist's first criterion [2], [3], [5].

Consequently, the shape of h(t) that gives no intersymbol interference is

$$h(t) = \frac{\mathrm{Sin}(\pi t/T)}{\pi t/T} \tag{1.4}$$

and its spectrum is an ideal characteristic

$$H(f) = \begin{cases} T & |f| \le \frac{1}{2T} \\ 0 & |f| > \frac{1}{2T} \end{cases} \tag{1.5}$$

The graphs of h(t) and H(f) are illustrated in figure 1.2 .

There are two basic problems associated with this pulse shape. One is the problem of realizing a pulse having the rectangular spectral characteristic H(f) given above. That is, H(f) is not physically realizable. The other problem is concerned with the fact that the tails of h(t) decay as $\frac{1}{t}$. Consequently a timing error in sampling results in an infinite series of intersymbol interference components. Such a series is not absolutely

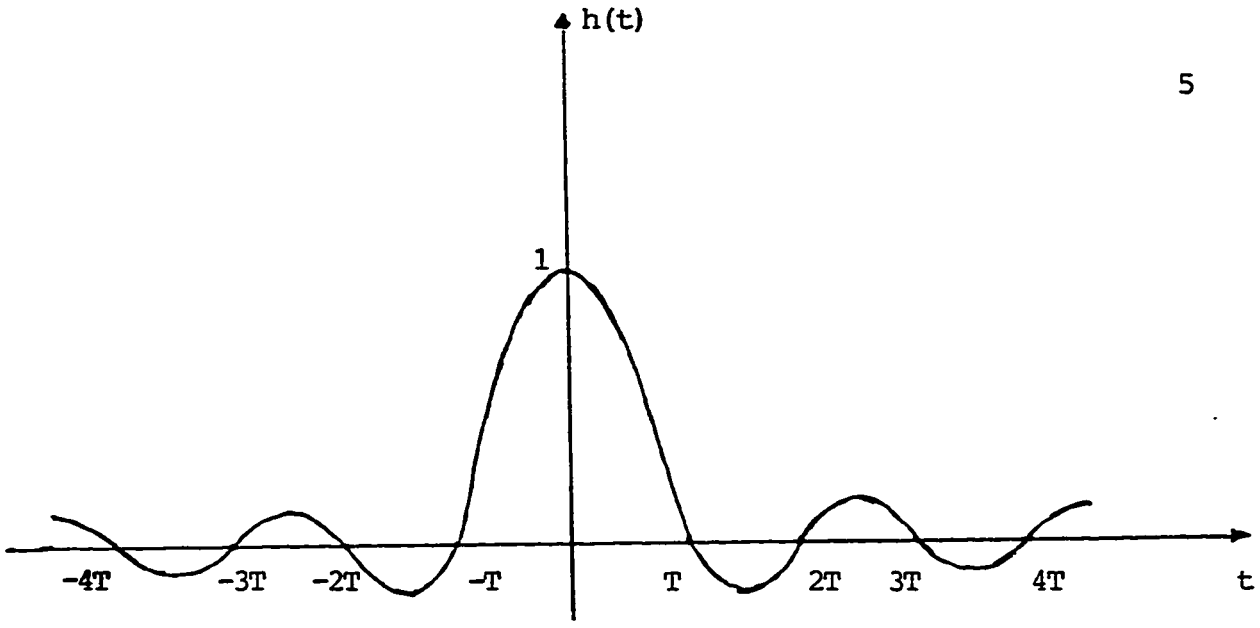

(a)

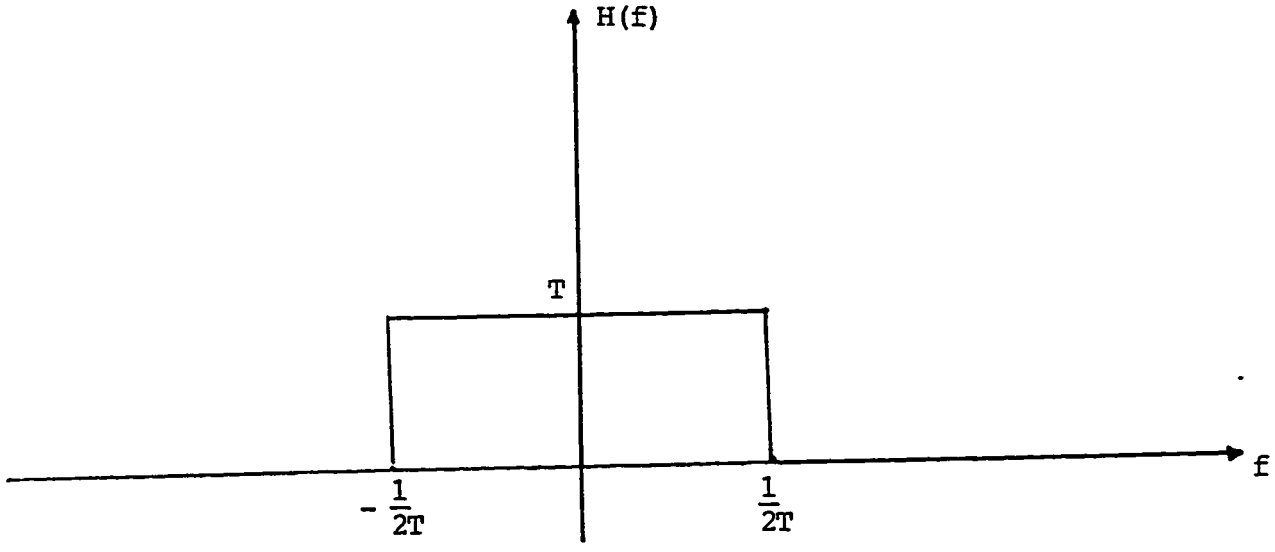

(b)

Figure 1.2: Band-Limited signal for no intersymbol interference.

summable and, hence, the sum of the resulting interference does not converge.

A pulse that has found wide use in digital transmission on band-limited channels such as telephone lines is one that has the raised cosine spectral characteristic [1],

$$H(f)=\begin{cases} T & 0\le |f| \le (1-\beta)/2T \\ \frac{T}{2}\{1-\mathrm{Sin}\frac{\pi T}{\beta}(f-\frac{1}{2T})\} & (1-\beta)/2T \le |f| \le (1-\beta)/2T \end{cases} \qquad (1.6)$$

where β is called the roll-off parameter. The pulse h(t) having this spectrum is

$$h(t)=\frac{\mathrm{Sin}(\pi t/T)}{\pi t/T}\frac{\mathrm{Cos}(\beta\pi t/T)}{(1-\frac{4\beta^2t^2}{T^2})} \qquad (1.7)$$

The tails of the pulse decay as $\frac{1}{t^3}$. Hence a timing error in sampling leads to a series of intersymbol interference components that converge. Figure 1.3 illustrates the spectral characteristic H(f) and the pulse h(t) for several values of β.

1.1.2 The transversal filter

To alleviate the effects of intersymbol interference it is necessary to equalize the channel. Thus equalization is the process of correcting channel-

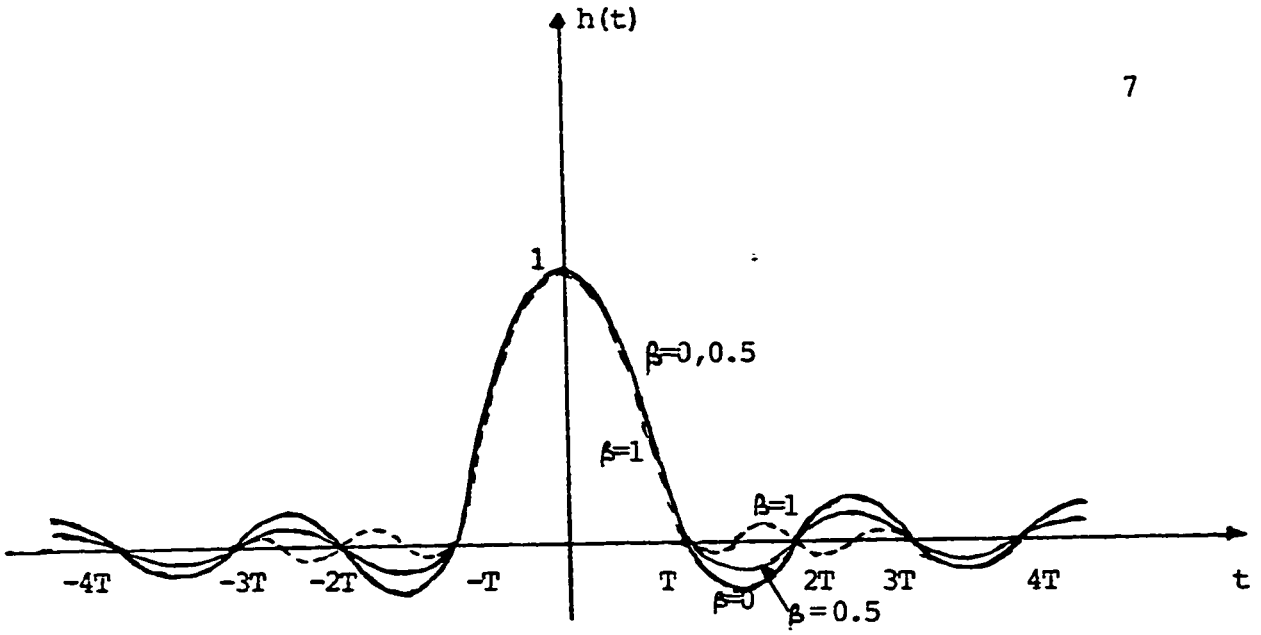

(a)

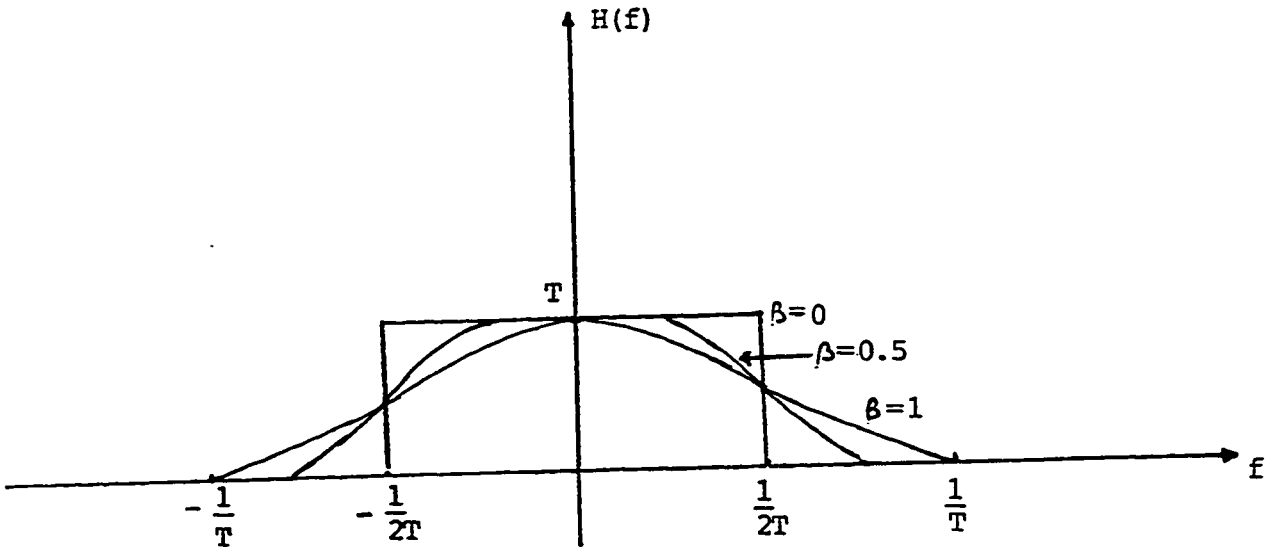

(b)

Figure 1.3: Pulses with ideal and raised cosine spectrum.

induced distortion, and the main idea of equalization is simply to compensate for nonideal characteristics by additional filtering. An equalizer is, then, an adaptive filter that is capable of high-speed digital signaling over slowly varying, band-limited channels whose impulse responses are unknown at the receiver [1], [5].

Most of these data sets use transversal filters for precise automatic equalization. The transversal filter was invented by Wiener and Lee in 1935 and described in the literature by Kalman in 1940 (see [3] for historical details). Figure 1.4 shows a linear transversal filter.

The essential element of the adaptive receiver is a tapped-delay-line (TDL) filter with an automatically adjustable gain at each tap. Figure 1.4 shows a practical model of an adaptive TDL filter. The tap gains are usually adjusted using a main cost function. The most widely used cost function is the mean square error (MSE), which is the standard performance measure at the equalizer output. Several algorithms can be used for adjusting the tap coefficients [6-8]; among these are the steepest descent algorithm, the Least Mean-Square (LMS) algorithm, and the Recursive Least-Squares (RLS) algorithm. The LMS algorithm is becoming a standard method [6]. The LMS algorithm is also referred to in the literature as the stochastic gradient algorithm.

Also, it must be emphasized that the theoretical results require an infinite transversal filter and that no optimality claim may be made for a finite transversal filter as an equalizer. However, the theory does provide a

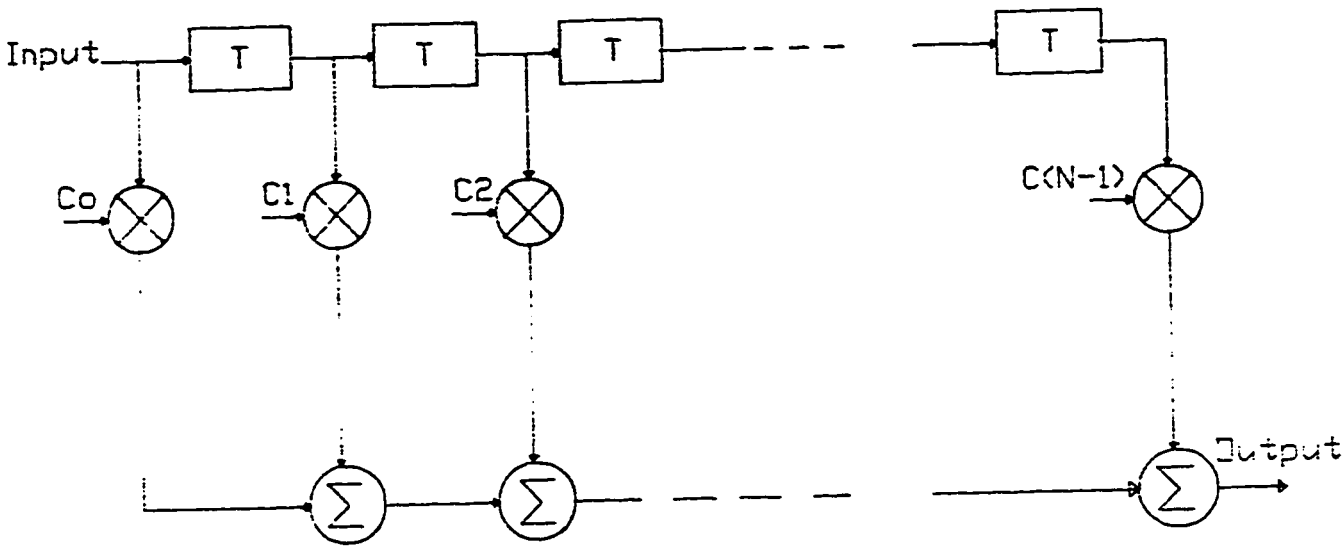

Figure 1.4 Linear transversal filter.

certain insight into the requirements for good equalization. It was shown that optimum filtering requires two filters [1]. One filter matches the channel and has the basic feature of minimizing the effect of noise. The other filter, a transversal filter, eliminates intersymbol interference. Then, the purpose of an equalizer, placed in the path of the received signal, is to cancel the effect of the ISI and the noise terms as much as possible so that the probability of error will be minimum.

Figure 1.5 shows a block diagram of an automatic adaptive equalizer. During the training period, a known signal is transmitted and a synchronized version of this signal is generated in the receiver to acquire information about the channel characteristics. The training sequence must be at least as long as the equalizer in order to make the transmitted signal spectrum adequatly dense in the bandwidth of the channel to be equalized.

When the initial training period is completed, the coefficients of the adaptive equalizer may be continually adjusted in a decision-directed manner. The receiver estimate is obtained by applying the adaptive equalizer output to a decision device, as shown in figure 1.5. During data mode, the receiver decisions are correct with a low probability of error.

Since we have an idea about an adaptive equalizer, why don't we take a look at the present and the previous work done on this field? The coming section is going to take care of this answer.

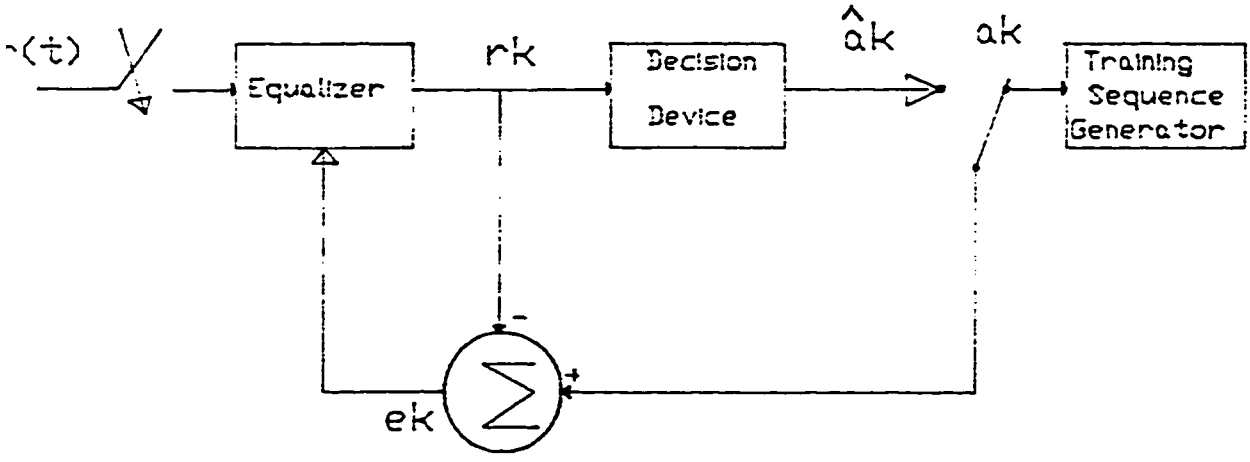

Figure 1.5 Automatic adaptive equalizer.

1.2 LITERATURE REVIEW

Adaptive equalizers are important building blocks in MOdulators-DEModulators (MODEMS) for digital data transmission over linear dispersive channels. They adaptively mitigate the adverse effects of ISI.

A large number of equalizer adjustment algorithms are conceivable, depending on the cost function. The currently prevailing technique is the so-called stochastic gradient algorithm. It was shown in [4], [7] that the Kalman, fast Kalman, and adaptive-lattice algorithms are the fastest known methods for the training of equalizers. The fast Kalman algorithm possesses the lowest complexity of these schemes. The adaptive-lattice algorithm requires more multiplications per update but has the advantage of being able to increase the equalizer length adaptively when needed; this is an advantage for off-line or batch processing but not for real-time applications [7]. The Kalman algorithm possesses the highest complexity and offers no advantage over the two other algorithms. All the above three mentioned algorithms use the least-squares cost function which minimizes the sum-of-error-squares.

Other algorithms for the design of transversal-filter equalizers are described in [8].

A critical parameter in the start-up performance of MODEMS is the speed of convergence of the equalizer adjustment algorithm. In [9] it was

shown that using a new configuration for the equalizer, the system's start-up time can be reduced significantly. Here, the new configuration was developed based on the following principles:

1)Equalizer setting time can be minimized by making the input signals orthonormal to the gain controls, and

2)such a minimization does not change the noise power, the mean-square equalization error, the convexity of the gain control adjustment, and the feedback control loops in the equalizer.

In [10] steps toward explaining a theory on the rapid initial convergence of least-squares equalizer adjustment algorithms are outlined.

An automatic and adaptive digital decision feedback equalizer with variable optimum step size for the adjustment is presented in [11]. Here, the computation of the step size in a gradient procedure can be achieved by multiplexing the equalizer structure.

The adaptive equalization of highly dispersive channels, e.g, a voice-grade telephone channel, for data transmission using the LMS algorithm was described by Gersho [12].

A major issue in the design of an adaptive digital equalizer is the determination of the minimum number of bits required to represent the adjustable equalizer coefficients, as well as all the internal levels of the equalizer. Gitlin et al. [13] consider the effect of digital implementation of an

adaptive equalizer using the LMS algorithm. They show that a digitally implemented LMS algorithm stops adapting whenever the correction term in the update recursion for any coefficient of the equalizer is smaller in magnitude then the least significant digit to within which the coefficient has been quantized. In a later work, Gitlin and Weinstein [14] developed a criterion for determining the number of bits required to represent the coefficients of an adaptive digital equalizer so that the mean squared error at the equalizer output is at an acceptable level.

So far, we have an idea about an adaptive equalizer and the updating schemes used to update the tap coefficients; but we do not have any information concerning the types of equalizers used and their corresponding problems associated to them. The next section will, hopefully, clear out this matter and suggest at the same time a proposed equalizer that will be a compromise between complexity and performance.

1.3 PROBLEM STATEMENT

The most widely used equalizers are the synchronous equalizer and the Fractionally-Spaced Equalizer (FSE). In the first equalizer, i.e., the synchronous equalizer, the equalizer taps are spaced at the reciprocal of the symbol rate. While in an FSE, on the other hand, the equalizer taps are spaced closer than the reciprocal of the symbol rate.

Figure 1.6 shows a simplified baseband-equivalent PAM data transmission system. The symbol rate and the receiver sampling rate are $\frac{1}{T}$ and $\frac{1}{T'}$, respectively. For a synchronous equalizer $T' = T$; while for FSE T' will be less than T. For the same time span NT, a synchronous equalizer will need N tap coefficients, while (2N) tap coefficients are needed for an FSE with tap spacing $T' = \frac{T}{2}$.

From the above discussion we see that the FSE requires a large number of tap coefficients than the synchronous equalizer. This will result in a great amount of computations needed to update the tap coefficients every symbol period, an important drawback of the FSE. Therefore, to overcome this defficiency, a new idea is presented.

1.4 THE PROPOSED SCHEME

The fractionally-spaced equalizer is superior to the synchronous equalizer, and this is in its ability to be not affected by aliasing problems and independent of the sampler phase. Hence, the idea behind our proposed method is as follows. Given that the FSE requires a larger number of tap coefficients than the synchronous equalizer, then one designs an unequally spaced fractional equalizer. The general configuration of the nonuniform

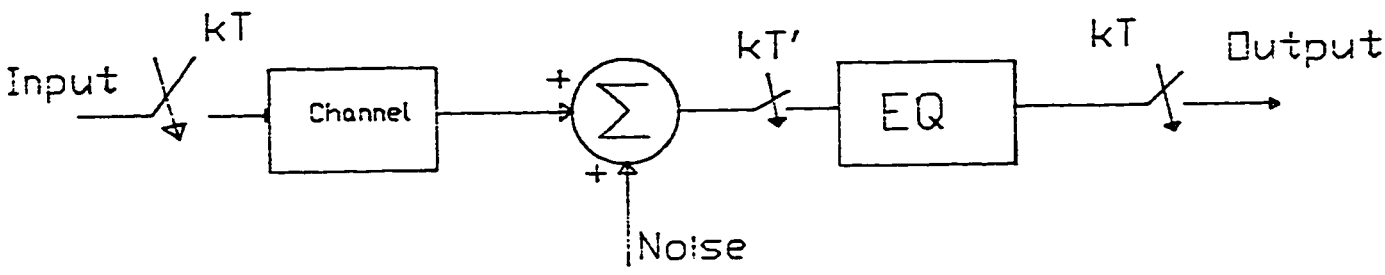

Figure 1.6 Simplified baseband-equivalent PAM data transmission system.

tap spacing is shown in figure 1.7, where each tap spacing , T_i , is confined to

$$T' \leq T_i \leq T \, , \, i = 1,2,...,N \qquad (1.8)$$

N is the number of taps. Hereafter, some of the C's, i.e., tap coefficients, will be forced to be zeros, and this is in the purpose of having a time span closer to that of the synchronous equalizer and the performance of an FSE.

Note that if C_i is zero, then $C_{(i-1)}$ and $C_{(i+1)}$ will be different from zero. The nonuniformity of the tap spacing is unknown and will be investigated, and the choice of these taps will be based on how the equalizer will perform. Performance is regarded here as the MSE as a function of the number of iterations, and the effect of delay of the sampler phase on the MSE as well. The effect of the jitter on the MSE is studied, too. Hence, investigation of the relative performance of the Non-uniformally-Fractional-Spaced Equalizer (NFSE) is carried out.

The performance of the proposed design will be evaluated based on the MSE at the output of the equalizer. Two channels are considered during this study, one for a baseband PAM system, and one for a baseband QAM system.

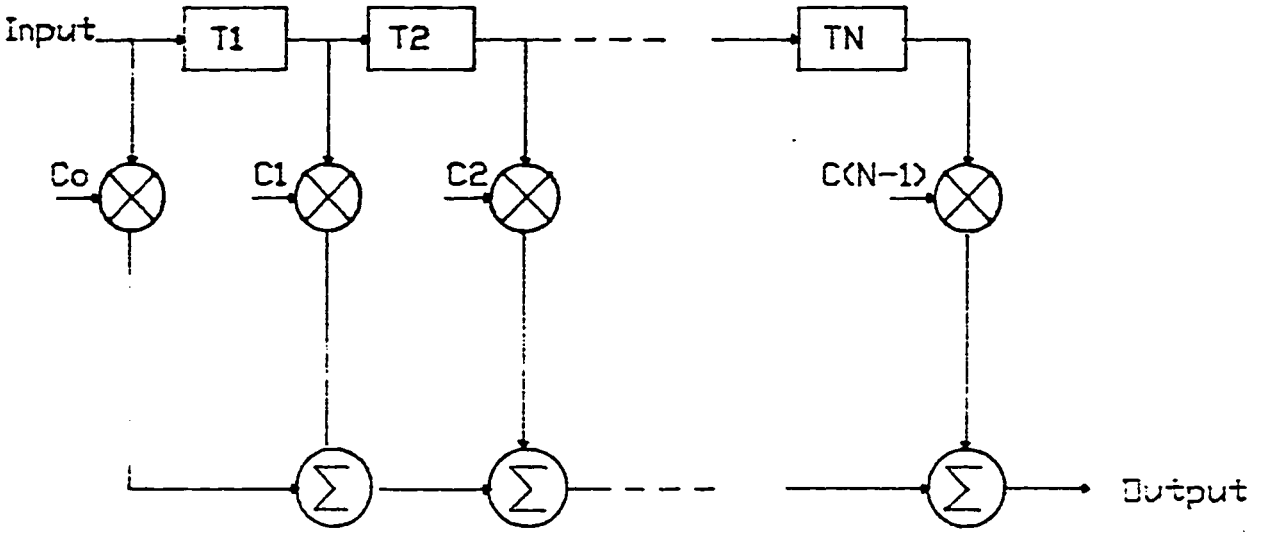

Figure 1.7 Nonuniform tap spacing equalizer.

1.5 THESIS ORGANIZATION

Chapter 2 will be totally devoted to adaptive equalization, including the LMS algorithm. While Chapter 3 will be concerned about fractionally-spaced equalization. The proposed method and simulation of the system will be presented in Chapter 4. Chapter 5 will elaborate equalizers used for QAM systems. Both equalizers are included in the analysis, the T spaced equalizer and the FSE equalizer.

The conclusion and suggestions for further work are presented in Chapter 6.

CHAPTER II

LINEAR ADAPTIVE EQUALIZATION

2.1 INTRODUCTION

The nonuniform transmission characteristics of the channel cause what might be termed a distortion barrier, prohibiting faster transmission. The distortion of data pulses by the channel results in these pulses being smeared out in time so as to overlap other transmission pulses. This intersymbol interference is one of the direct chief degrading factors in present systems and becomes the determining factor in the design of high-rate systems [1].

The variation in the characteristics within a class of channels, as in the lines found in the switched telephone network, is large enough so that automatic adaptive equalization is used nearly universally for speeds higher than 2400 b/s [2].

The transversal filter of figure 2.1 has a sampled impulse-response given by the N-component row vector

$$C^T=[C_0C_1...C_{N-1}] \tag{2.1}$$

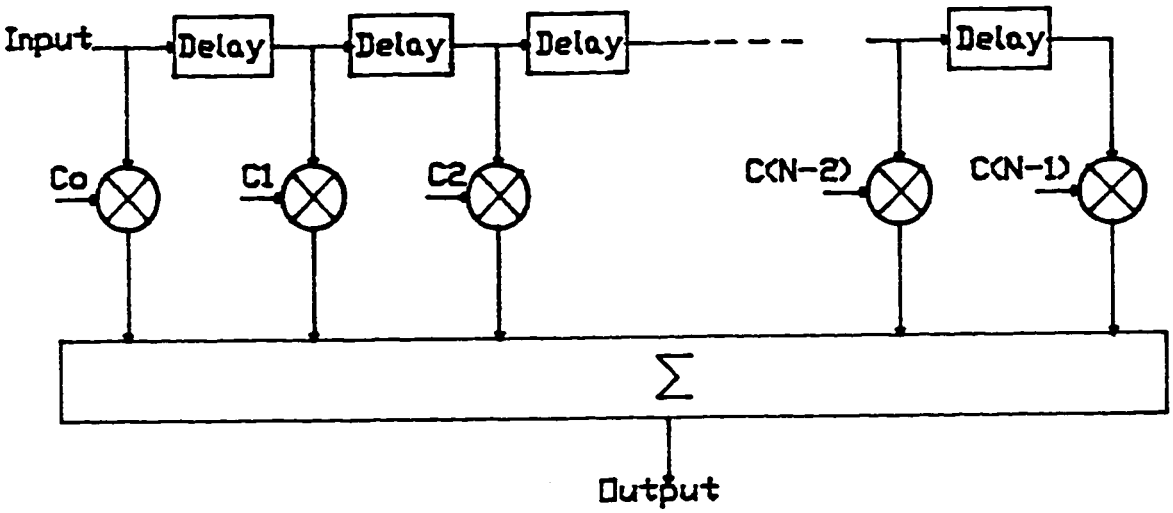

Figure 2.1 Tapped-delay-line filter

and the z transform of this sampled impulse response is

$$C(z) = C_0 + C_1 z^{-1} + \ldots C_{N-1} z^{-N+1} \tag{2.2}$$

Notice that the sampled impulse-response of the filter is given by the sequence of its tap gains, which also form the coefficients in the corresponding z-transform.

Various design techniques are available for evaluating the tap gains of the linear equalizer. Let **H** (z) be the sampled impulse-response of the baseband channel given by

$$H(z) = h_0 + h_1 z^{-1} + \ldots h_g z^{-g} \tag{2.3}$$

The output of a finite transversal filter is given by the (N+g)-component row vector

$$CH = [e_0 e_1 \ldots e_{N+g-1}] \tag{2.4}$$

Ideally we want $e_h = 1$ (where h is a nonnegative integer in the range 0 to N+ g-1, and represents the maximum delay), and the rest of e_i's equal to zero.

The peak distortion in the equalized signal is defined to be [1]

$$D_p = \frac{1}{|e_h|} \sum_{\substack{i=0 \\ i \neq h}}^{N+g-1} |e_i| \tag{2.5}$$

The mean-square distortion is

$$D_m = \frac{1}{e_h^2} \sum_{\substack{i=0 \\ i \neq h}}^{N+g-1} e_i^2 \qquad (2.6)$$

and the mean-square error will be defined later.

In the early work on linear equalizers these were generally designed to minimize the peak distortion. This is achieved, under conditions, by a technique known as zero forcing. Figure 2.2 illustrates in block diagram the equivalent discrete-time channel and equalizer.

The peak distortion is simply defined as the worst-case intersymbol interference at the output of the equalizer [4]. The point that should be emphasized about the zero-forcing algorithm is that the algorithm is optimum only if peak distortion of the received signal is less than unity, in the sense of minimizing D [1]. Another point is that the peak distortion criterion and, hence, the zero-forcing algorithm neglects the effects of additive noise. These limitations do not exist if the mean-square-error criterion is used in the adjustment of the equalizer coefficients [4].

In the LMS equalizer the tap coefficients are chosen to minimize the mean-square error which is the sum of squares of all the ISI terms plus the noise power at the output of the equalizer. Therefore, the LMS equalizer maximizes the signal-to-distortion ratio at the equalizer output within the constraints of the equalizer length and delay [2].

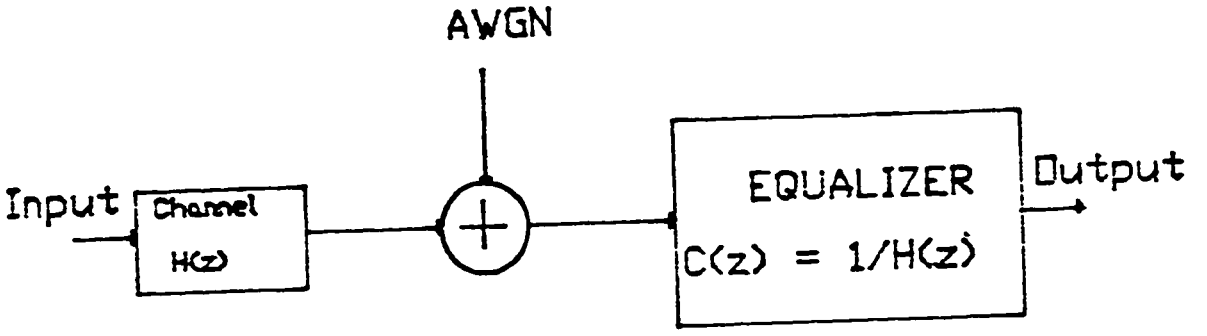

Figure 2.2 Block diagram of the equivalent discrete-time channel and equalizer.

Most current high-speed MODEMS use LMS equalizers because they are more robust and superior to the zero-forcing equalizers in their convergence properties [3].

2.2 THE MEAN-SQUARED ERROR (MSE) AND THE LMS ALGORITHM

2.2.1 The mean-squared error criterion

In the MSE criterion the tap coefficients $\{C_i\}$ of the equalizer are adjusted to minimize the mean square value of the error

$$e_k = d_k - y_k \tag{2.7}$$

where d_k is the desired signal and y_k is the output signal of the equalizer, defined as

$$y_k = \sum C_i r_{k-i}$$

$$= \mathbf{R}_k^T \mathbf{C} \tag{2.8}$$

where $\{r_k\}$ is the input to the equalizer, and

$$\mathbf{R}_k = [r_0 r_1 \ldots r_k]^T$$

In most practical instances the adaptive process is oriented toward minimizing the mean-square value, or average power of the error signal. The

performance index for the MSE criterion, denoted J, is defined as

$$J = E[e_k^2] \tag{2.9a}$$

or, equivalently

$$J = E[(d_k - y_k)^2] \tag{2.9b}$$

finally

$$J = E[d_k^2] - 2\sum_i C_i E[d_k r_{k-i}] + \sum_i \sum_j C_i C_j E[r_{k-i} r_{k-j}] \tag{2.9c}$$

Note that the expected value of any sum is the sum of expected values, but that the expected value of a product is the product of expected values when the variables are statically independent.

The mean-square-error function can be more conveniently expressed as follows. Let **A** be defined as an (N × N) square matrix with elements a_{ij} given by

$$a_{ij} = E[(r_{k-i} r_{k-j})], \qquad i,j = 0,1,...,N-1 \tag{2.10}$$

This matrix is designated the input correlation matrix. The main diagonal terms are the mean squares of the input components, and the cross terms are the cross correlations among the input components. This matrix has the following properties [15].

Property 1. The correlation matrix **A** is symmetric, that is $\mathbf{A}^T = \mathbf{A}$ where $\mathbf{A}^T$ is the transpose of **A**.

Property 2. The correlation matrix **A** is Toeplitz, that is, the elements on its main diagonal are equal and so are the elements on any other diagonal parallel to the main diagonal.

Property 3. The correlation matrix **A** is almost always positive definite.

Let **b** be similarly defined as the column vector with elements b_i given by

$$b_i = E[(d_k r_{k-i})] \quad , \qquad i = 0,1,...,N-1 \tag{2.11}$$

This vector is the set of cross correlations between the desired response and the input components.

We now let the mean-square error defined in (2.9) expressed in terms of equations (2.10) and (2.11) as

$$J = E[d_k^2] - 2\mathbf{C}^T\mathbf{b} + \mathbf{C}^T\mathbf{A}\mathbf{C} \tag{2.12}$$

It is clear from this expression that the mean-square error J is precisely a quadratic function of the components of the tap coefficients **C** when the input components and desired response input are stationary stochastic variables.

The shape associated with this MSE is hyperboloid. This bowl-shape quadratic error function, or performance surface, must be concave upward;

otherwise, there would be tap coefficients that would result in a negative MSE, an important result with real, physical signals [16].

2.2.2 Gradient and Minimum MSE

The point at the bottom of the performance surface corresponds to the optimal tap coefficients, $\mathbf{C}_{op}$, or minimum MSE. The gradient method is used to cause the tap coefficients vector to seek the minimum of the performance surface. It is defined as

$$\mathbf{G}_k = \frac{dJ}{2d\mathbf{C}} = \mathbf{AC} - \mathbf{b} = -E[e_k \mathbf{R}_k] \tag{2.13}$$

To obtain the minimum MSE, the tap-coefficients vector $\mathbf{C}$ is set to its optimal value $\mathbf{C}_{op}$, where the gradient is zero, that is,

$$\mathbf{G}_k = 0 = \mathbf{AC}_{op} - \mathbf{b} \tag{2.14}$$

Assuming that $\mathbf{A}$ is nonsingular, the optimal tap-coefficients vector $\mathbf{C}_{op}$, sometimes called the Wiener vector [15], [16], is found from (2.14) to be

$$\mathbf{C}_{op} = \mathbf{A}^{-1}\mathbf{b} \tag{2.15}$$

The minimum MSE is found by substituting $\mathbf{C}_{op}$ from (2.15) for $\mathbf{C}$ in

(2.12)

$$J_{min} = E[d_k^2] - \mathbf{b}^T \mathbf{C}_{op} \tag{2.16}$$

Since the MSE is a quadratic form in **C** which reaches its minimum value when **C** equals $\mathbf{C}_{op}$, one might expect that it could be expressed as

$$J = J_{min} + (\mathbf{C} - \mathbf{C}_{op})^T \mathbf{A} (\mathbf{C} - \mathbf{C}_{op}) \tag{2.17}$$

See appendix for the proof of equation (2.17).

2.2.3 The LMS Algorithm

The solution for $\mathbf{C}_{op}$ involves inverting the input correlation matrix **A**. Alternatively, an iterative procedure may be used to determine $\mathbf{C}_{op}$. Probably the simplest iterative procedure is the method of steepest descent, in which one begins by choosing an initial tap-coefficient vector. This initial choice of coefficients corresponds to some point on the performance surface in the N-dimensional space of coefficients. The initial gradient vector $\mathbf{G}_0$ is then computed at this point of the performance surface, and each tap coefficient is changed in the direction opposite to its corresponding gradient component. Then, succeeding values are obtained according to the relation

$$\mathbf{C}_{k+1} = \mathbf{C}_k - \Delta \mathbf{G}_k \ , \quad k = 0,1,2,..., \tag{2.18}$$

where $\mathbf{C}_k$ represents the set of coefficients at the kth iteration, and Δ is a positive number chosen small enough to insure convergence of the iterative

procedure. If the minimum MSE is reached for some $k = k_0$, then $\mathbf{G}_k$ is equal to zero so that no further change occurs in the tap coefficients. In general, J_{min} cannot be attained for a finite value of k_0 with the steepest-descent method; however, it can be approached as closely as desired for some finite value of k_0 [4],[5].

Given that the gradient vector $\mathbf{G}_k$ depends on both the autocorrelation matrix **A** and the vector **b** of cross correlations, this makes the steepest descent difficult for determining the optimum tap coefficients. Instead, estimates of the gradient vector may be used. That is, the algorithm for adjusting the tap coefficients may be expressed in the form

$$\mathbf{C}_{k+1} = \mathbf{C}_k - \Delta \hat{\mathbf{G}}_k \tag{2.19}$$

where $\hat{\mathbf{G}}_k$ denotes an estimate of the gradient vector $\mathbf{G}_k$, and is defined as

$$\hat{\mathbf{G}}_k = -e_k \mathbf{R}_k \tag{2.20}$$

Since $E\{\hat{\mathbf{G}}_k\} = \mathbf{G}_k$, the estimate $\hat{\mathbf{G}}_k$ is an unbiased estimate of the true gradient vector. The LMS algorithm for recursively adjusting the tap coefficients of the equalizer is given then as

$$\mathbf{C}_{k+1} = \mathbf{C}_k + \Delta e_k \mathbf{R}_k \tag{2.21}$$

figure 2.3 depicts a linear adaptive equalizer based on the LMS algorithm.

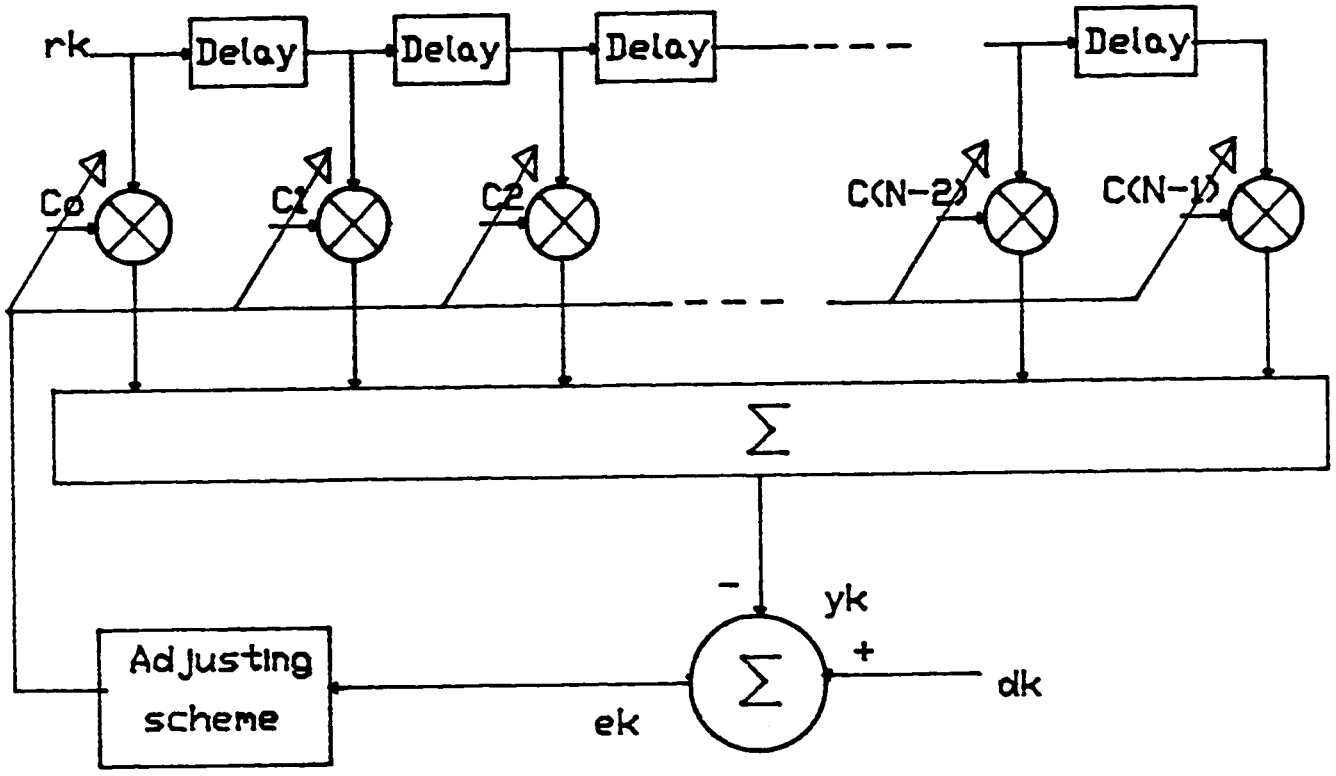

Figure 2.3 Linear adaptive equalizer based on the LMS algorithm.

2.2.4 Convergence behavior of the LMS algorithm

As with all adaptive algorithms, a primary concern with the LMS algorithm is its convergence to the optimum coefficient vector solution, where J is minimized. The convergence behavior of the LMS algorithm given in (2.21) is governed by the step size parameter Δ. To ensure convergence, the choice of this parameter Δ is considered. The effect of Δ in (2.21), which uses noisy, but unbiased estimates of the gradient vector, will be the same on the average as the effect of Δ on the steepest-descent algorithm in (2.14), which employs the exact value of the gradient [5].

From (2.13) and (2.18) we have

$$\mathbf{C}_{k+1} = \mathbf{C}_k - \Delta \mathbf{G}_k$$

$$= (\mathbf{I} - \Delta \mathbf{A})\mathbf{C}_k + \Delta \mathbf{b} \qquad (2.22)$$

where $\mathbf{I}$ is the identity matrix. It is shown in [5], and [15] that the iterative process given in (2.21) will converge to the optimum coefficient-vector $\mathbf{C}_{op}$ provided that the eigenvalues of the matrix $(\mathbf{I} - \Delta \mathbf{A})$ are less than one in absolute value, that is,

$$|1 - \Delta\lambda_k| < 1 \quad , k = 0,1,...,N-1 \qquad (2.23)$$

where $\{\lambda_k\}$ is the set of the N eigenvalues of $\mathbf{A}$. Since $\mathbf{A}$ is an autocorrelation matrix, it is positive definite and, hence, λ_k is greater than zero for all k [15]. Consequently, the tap coefficients will converge to their optimum values if Δ

satisfies the inequality

$$0 < \Delta < \frac{2}{\lambda_{max}} \tag{2.24}$$

where λ_{max} is the largest eigenvalue of **A**.

Within these bounds, the speed of adaptation and also the noise in the tap coefficient vector solution are determined by the step size of Δ. Note that λ_{max} cannot be greater than the trace of **A**, which is the sum of the diagonal elements of **A** [5], that is,

$$\lambda_{max} < \mathrm{tr}\{\mathbf{A}\} = \sum(\text{diagonal elements of } \mathbf{A}) \tag{2.25}$$

Furthermore, with a transversal adaptive filter, equation (2.10) gives

$$\mathrm{tr}\{\mathbf{A}\} = N \times E\{r_{k-j}^2\} \tag{2.26}$$

or N times the input signal power. Thus convergence of the tap coefficient vector is assured by

$$0 < \Delta < \frac{1}{N \times (\text{signal power})} \tag{2.27}$$

It is observed that rapid convergence occurs when $|1-\Delta\lambda_k|$ is small. Slow convergence, however, will occur if there is a large spread between the largest

and smallest eigenvalues of **A**. Consequently the ratio $\frac{\lambda_{max}}{\lambda_{min}}$ ultimately determines the convergence rate [4]. If the ratio $\frac{\lambda_{max}}{\lambda_{min}}$ is small, Δ can be selected as to achieve rapid convergence. However, if the ratio $\frac{\lambda_{max}}{\lambda_{min}}$ is large, the convergence rate of the algorithm will be slow.

Gersho [12] showed that

$$\Delta = \frac{2}{\lambda_{max} + \lambda_{min}} \tag{2.28}$$

gives the fastest convergence. Here the step size results in a mean square error 3 dB worse than the minimum achievable MSE.

2.2.5 Excess MSE

The recursive algorithm for adapting the tap coefficients of the TDL filter, given in (2.21), employs unbiased noisy estimates of the gradient vector. The noise in these estimates causes random fluctuations in the tap coefficients about their optimal values and thus leads to an increase in the MSE at the output of the equalizer, which is called excess MSE [5].

The excess MSE at the output of the equalizer, can be seen from equation (2.17) which is

$$J = J_{min} + (\mathbf{C} - \mathbf{C}_{op})^T \mathbf{A} (\mathbf{C} - \mathbf{C}_{op})$$

It is represented in the second term of the right hand side of the above mentioned equation. When C equals C_{op} the excess MSE will be zero and J will be exactly equals to J_{min}.

Notice that the MSE is directly related to Δ. Thus, an increase in Δ will have a direct affect on the MSE. Hence, the choice of Δ involves a tradeoff between the speed of convergence of the recursive algorithm and the amount of excess MSE that can be tolerated. In practice, the value of the step is selected for fast convergence during the training period and then reduced for fine tuning during the steady-state operation (or data mode) [2].

2.3 IMPLEMENTATION OF ADAPTIVE FILTERS

The methods of implementing adaptive filters may be divided into two broad categories: analog and digital.

The analog approach is primarily based on the use of charge-coupled device (CCD) technology or switched-capacitor technology. The basic circuit realization of the CCD is a row of field-effect transistors drains and sources connected in series, and the drains capacitively coupled to the gates. The set of adjustable coefficients are stored in digital memory locations, and the multiplications of the analog sample values by the digital coefficients take place in an analog fashion. This approach has significant potential in applications where the sampling rate of the incoming data is too high for digital implementation [15].

In the digital implementation of an adaptive filter, the filter input is sampled and quantized into a form suitable for storage in shift registers. The set of adjustable coefficients are also stored in shift registers. Logic circuits are used to perform the required digital arithmetic, e.g., multiply and accumulate. In this approach, the circuitry may be hard-wired for the sole purpose of performing adaptive filtering. Alternatively, it may be implemented in programmable form on a microprocessor. The use of a microprocessor also offers the possibility of integrating the adaptive filter with other signal-processing operations, which can be attractive in some applications [15].

2.4 SUMMARY

Linear adaptive equalization is a subject used for both equalizers, the synchronous equalizer and the fractionally-spaced equalizer. The different cost functions, like the peak distortion, the mean-square distortion, and the MSE were defined. The application of these cost functions to the zero forcing algorithm and to the LMS algorithm were presented. The LMS algorithm was more elaborated and this is due to its wide use and its need during our simulation process. Since, it was only presented for the synchronous equalizer, the application of the LMS algorithm to fractionally-spaced equalizers and their performance compared to the synchronous equalizers is presented in the following chapter. The proposed method will be presented in Chapter 4.

CHAPTER III

FRACTIONALLY-SPACED EQUALIZATION

Many years have elapsed between Lucky's invention of the adaptive synchronous equalizer, and the present interest in fractionally-spaced equalization [16]. This is due to both the increased complexity required to implement the FSE, and the relatively satisfactory performance of the conventional synchronous equalizer.

A fractionally-spaced transversal equalizer is shown in figure 3.1. The delay line taps of such an equalizer are spaced an interval T′ which is less than, or a fraction of, the symbol period T. The tap spacing T′ is typically selected such that the bandwidth occupied by the signal at the equalizer input is

$$|f| < \frac{1}{2T'} \tag{3.1}$$

that is T′-spaced sampling satisfies the sampling theorem. The general tap spacing formula for an FSE may be written as

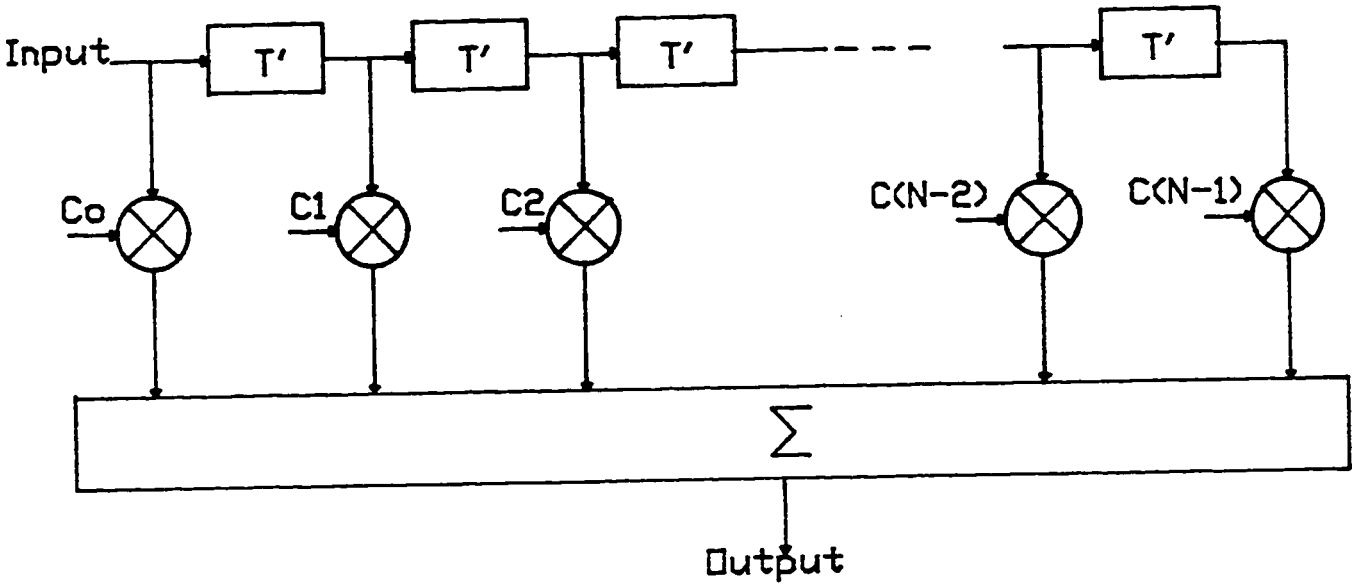

Figure 3.1 Fractionally-spaced transversal equalizer.

$$T' = \alpha T \tag{3.2}$$

where

$$\alpha = \frac{K}{M} < 1 \tag{3.3}$$

where K and M are integers and M > K. For digital implementation K and M should be prime integers [6]. The cost of fractional tap spacing would then primarily be an M-times higher Analog-to-Digital (AD) converter rate, M-times more memory stages for the equalizer delay line, and $\frac{L}{K}$ -times more multiplications for the same length, L, of the equalizer delay line in terms of total delay.

Figure 3.2 shows a digital implementation for an FSE with a tap spacing $T' = \frac{T}{2}$. The received signal r(t) is sampled and shifted into the equalizer delay line at a rate $\frac{2}{T}$ and one output is produced each symbol period according to

$$y_n = \sum_{k=0}^{N-1} C_k r(nT - \frac{kT}{2}) \tag{3.4}$$

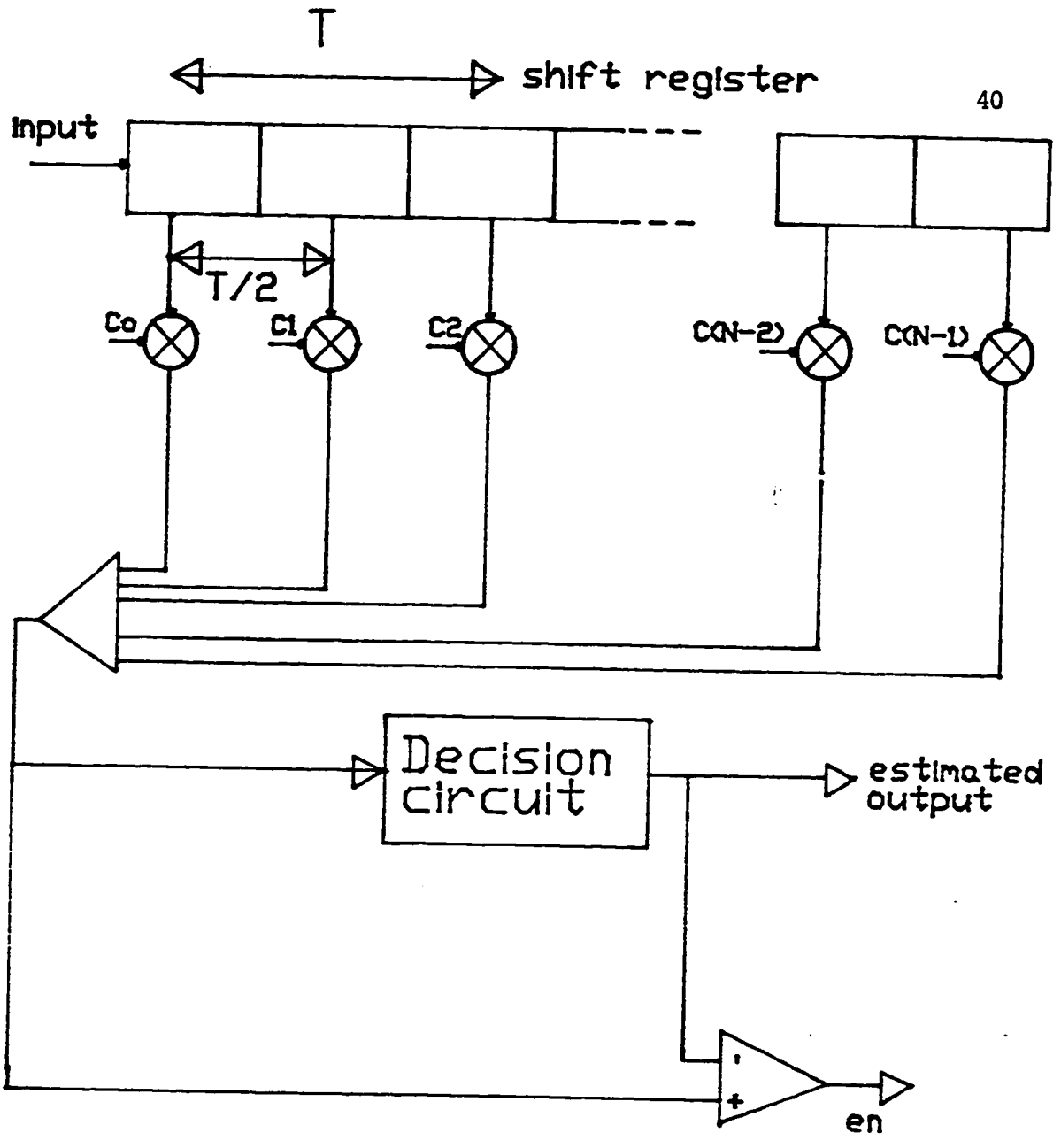

Figure 3.2 Digital Implementation for an FSE with tap spacing T/2

3.1 SUPERIORITY OF FRACTIONALLY-SPACED EQUALIZERS

We begin with a brief discussion of the ability of a fractionally-spaced equalizer to compensate for any receiver timing phase. To do this we use the transfer function of the fractionally-spaced equalizer.

Consider first the received signal

$$r(t) = \sum_m a_m h(t-mT) + n(t) \tag{3.5}$$

where $\{a_n\}$ is the discrete-valued data symbols, $\frac{1}{T}$ is the symbol rate, h(t) is the impulse response of the channel, and n(t) is additive noise. The input to a conventional synchronous equalizer are samples of the filtered received signal at the instants $t = nT + \tau$, i.e.,

$$r(nT+\tau) = \sum_m a_m h(nT+\tau-mT) + n(nT+\tau) \tag{3.6}$$

The output of this synchronous equalizer, with tap coefficients $\{C_i\}$ spaced at the symbol period, T, have a Fourier transform

$$Y_T(\omega) = C_T(\omega) H_T(\omega) \tag{3.7}$$

Here, $H_T(\omega)$ is the aliased spectrum of $H(\omega)$, $C_T(\omega)$ is the transfer function of the synchronous equalizer, and, ideally, the equalizer output is the transmited data symbol, i.e.,

$$y(nT+\tau)=a_n \tag{3.8}$$

Since

$$C_T(\omega)=C_T(\omega+\frac{2\pi k}{T}) \tag{3.9}$$

the synchronous equalizer can only act to modify $H_T(\omega)$, as opposed to directly modifying $H(\omega)e^{j\omega\tau}$. In other words, the synchronous equalizer cannot exercise independent control over both sides of the roll-off region about $\omega=\frac{\pi}{T}$. This is shown in figure 3.3 where α denotes the excess bandwidth of h(t). If, because of a severe phase characteristics and a poor choice of τ , a null is created in the roll-off portion of the folded spectrum $H_T(\omega)$, hence all the synchronous equalizer can do to compensate for this null is to synthesize a rather large gain in the affected area; this leads to a severe performance degradation because of the noise enhancement at these frequencies.

Let us consider now a fractionally-spaced equalizer with tap spacing $T' < T$. This equalizer has the following transfer function

$$C_{T'}(\omega)=\sum_i C_i e^{-j\omega iT'} \tag{3.10}$$

For a fractionally-spaced equalizer the equalizer input is sampled at the rate $\frac{1}{T'}$, while the output is sampled at the rate $\frac{1}{T}$, since data decision is made

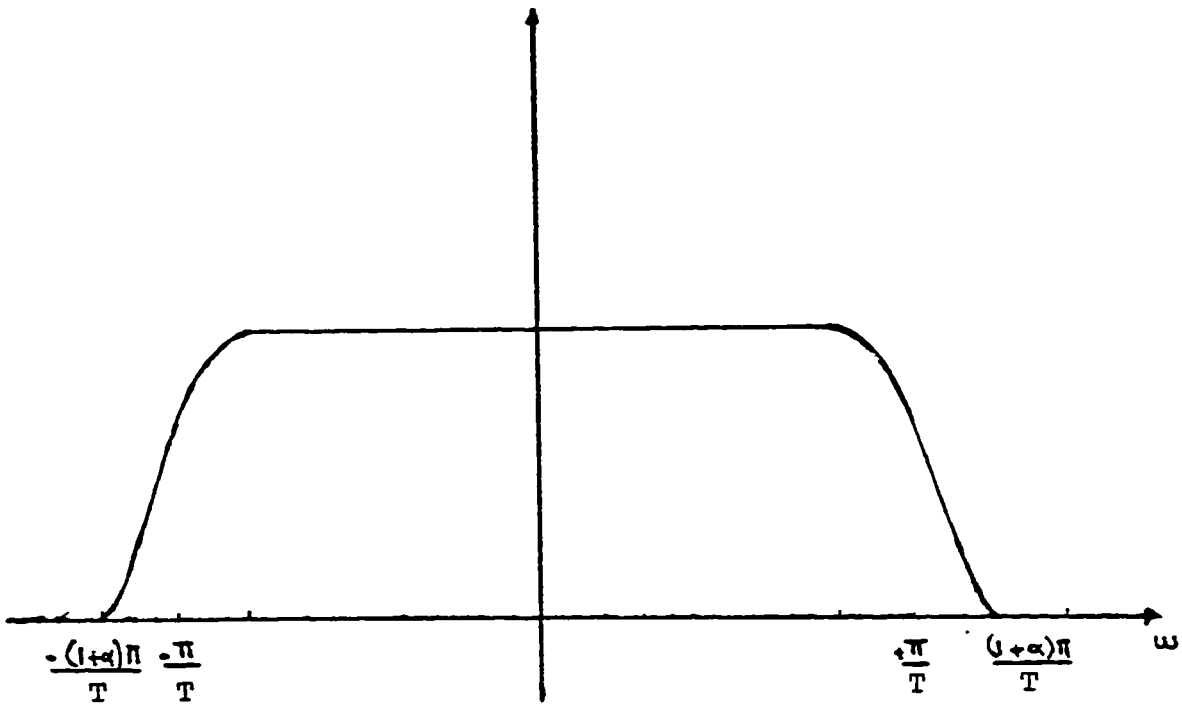

Figure 3.3: Fourier transform of h(t).

every symbol period, T. A PAM data transmission system is shown in figure 3.4 to clearify the idea.

The output of the fractionally-spaced equalizer, just prior to the output sampler, is periodic, with period $\frac{2\pi}{T'}$, and is given in the frequency domain as

$$Y_{T'}(\omega) = C_{T'}(\omega)\sum_{k} H(\omega + \frac{2k\pi}{T'})\exp\{j(\omega + \frac{2k\pi}{T'})\tau\} \qquad (3.11)$$

and for systems where $\frac{(1+\alpha)\pi}{T} \leq \frac{\pi}{T'}$ only the $k=0$ term survives [17], i.e., the output of the fractionally-spaced equalizer is given by the following expression

$$Y_{T'}(\omega) = C_{T'}H(\omega)e^{j\omega\tau} \qquad (3.12)$$

Hence, $C_{T'}(\omega)$ acts on $H(\omega)e^{j\omega\tau}$ before aliasing, with respect to the output sampling rate, takes place. Thus $C_{T'}(\omega)$ can compensate for any timing phase [2], [6], [17]. Clearly, such compensation is highly desirable since it minimizes noise enhancement and avoids the extreme sensitivity to timing phase associated with the synchronous equalizer [2], [17]. The equalizer output is sampled at T and the spectrum of this output is periodic with period $\frac{2\pi}{T}$ and has the following expression

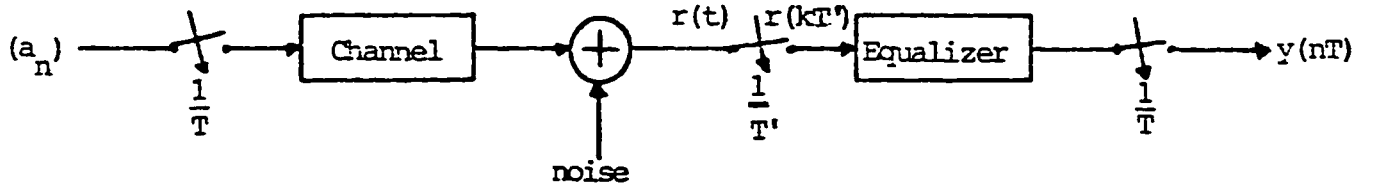

Figure 3.4: PAM data transmission system.

$$Y_T(\omega) = \sum_i C_T(\omega + \frac{2i\pi}{T}) H(\omega + \frac{2i\pi}{T}) \exp\{j(\omega + \frac{2i\pi}{T})\tau\} \qquad (3.13)$$

We can see that equations (3.13) and (3.7) are different, where in this equation, i.e., equation (3.13), the equalized output is the sum of equalized aliased components rather than equalization of an already formed sum of aliased components.

With this property, we can see why the fractionally-spaced equalizer is superior to the synchronous equalizer, and this is in its ability to be not affected by aliasing problems and independent of the timing phase. Here then comes the superiority of fractionally-spaced equalizers over the synchronous equalizers.

3.2 THE LEAST MEAN SQUARE (LMS) ALGORITHM

The coefficients of a fractionally-spaced equalizer are updated once per symbol period T, based on the error computed for that symbol. The commonly adopted version of the LMS algorithm for adjusting the tap gains by unbiased gradient estimate is used

$$\mathbf{C}_{k+1} = \mathbf{C}_k + \Delta e_k \mathbf{R}_k \qquad (3.14)$$

Where $\mathbf{C}_k$ is the tap vector at the kth iteration, Δ is a positive number called the step size, $\mathbf{R}_k$ is the received vector defined as

$$\mathbf{R}_k = \{r_0 r_1 \ldots r_k\}^T \tag{3.15}$$

and e_k is the error computed at the kth iteration is given by the following expression

$$e_k = d_k - y_k \tag{3.16}$$

where d_k is the desired signal and y_k is the output signal of the equalizer, defined as

$$y_k = \sum C_i r_{k-i}$$

$$= \mathbf{R}_k^T \mathbf{C} \tag{3.17}$$

The mean-squared error at the output of the equalizer is the performance measure for data transmission systems and is defined as

$$J = E\{e_n^2\} \tag{3.18}$$

When replacing e_n by the expression given by (3.16) and expanding (3.18), the mean-squared error will be then

$$J = E\{d_n^2\} - 2\mathbf{C}^T\mathbf{b} + \mathbf{C}^T\mathbf{A}\mathbf{C} \tag{3.19}$$

where **A** is the channel correlation matrix and **b** is the cross correlation

vector and are defined in (2.10) and (2.11), respectively. It is shown [13], [17] that the channel correlation matrix, **A** , which is Toeplitz for a synchronous equalizer, is no longer Toeplitz for a fractionally-spaced equalizer.

Minimizing J with respect to the tap coefficients, i.e.,

$$\frac{dJ}{d\mathbf{C}} = 0 \tag{3.20}$$

gives the familiar optimum tap coefficients

$$\mathbf{C}_{op} = \mathbf{A}^{-1}\mathbf{b} \tag{3.21}$$

From the above equation we can see that the attractive feature of the LMS algorithm, defined in equation (3.14), is shown in its relative simplicity; it does not require measurements of the pertinent correlations functions, nor does it require matrix inversion.

The corresponding minimum MSE, J_{min} , is given by

$$J_{min} = J - \underline{\mathbf{C}}^{T}\mathbf{A}\underline{\mathbf{C}} \tag{3.22}$$

where $\underline{\mathbf{C}}$ is defined as

$$\underline{\mathbf{C}} = \mathbf{C} - \mathbf{C}_{op} \tag{3.23}$$

The excess MSE is represented in the second term of the right hand side of

equation (3.22). When $\mathbf{C}=\mathbf{C}_{op}$, J_{min} will be exactly equal to J, and the excess MSE will vanish.

Fractional tap spacing could in practice, if one made the tap spacing significantly smaller than T [6], lead to a serious range problem for the element values of **C**, due to the fact that the uniqueness of $\mathbf{C}_{op}$ disappears as the autocorrelation matrix A becomes singular. A simple method for counteracting would be to introduce in (3.14) a rebound mechanism in the form of a small leakage [6]; this is shown in the following expression

$$\mathbf{C}_{k+1}=(1-\beta)\mathbf{C}_k+\Delta e_k\mathbf{R}_k \tag{3.24}$$

by an amount $\beta\mathbf{C}_k$, where

$$\Delta >> \beta > 0 \tag{3.25}$$

An important factor in the speed of the convergence of the LMS algorithm is the choice of the step size Δ

Ungerboeck [6] showed for the same equalizer delay-line length, a conventional equalizer and a fractional tap-spacing equalizer converge at practically the same speed with respect to the MSE, when using the LMS algorithm in updating the tap coefficients. Fastest convergence is generally obtained by using the step-size parameter

$$\Delta_{op} = \frac{1}{N \times E\{|r^2|\}} \tag{3.26}$$

where $E\{|r^2|\}$ is the average power of r(t). This result applies to an equalizer with fractional tap spacing as well.

From [2], [1] we know that, for the known-LMS algorithm to converge, it is required that

$$|1 - \Delta\lambda_i| < 1 \tag{3.27}$$

where $\{\lambda_i\}$ is the set of the N eigenvalues of the channel correlation matrix **A**, or equivalently

$$0 \le \Delta \le \frac{2}{\lambda_M} \tag{3.28}$$

where λ_M is the largest eigenvalue of the channel correlation matrix **A**.

3.3 PERFORMANCE OF FRACTIONALLY-SPACED EQUALIZERS

One important property of an FSE is the insensitivity of its performance to the choice of the sampler phase. This distinction between the conventional synchronous equalizer and fractionally-spaced equalizers can be explained as follows: First, symbol-rate sampling at the input of a T-spaced equalizer causes spectral overlap or aliasing. Second, variation in the sampler phase or timing instant corresponds to a variable delay in the signal path. Thus, changes in the sampler phase strongly influence the effects of aliasing, i.e., they influence the amplitude and delay characteristics in the spectral overlap region of the sampled equalizer input. Therefore, the minimum MSE achieved by the synchronous equalizer is a function of the sampler phase [2]. In particular, when the sampler phase causes cancellation of the band-edge ($f = \pm \frac{1}{2T}$ Hz) components, the equalizer cannot manipulate the null into a flat spectrum at all [2], [6].

In contrast, there is no spectral overlap at the input to an FSE. Therefore, such an equalizer can adjust the channel spectrum (amplitude and phase) at the band-edge regions before symbol-rate sampling at the equalizer output. Hence, the sensitivity of the minimum MSE, achieved with an FSE with respect to the sampler phase, is typically smaller than that achieved with a T-spaced equalizer [2]. Then, data transmission can begin with an arbitrary sampler phase, since the FSE synthesizes the correct delay

during adaptation [16].

Another point is, as Gitlin and Weinstein [17] showed, since the optimum receive filter in a linear modulation system is the cascade of a filter matched to the actual channel, with a transversal T-spaced equalizer. The FSE, by virtue of its sampling rate, can synthesize the best combination of the characteristics of an adaptive filter and a T-spaced equalizer, within the constraints of its length and delay. A synchronous equalizer, with symbol-rate sampling at its input, cannot perform matched filtering. However, an FSE can effectively compensate for more severe delay distortion and deal with amplitude distortion with less enhancement than a synchronous equalizer.

In a comparison, done by [18], between a synchronous equalizer and a $\frac{T}{2}$ fractionally-spaced equalizer for QAM systems with severe band-edge delay distortion, the synchronous equalizer performs noticeably worse than a $\frac{T}{2}$ FSE regardless of the choice of sampler phase.

3.4 SUMMARY

We have given an overview about the synchronous and the fractionally-spaced equalizers and their associated problems, the type of algorithm used in updating the tap coefficients, i.e., the LMS algorithm. The fractionally-spaced equalizer requires more tap coefficients than the synchronous

equalizer, that is more computations needed to update the tap coefficients of the FSE. For the same time span, NT, where T is the symbol period, the synchronous equalizer will need N tap coefficients, whereas an FSE with tap spacing $\frac{T}{2}$ will need (2N) tap coefficients. This will make the FSE with tap spacing $\frac{T}{2}$ more complex than the synchronous equalizer. On the other hand, once it comes to the performance side, the FSE outperforms the synchronous equalizer as far as the sensitivity of the MSE with the choice of the sampler phase is concerned.

Now, we are in a position where we can propose an idea that will be a compromise between complexity and performance. This idea consists of setting some of the tap coefficients of the FSE with tap spacing $\frac{T}{2}$ to zero. Detailed explanation of this idea and its simulation are treated in the coming chapter.

CHAPTER IV

PROPOSED METHOD AND SIMULATION OF THE SYSTEM

The previous chapters have given us an overview about the synchronous equalizer and the fractionally-spaced equalizer. We saw that the fractionally-spaced equalizer required more computations than the synchronous equalizer. A remedy can be made if some of the tap coefficients of the FSE are set to zero. Thus less computations are needed to update the tap coefficients of the FSE at every symbol period, T. Every time that the FSE with some of its tap coefficients are set to zero, a configuration is obtained from the FSE. Then we will call the modified FSE a configuration, that is the proposed method which is presented next.

4.1 PROPOSED METHOD

In this part of the chapter we are going to present the different possible configurations of our proposed method. The idea behind this proposed method is to set some of the tap coefficients of the fractionally spaced

equalizer to zero, with tap spacing $\frac{T}{2}$ as an example (where T is the symbol period), and this is for the purpose of having a time span closer to that of the synchronous equalizer and the performance of an FSE. The distribution of these coefficients, the zero coefficients, is taken from the sampled impulse response of the $\frac{T}{2}$ equalizer. For the new configuration the tap spacing T_i will be confined to

$$T' \leq T_i \leq T \qquad , i=1,2,...,N \tag{4.1}$$

where N is the number of tap coefficients and T′ will be less than T. Figure 4.1 depicts an example of the new idea with $T' = \frac{T}{2}$. Figure 4.2 is exactly identical to figure 4.1. As can be seen from figure 4.1, a reduction by two arithmetic multiplications and two arithmetic additions has occured when tap coefficients C_3 and C_5 have been set to zero.

Many configurations come up in mind. Among these are those which can have some coefficients to be set to zero at the begining of the sampled impulse response of the $\frac{T}{2}$ equalizer, or in the middle (near the main tap), or at the end, or a mixture of these configurations. The zero tap coefficients are neither updated nor entered in the computational process, thus leading to simplified algorithms.

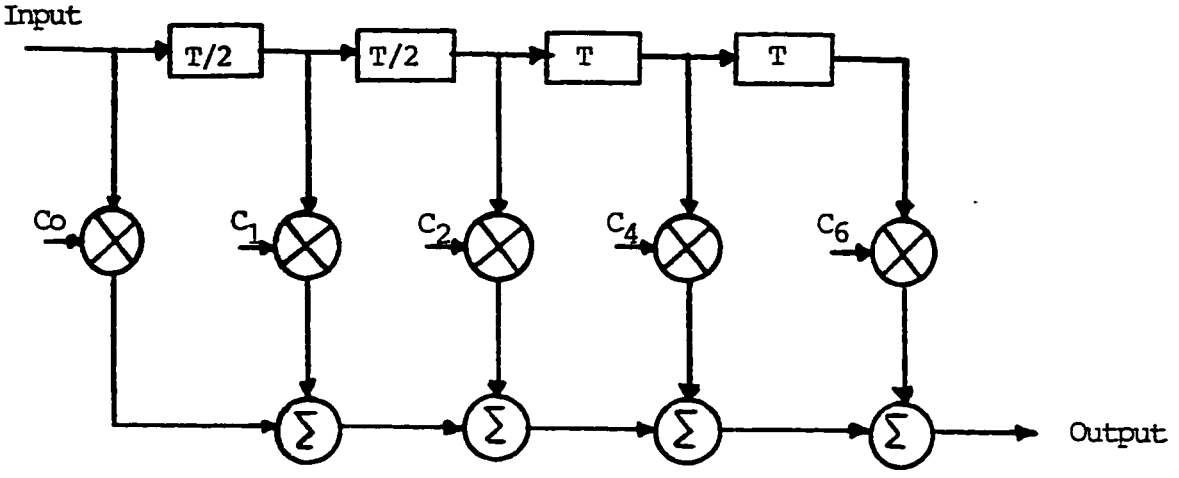

Figure 4.1: Block diagram of the proposed design with $T' = \frac{T}{2}$

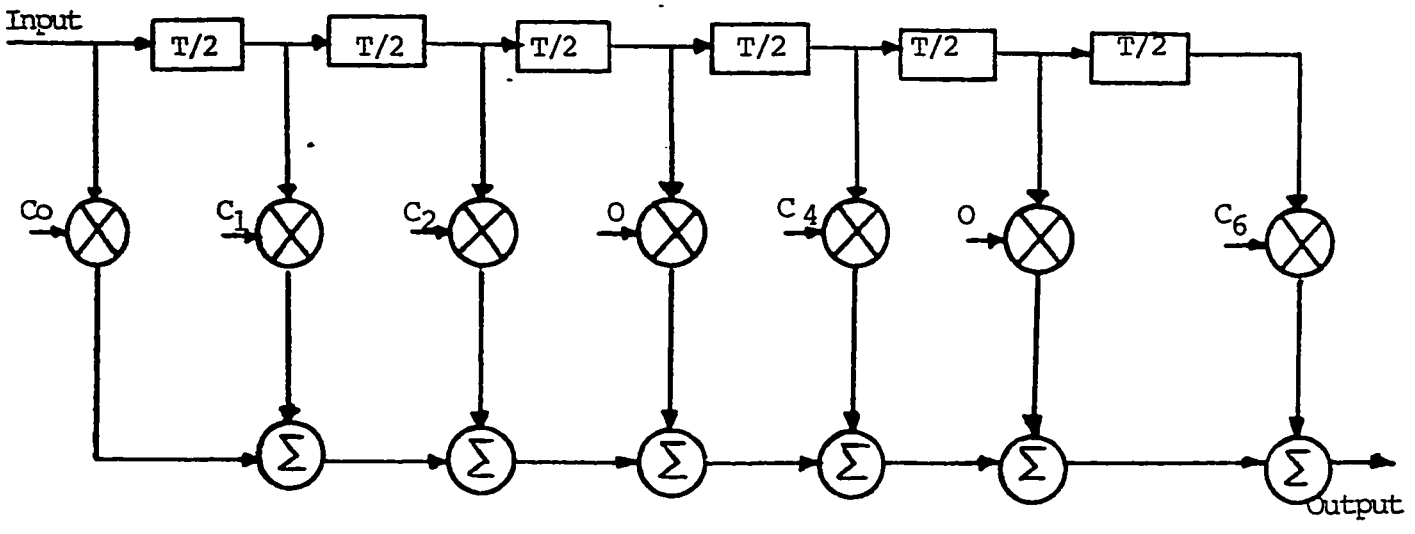

Figure 4.2: Equivalent block diagram to that of Figure 4.1

By no means can one say that this configuration is better than the other one until it has outperformed the different possible ones, or its behaviour is closer to that of an FSE. The performance evaluation is based on the residual MSE and specifically the sensitiveness of the MSE due the sampler phase. Computation and implementation complexity are taken into account, too.

The output of all configurations will be given by

$$y_n = \sum_{k=0}^{N-1} C_k r(nT - \frac{kT}{2}) \tag{4.2}$$

with some of the tap coefficients C_k being zeros. The coefficients of this new configuration are updated once per symbol period T, and this is based upon the error computed for that symbol. This is done through the commonly adopted version of the LMS algorithm for adjusting the tap gains by unbiased gradient estimate given by equation (3.5).

In this work, we are going to investigate the performance of this proposed idea. First, let us have an overlook about the overall system and investigate the T and the $\frac{T}{2}$ equalizers, the proposed method will be treated later.

4.2 SIMULATION OF THE SYSTEM

4.2.1 The overall system

The block diagram shown in figure 4.3 illustrates the basic elements of the overall system that will be considered in the study of the proposed method. The transmitted signal consists of a Pseudo-Noise (PN) sequence generator. More details are given about PN sequences in the next section. The output of the channel is the response of this channel to the transmitted signal. The sampled impulse response of this channel is assumed to be spaced by T (the symbol period). This output is added to an additive white Gaussian noise with zero mean and controllable variance to give the desired Signal to Noise Ratio (SNR). This will result in the receive signal. The signal to noise ratio here is defined to be the ratio of the average power of the transmitted signal to the average power of the noise.

Given that the channel impulse response and the transmitted signal are spaced by T, the symbol period, data sampled at lower rate are needed during this simulation process. Then an interpolating scheme will solve the problem in obtaining these samples.

An interpolating scheme is used to derive points sampled at a rate of $\frac{16}{T}$. This is due to the need for samples spaced at $\frac{T}{2}$. It will be used also in the evaluation of the mean-square-error as a function of the sampler phase.

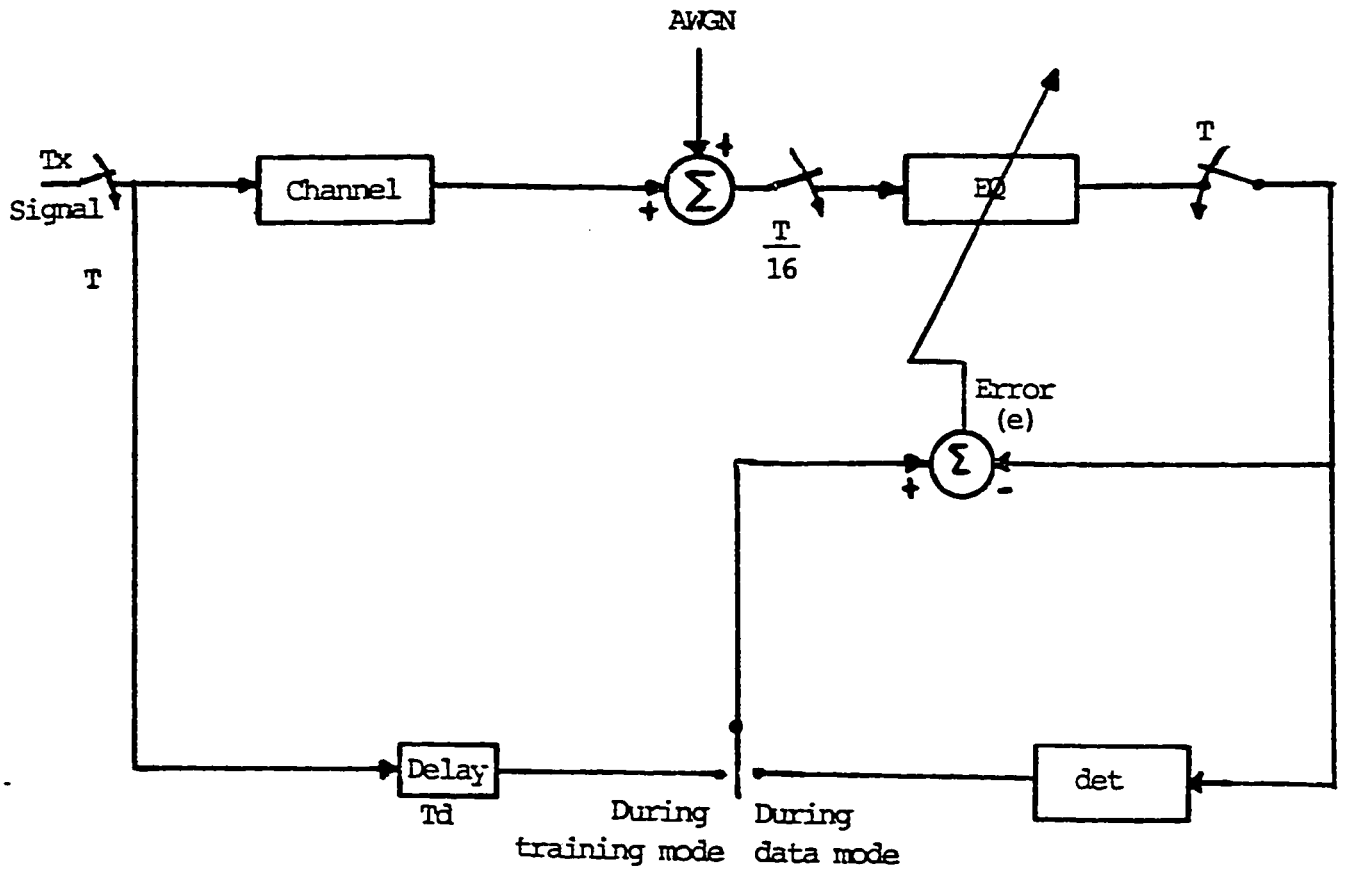

Figure 4.3: Block diagram of the overall system.

The equalizer here, could be a synchronous equalizer, or a fractionally-spaced equalizer, or one of the proposed configurations. The output of each equalizer under study is obtained at every symbol period T, and the tap coefficients of each one of them are updated at every symbol period too. An error is calculated between each transmitted symbol and the corresponding received element. This error is used in updating the tap coefficients and in the evaluation of the MSE.

During the training mode, the unit delay (T_d) is used to determine the location of the equalizer main tap. The phase of the sampling period as well as the unit delay is made under program control.

4.2.2 PN Generator

For synchronization problems a random sequence is needed. Among these random sequences is the maximum-length sequence, also referred to as pseudo-noise (PN) sequence, which is a cyclic binary sequence generated by a feedback shift register. A shift register of degree m is a device consisting of m consecutive memory stages clocked by a single clock. At each clock pulse, the state, represented by binary symbol 1 or 0, of each memory stage is shifted to the next stage down the line. In order to prevent the shift register from getting empty by the end of m clock pulses, a logical Boolean function of the states of the m memory stages is used to compute a feedback term that is applied to the first memory stage of the shift register. An m-stage

shift register with linear feedback is illustrated in figure 4.4.

The sequence generated by this sequence is periodic [4] with period given by

$$L = 2^m - 1 \tag{4.3}$$

where m is the degree of the shift register. We see from equation (4.3) that the longer the degree of the shift register, the longer the period will be.

Figure 4.5 shows the shift register used in the simulation with m = 23. If X(I) represents the state of memory I, then the input to memory 1 is given by the following relation

$$X(1) = 1 + X(5) + X(23) \tag{4.4}$$

where + here is modulo-two addition. Equation (4.4) is the answer mode modem generating polynomial of the V.32 [19].

If the symbols 1 and 0 are represented by the values +1 and -1, respectively, we find that the autocorrelation of a PN sequence is periodic [4], [20] with period LT, where T is the symbol duration of symbols 1 and 0, and it is defined as the following

$$R(\tau) = \begin{cases} (1 - \frac{|\tau|}{T}) & , \quad |\tau| \le T \\ 0 & , \quad \text{elsewhere} \end{cases} \tag{4.5}$$

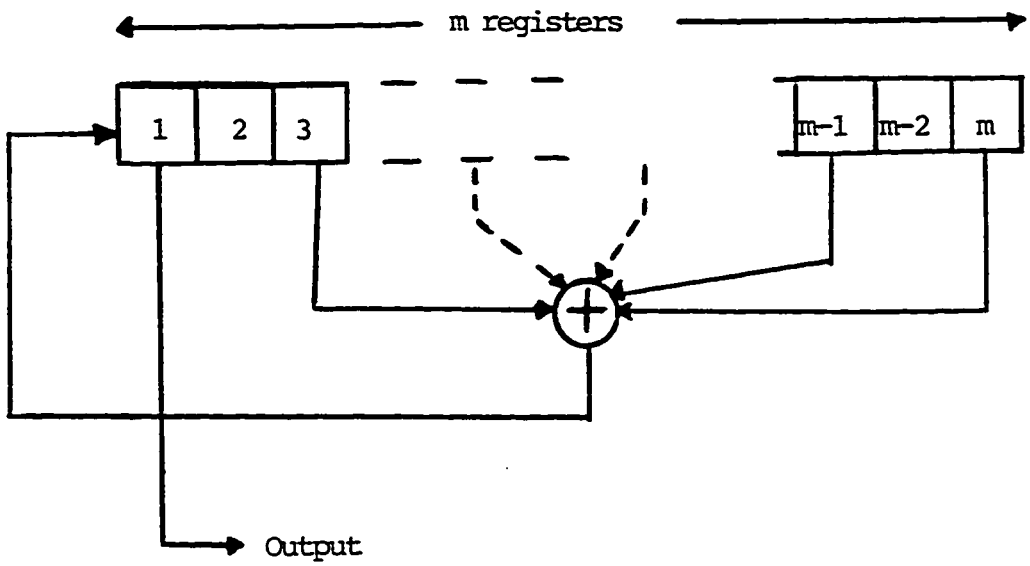

Figure 4.4: m-stage shift register.

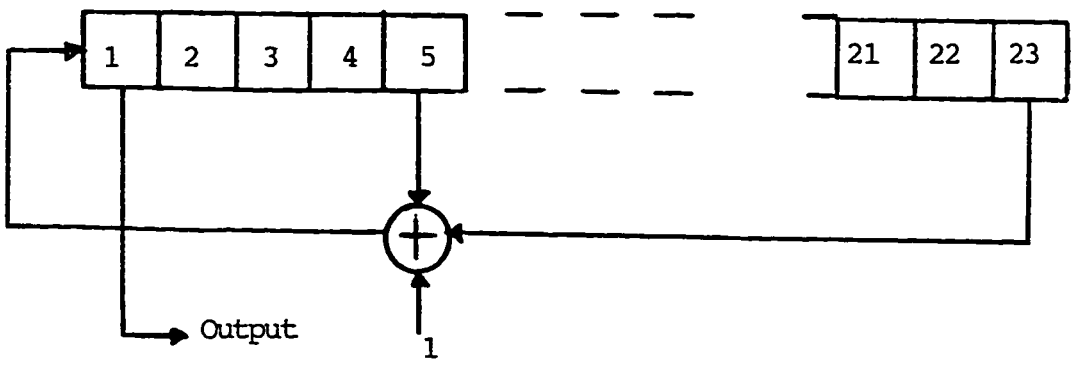

Figure 4.5: 23-stage shift register used in the simulation.

its graph is depicted in figure 4.6.

4.2.3 Interpolation

In some applications, it is necessary to increase the effective sampling frequency (f_s) of a discrete signal. Two methods can be used in doing this scheme. One way is to convert the signal from digital to analog and resample the latest signal at the desired new rate. This technique, however, is expensive and introduces many potential sources of noise and distortion [21]. The second approach is performed by means of digital signal processing. The process of increasing the sampling rate by a factor L, positive integer, is called interpolation.

In numerical analysis, interpolation of arbitrary functions is often done by fitting polynomials to some number of discrete values. However, in digital signal processing, the sampled signals must be bandlimited, and this additional constraint on the signal spectrum implies that lowpass filtering is the appropriate method of interpolation for theses signals [21].

The operations required to implement interpolation become clear in the frequency domain as illustrated in figure 4.7, where X(f) and X'(f), the transforms of x(n) and x'(n), respectively, are both depicted. Here, the new sampling frequency f'_s is four times the original frequency f_s. This process requires the insertion of three zeros between each pair of consecutive samples x(n) and x(n-1). Then as shown in figure 4.7, this modified signal is

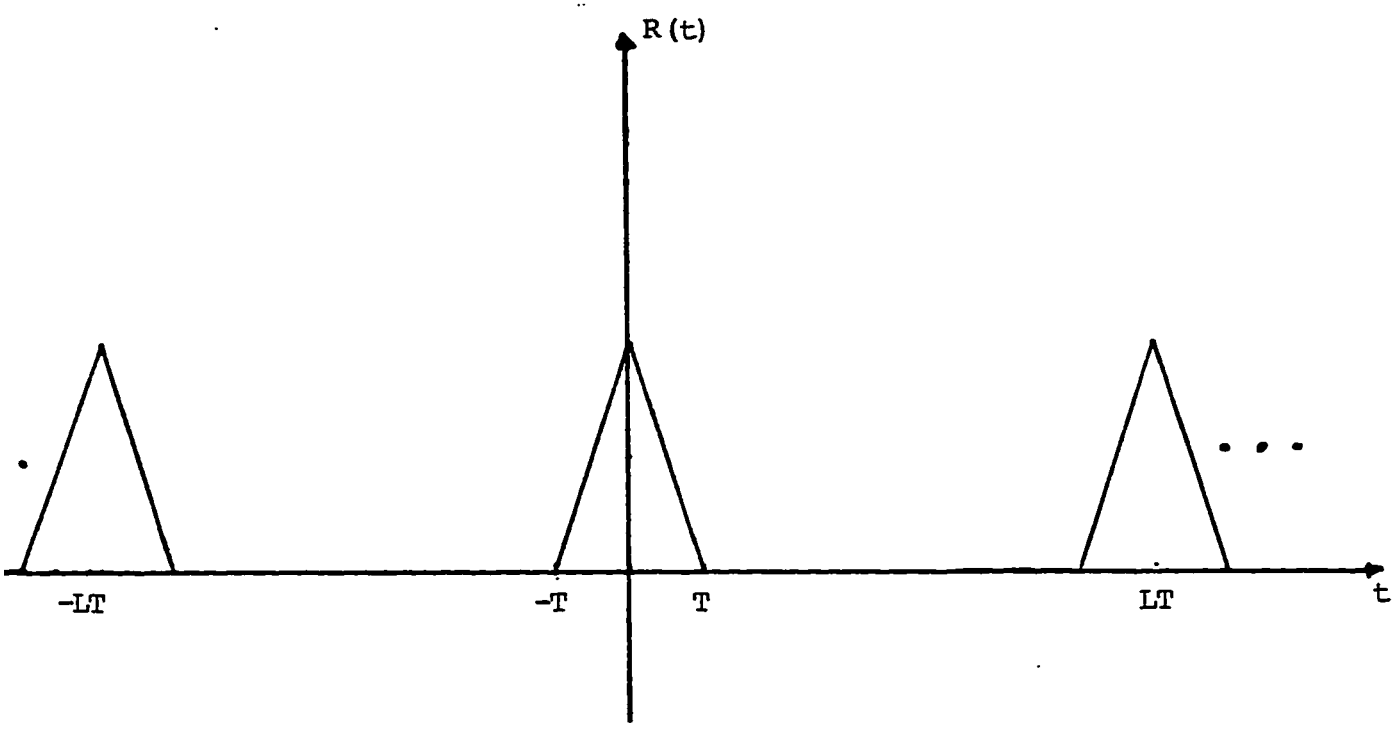

Figure 4.6: Autocorrection of a PN sequence.

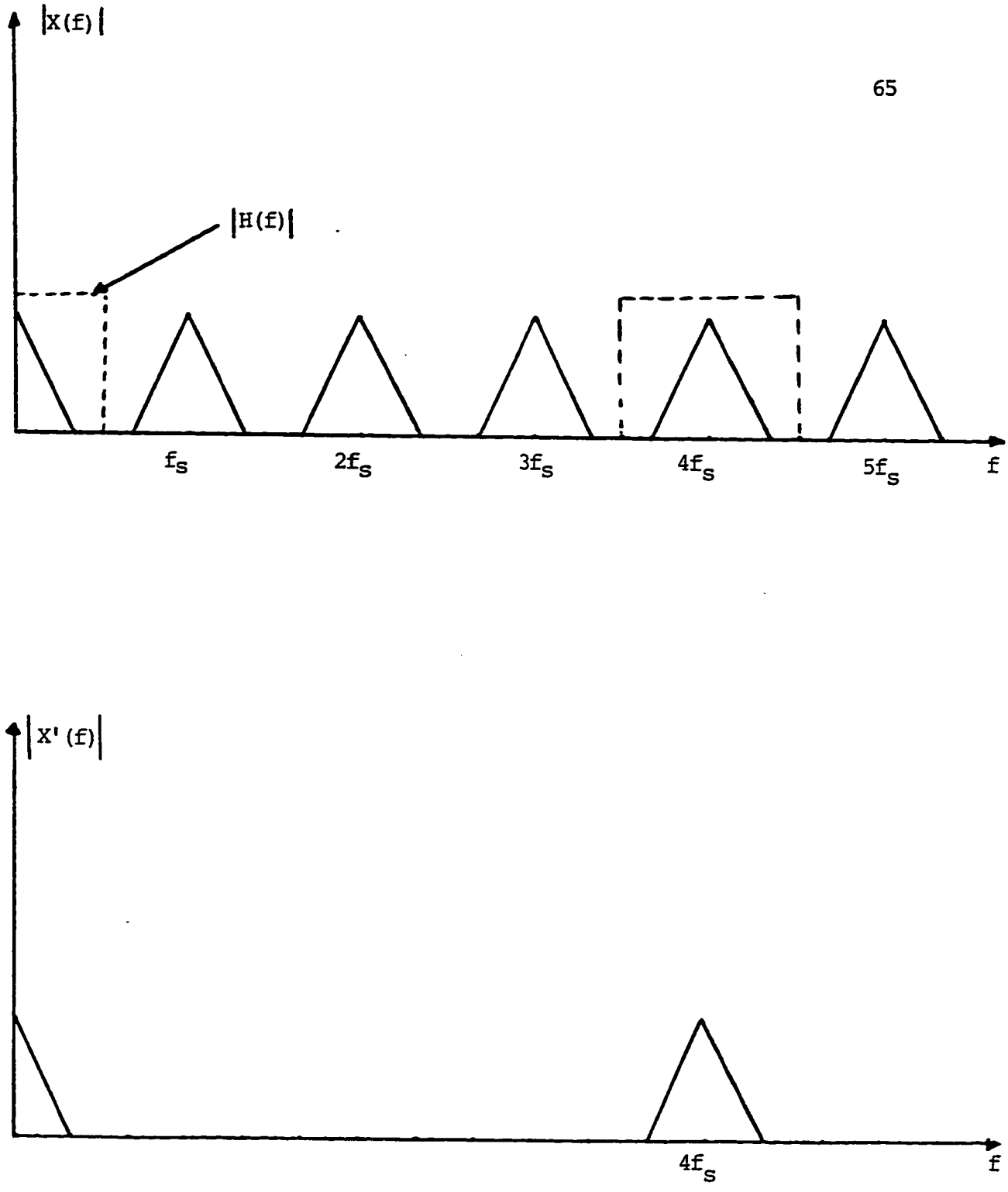

Figure 4.7: Frequency-domain illustration for L=4

now lowpass filtered by H(f), with f'_s being the new rate of operation, to produce the interpolated signal x'(n) with spectrum X'(f). The overall interpolating system is depicted in figure 4.8. The lowpass filter is in general a direct form FIR filter.

For the implementation of the interpolation scheme we will give an example for L=2, and then generalize it. Interpolating by 2 is equivalent to insert a zero between each pair of samples x(n) and x(n-1). Then have a lowpass filter with a certain number of coefficients; say eight coefficients. Now, two outputs will be produced at time $(n\frac{T}{2})$ and at time $\{(n+1)\frac{T}{2}\}$ if the original samples where sampled at T. The zeros are not involved in the calculation process, thus a simplified procedure will result. The outputs are shown in figure 4.9. As can be seen figures 4.9.a and 4.9.b are equivalent and so are figures 4.9.c and 4.9.d. These two implementations are equivalent to the implementation depicted in figure 4.10, where two banks of filters are set up to give two outputs sampled at $\frac{T}{2}$ and spaced by one in time.

This was the case when L=2. In general for a certain number of interpolated points (L), the configuration of the lowpass filter will look like the one shown in figure 4.11, with L banks.

In the case of our design we had to interpolate by sixteen. To do this, we had to use a lowpass filter with a sampling frequency four times the original sampling frequency, and then cascading the same lowpass filter to

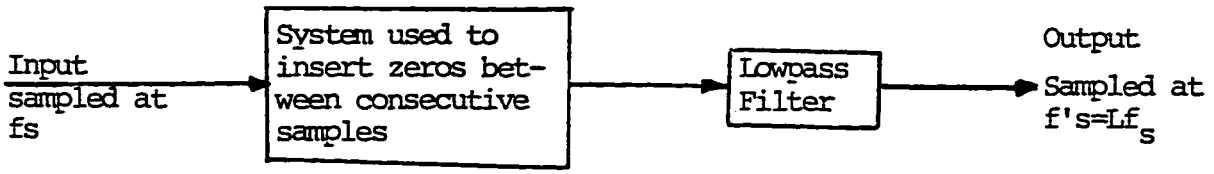

Figure 4.8: Overall system for interpolation.

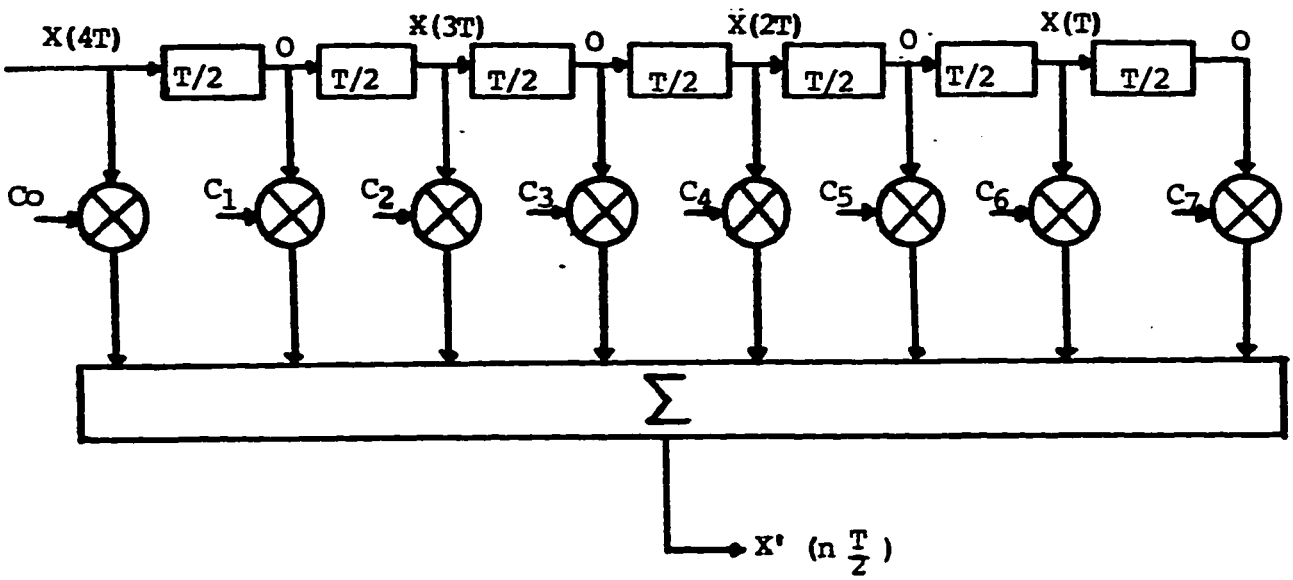

Figure 4.9a: Output at time $n\frac{T}{2}$ for the interpolating system.

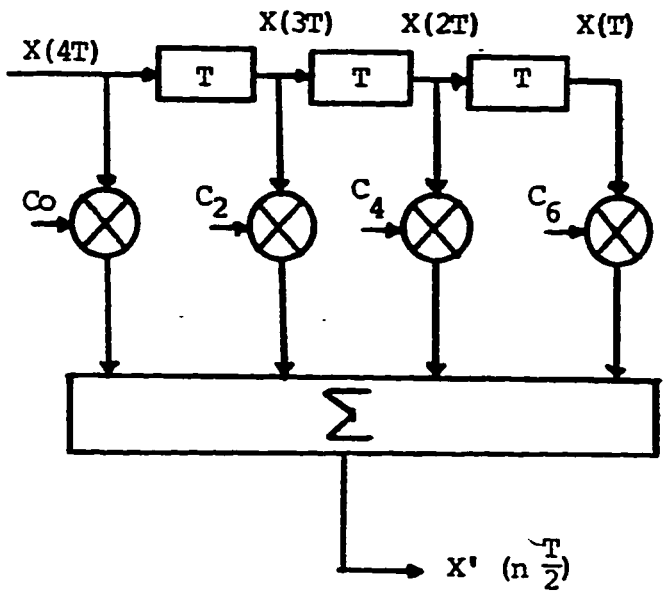

Figure 4.9.b: Equivalent configuration to that of Figure 4.9.a

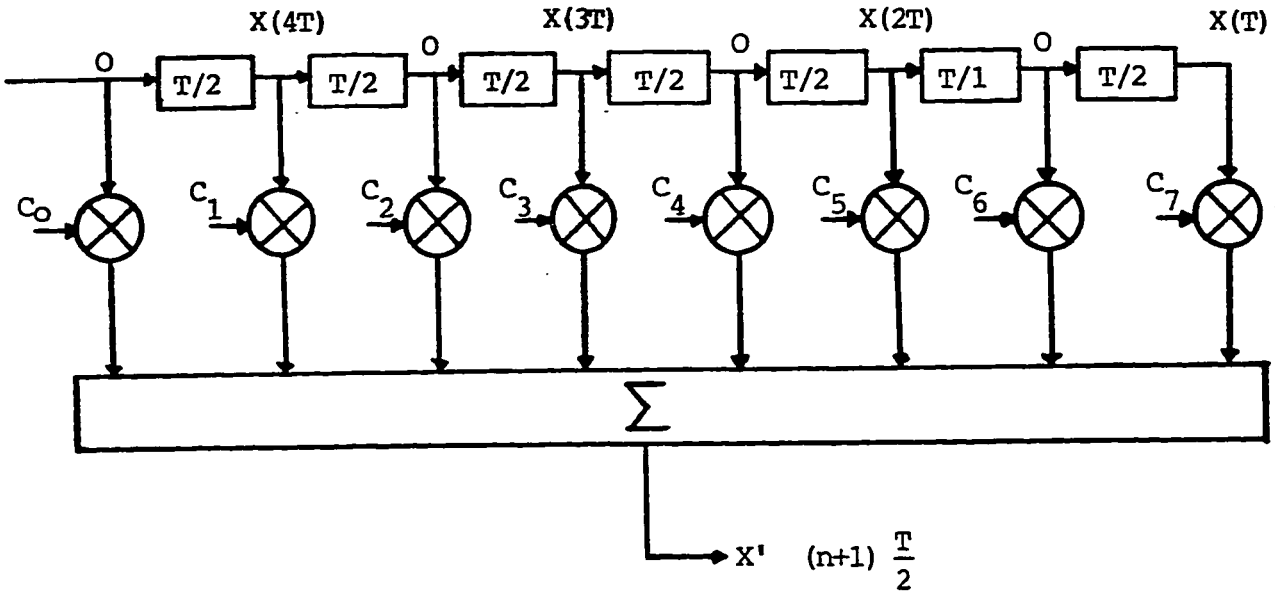

Figure 4.9.C: Output at time (n+1) $\frac{T}{2}$ for the interpolating system.

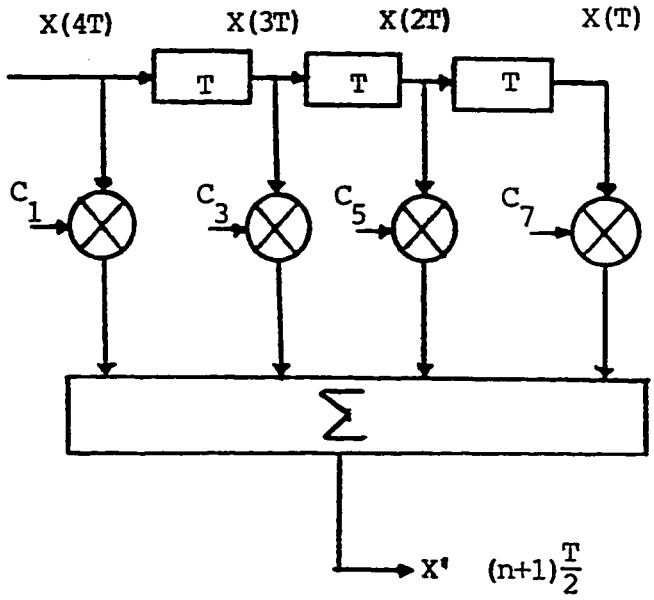

Figure 4.9.d: Equivalent configuration to that of Figure 4.9.C

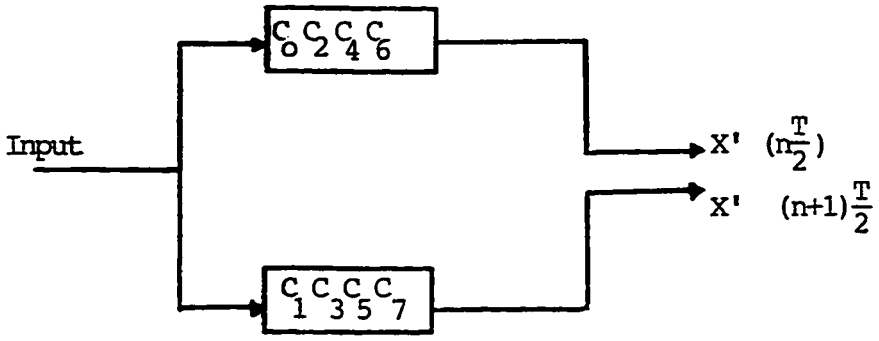

Figure 4.10: Equivalent implement to those of Figure 4.9

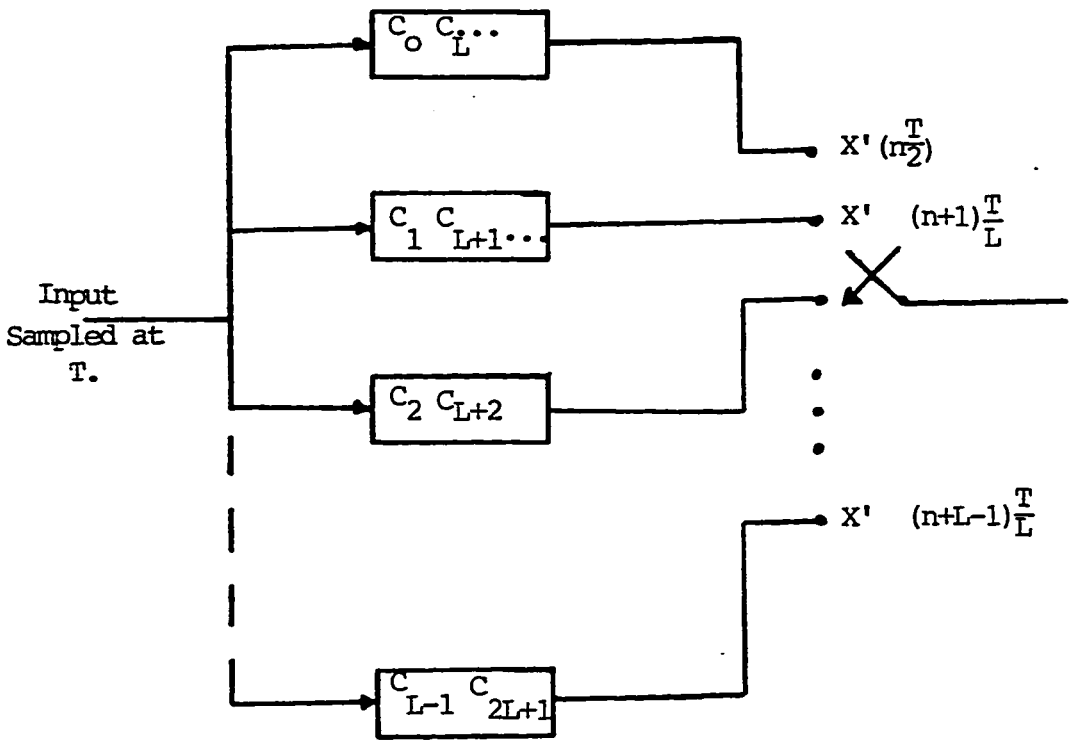

Figure 4.11: General configuration of interpolating system.

give an overall sampling frequency of sixteen times the original one. Then, we can see that the process is done in two stages. Each stage consists of interpolating by 4. This is depicted in figure 4.12. The filter designed was chosen to be an FIR filter with 64 coefficients.

Figures 4.13.a and 4.13.b show the input and output, respectively, of the designed lowpass filter used in the implemented system.

Since the overall system is well defined, and every part of the system is elaborated in details, then we can use this system to study the synchronous equalizer, the FSE, and the proposed method. Let us start with a comparison between a T equalizer and $\frac{T}{2}$ equalizer.

4.2.4 Comparison between T and $\frac{T}{2}$ equalizers

Before we try to investigate the new proposed method, let us investigate first the T and $\frac{T}{2}$ equalizers, so that a comparison between the proposed method and these equalizers can be made.

In this section we will try to investigate the performance of each one of the equalizers. This is regarding the convergence rate, the MSE with respect to the sampler phase, and the effect of the MSE due to the position of the main tap. Different SNR's are considered in the analysis.

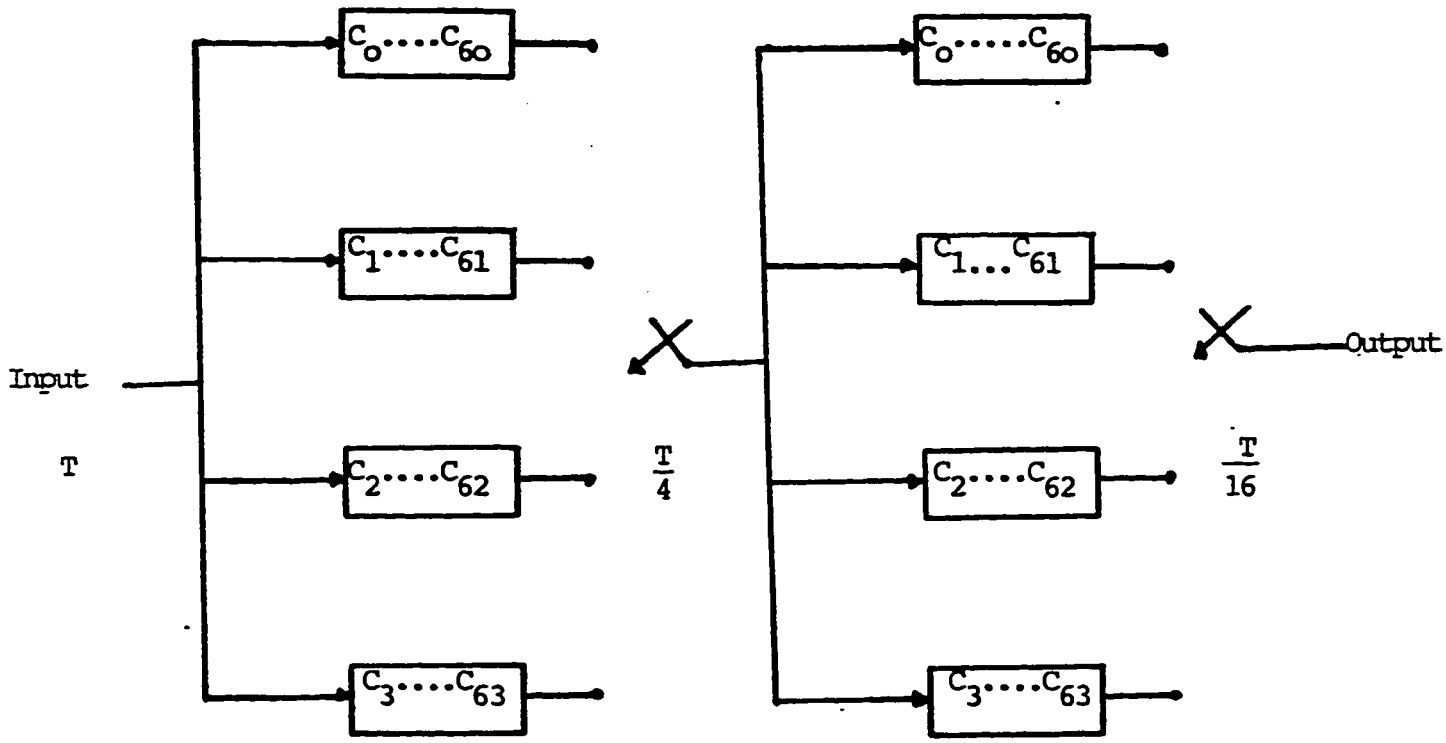

Figure 4.12: Configuration used in the simulation.

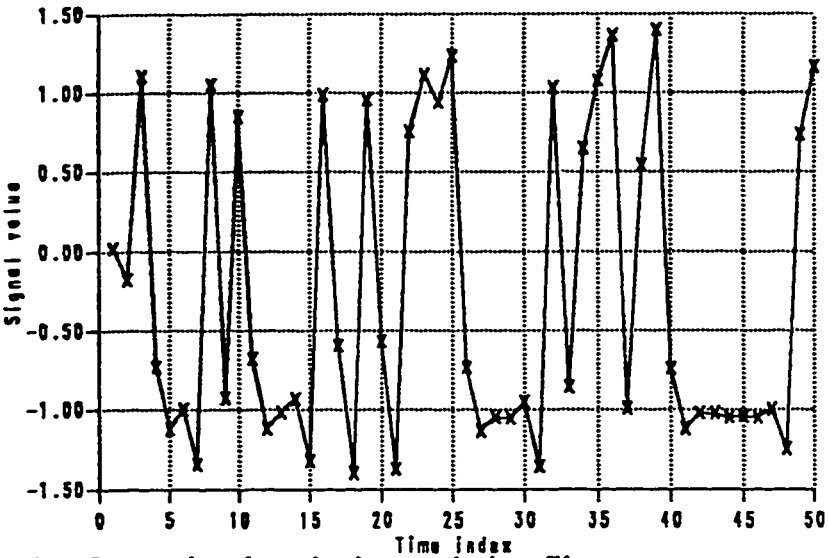

Figure 4.13.a: Input signal to the interpolating filter.

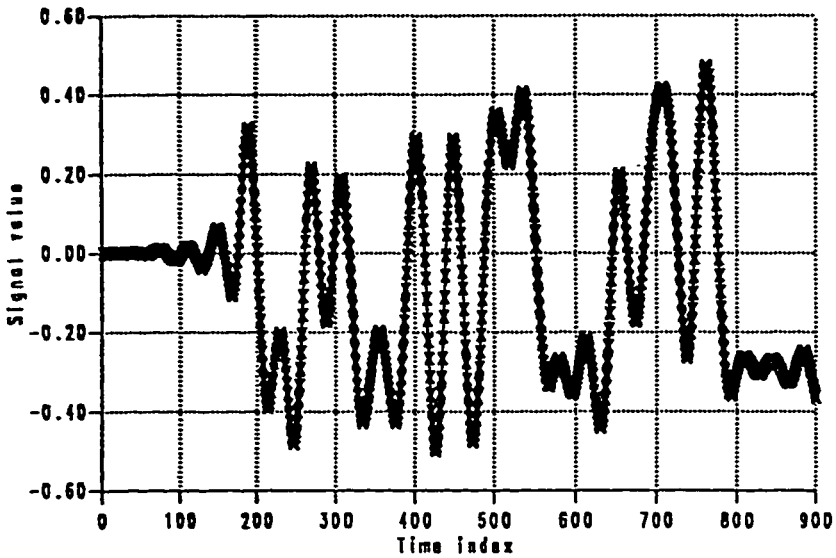

Figure 4.13.b: Output signal from the interpolating filter.

The channel considered in this study is the one chosen by Lucky [1]. The sampled impulse response of this channel is given by {0.04,-0.15,1.0,0.2,-0.05}. The T equalizer was chosen to have 15 coefficients whereas the $\frac{T}{2}$ equalizer had 29 coefficients only so that a total delay of 14T was spanned by both equalizers, where T is the symbol period.

A random sequence of polar binary data symbols (± 1) was transmitted over the channel which in the receiver was available as an ideal reference signal. The MSE represents the result of averaging e_n^2 over 50 runs, where e_n is the error at time nT. Each run started at $n=1$ and tap coefficients exhibit zero values. The LMS algorithm was chosen to update the tap coefficients at every symbol period, which is given by equation (2.21).

Three important factors are investigated in this analysis. These are the effect of the location of the main tap on the the MSE, the convergence rate, and the effect of the sampler phase on the MSE.

In the case where the main tap was in the right position, i.e., the center of the impulse response, the MSE versus the number of iterations, with an SNR of 30 dB, both equalizers converged approximately on the same speed. A step size of 0.06 and 0.031 was chosen to the T equalizer and the $\frac{T}{2}$ equalizer, respectively. Both of these values satisfy equation (2.27). We shall see shortly that the MSE versus the number of iterations converges after iteration 400 has occured. Then, the average MSE is taken here for

only the last 400 iterations, in a total 1000 iterations, that is after convergence has been reached. This has given 0.0549 and 0.0508 for the T equalizer and the $\frac{T}{2}$ equalizer, respectively. The same thing was repeated for an SNR of 20 dB and 10 dB. These values are tabulated in table 4.1. The values obtained for the case of 20 dB are 0.0591 and 0.0558 for the T equalizer and the $\frac{T}{2}$ equalizer, respectively, and 0.1042 for the T equalizer and 0.0994 for the $\frac{T}{2}$ equalizer in the case of 10 dB. Figures 4.14 through 4.19 show the simulation results for the above mentioned cases.

Now let us change the position of the main tap from the central position and see what would happen to the MSE. Starting with a position for the main tap in the begining of the sampled impulse response of the equalizer, as depicted in figures 4.20.b and 4.21.b, has given the following results. For an SNR of 30 dB the average MSE was 0.0569 for the T equalizer while it was only 0.0542 for the $\frac{T}{2}$. Figures 4.20.a and 4.21.a depict the behavior of the MSE with respect to the number of iterations. From these results we see that a change in the position of the main tap will result in a larger amount of the MSE at the equalizer output.

If, however, the main tap is moved to the end of the sampled impulse response as shown in figures 4.22.b and 4.23.b with an SNR of 30 dB, the average MSE is found to be equal to 0.0886 and 0.0658 for the T equalizer

SNR / Equalizer	10 dB	20 dB	30 dB
T	0.1042	0.0591	0.0549
T/2	0.0994	0.0558	0.0508

Table 4.1: Average MSE for T and T/2 equalizers with different SNR's.

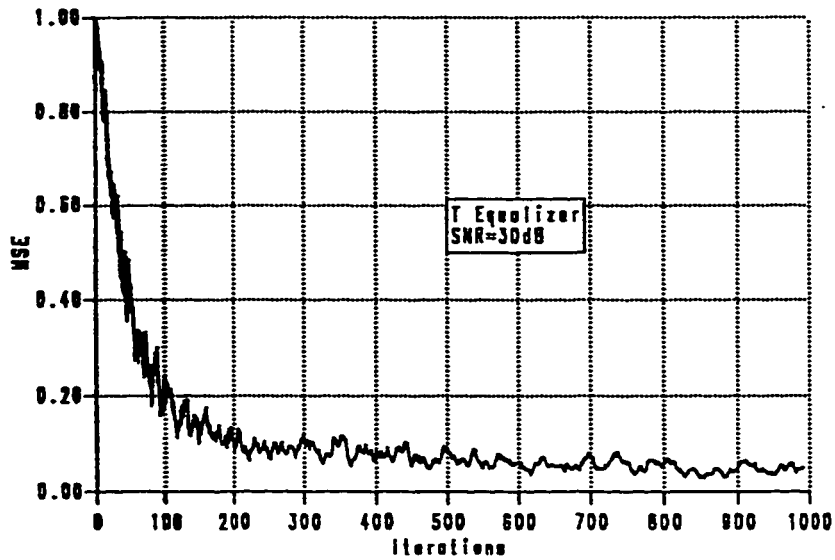

Figure 4.14.a: MSE using the LMS algorithm for the T equalizer with SNR = 30 dB.

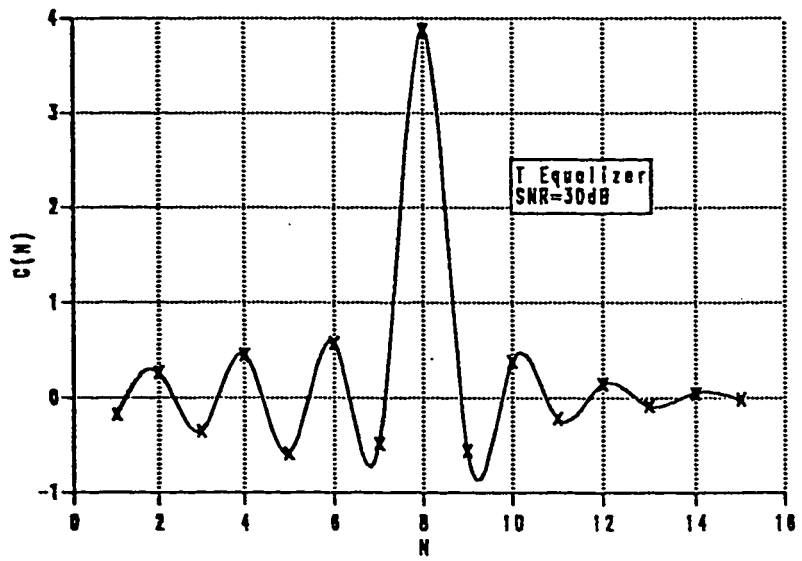

Figure 4.14.b: Sampled impulse response of the T equalizer with SNR = 30 dB.

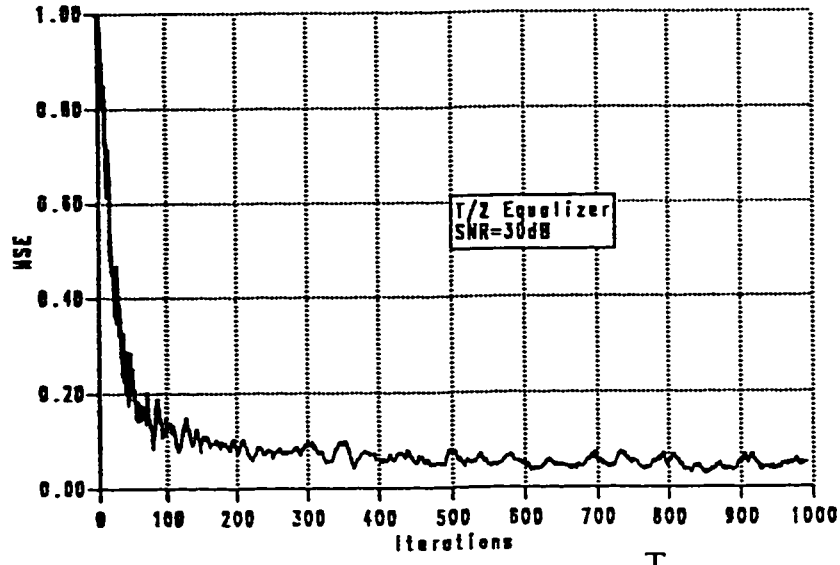

Figure 4.15.a: MSE using the LMS algorithm for the $\frac{T}{2}$ equalizer with SNR = 30 dB.

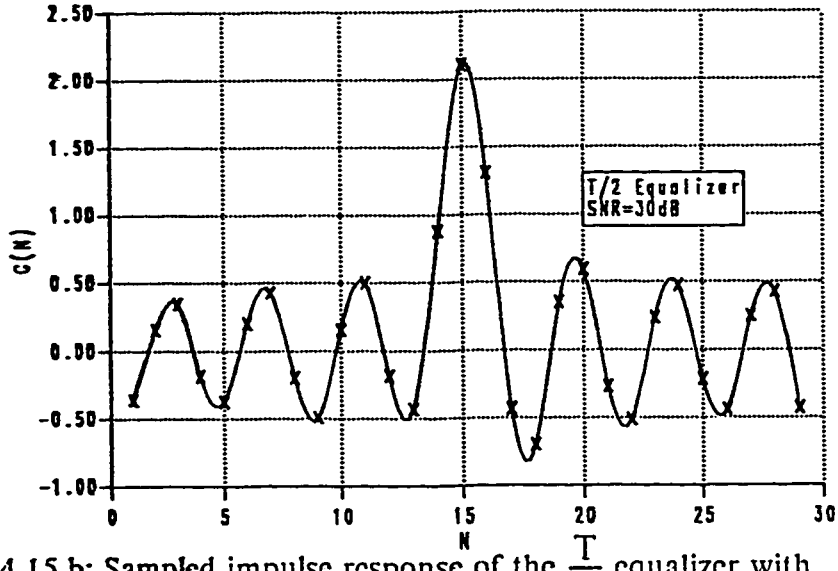

Figure 4.15.b: Sampled impulse response of the $\frac{T}{2}$ equalizer with SNR = 30 dB.

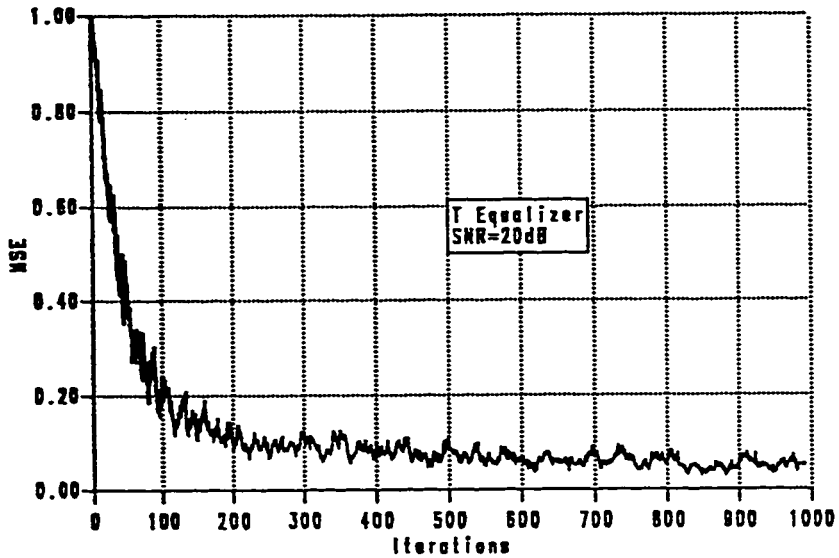

Figure 4.16.a: MSE using the LMS algorithm for the T equalizer with SNR = 20 dB.

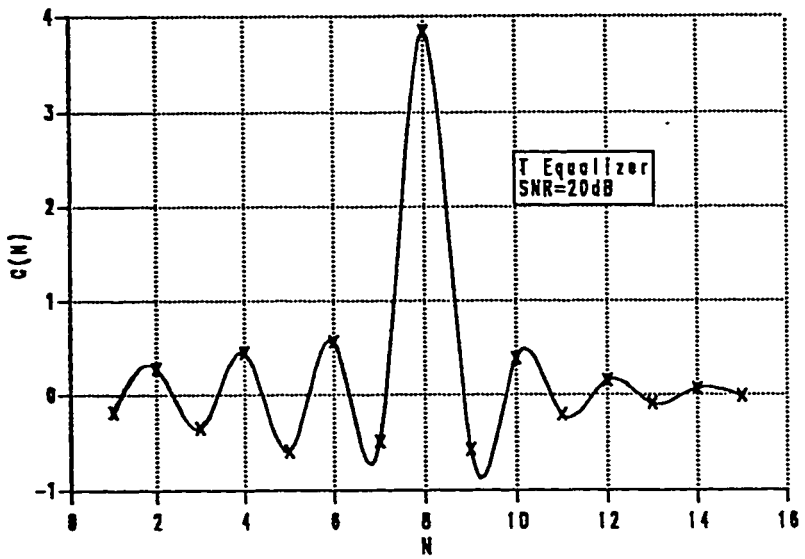

Figure 4.16.b: Sampled impulse response of the T equalizer with SNR = 20 dB.

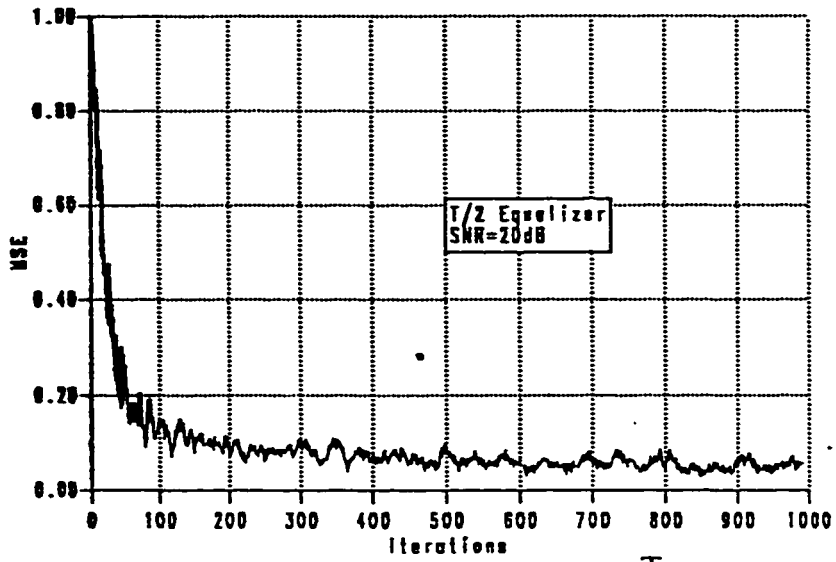

Figure 4.17.a: MSE using the LMS algorithm for the $\frac{T}{2}$ equalizer with SNR = 20 dB.

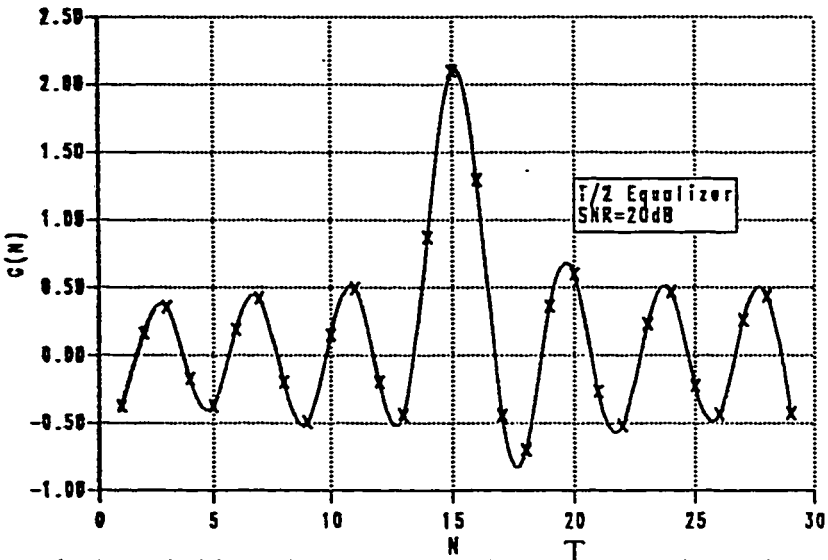

Figure 4.17.b: Sampled impulse response of the $\frac{T}{2}$ equalizer with SNR = 20 dB.

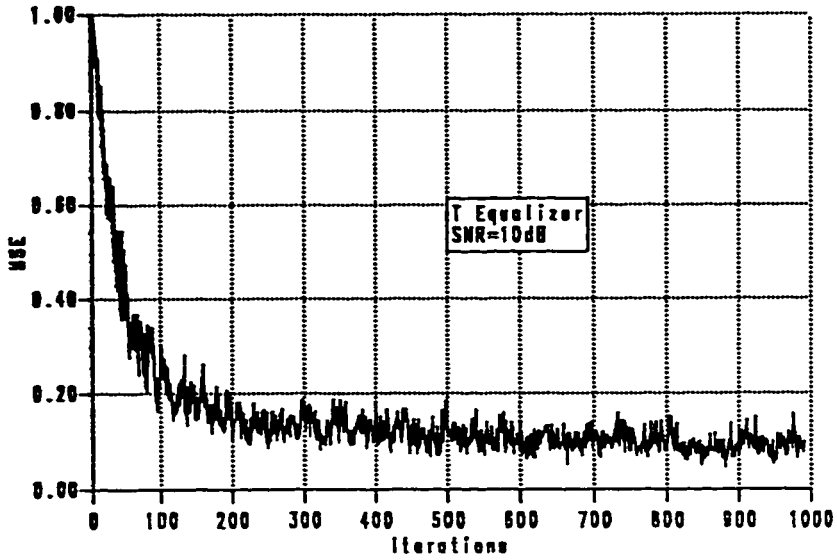

Figure 4.18.a: MSE using the LMS algorithm for the T equalizer with SNR = 10 dB.

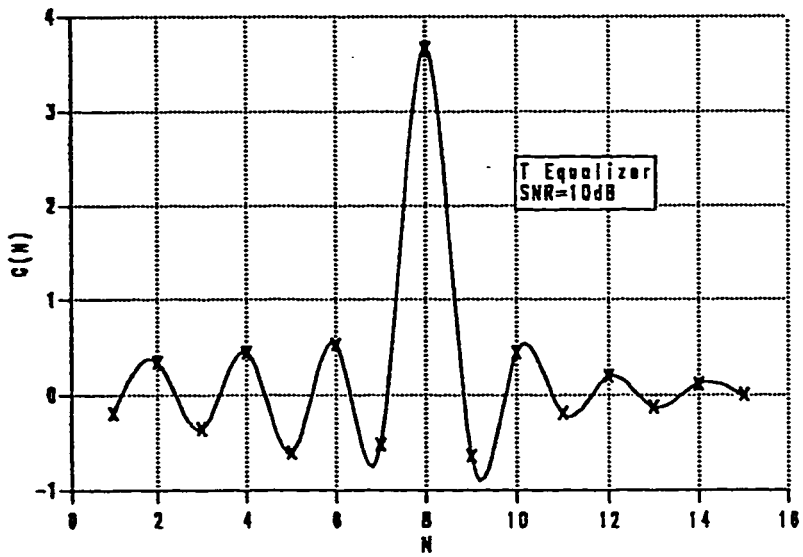

Figure 4.18.b: Sampled impulse response of the T equalizer with SNR = 10 dB.

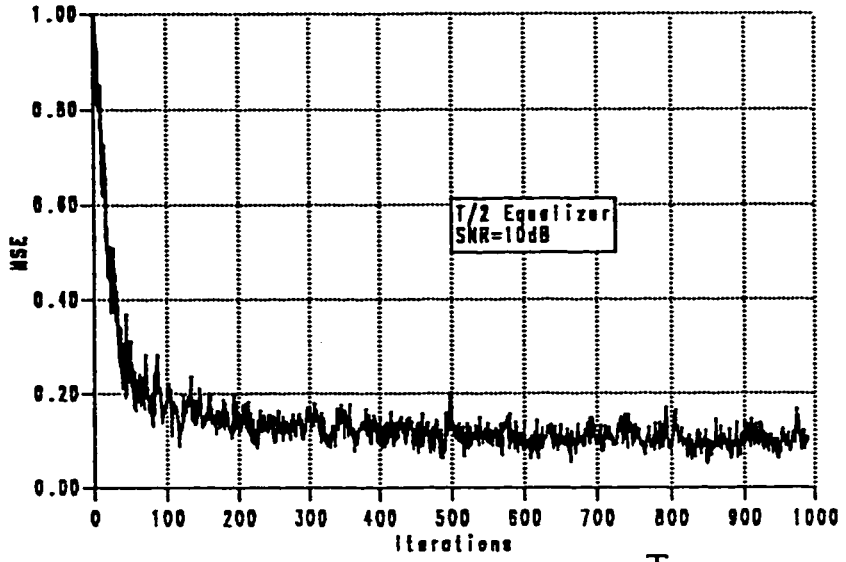

Figure 4.19.a: MSE using the LMS algorithm for the $\frac{T}{2}$ equalizer with SNR = 10 dB.

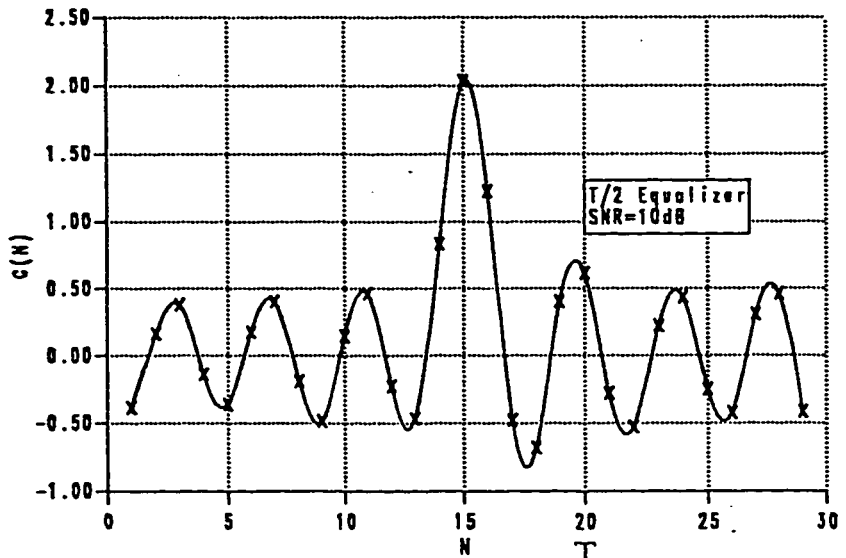

Figure 4.19.b: Sampled impulse response of the $\frac{T}{2}$ equalizer with SNR = 10 dB.

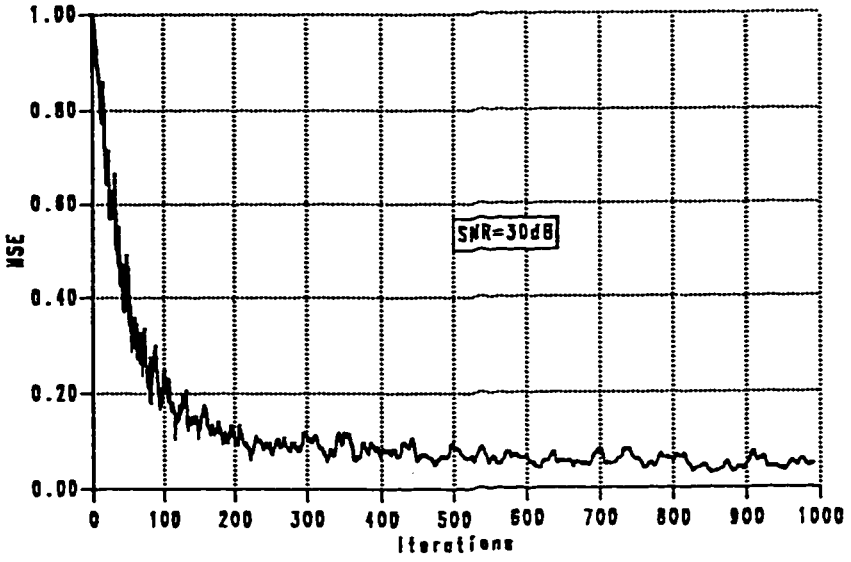

Figure 4.20.a: MSE using the LMS algorithm for the T equalizer with main tap moved from main position and SNR = 30 dB.

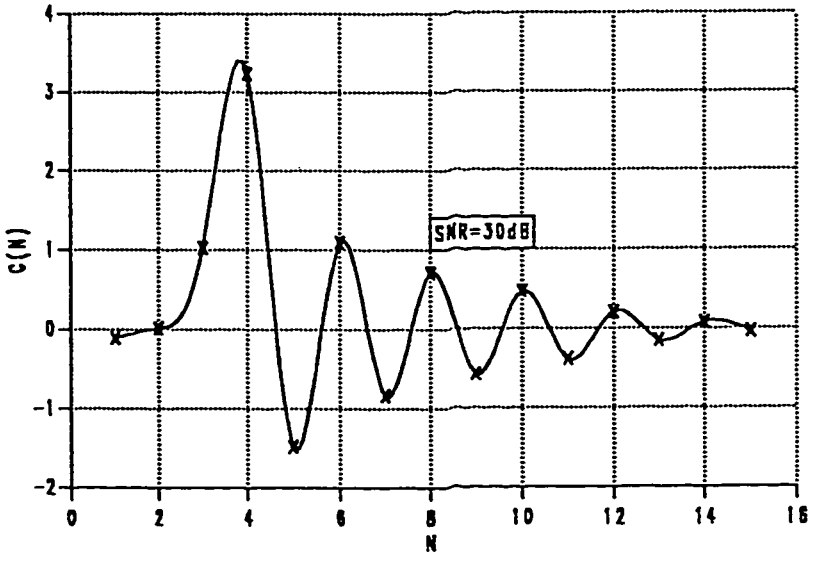

Figure 4.20.b: Sampled impulse response of the T equalizer with main tap moved from main position and SNR = 30 dB.

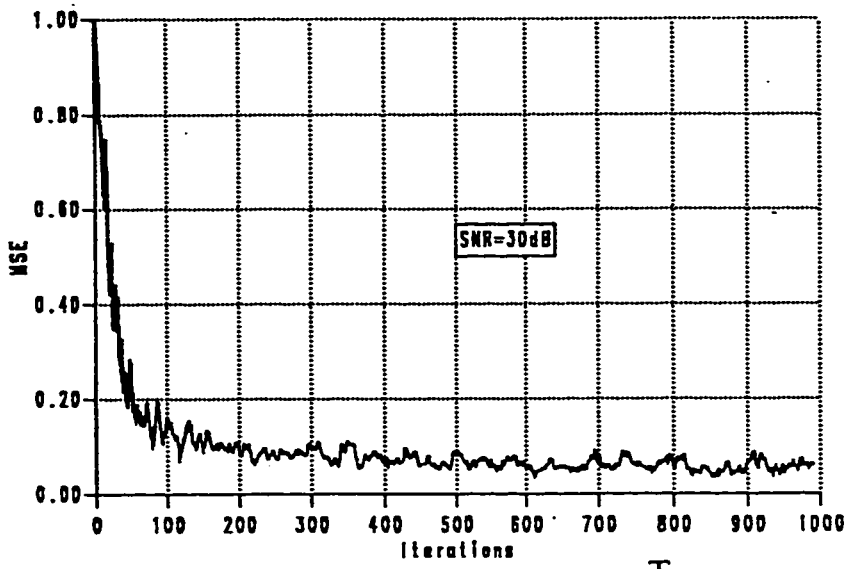

Figure 4.21.a: MSE using the LMS algorithm for the $\frac{T}{2}$ equalizer with main tap moved from main position and SNR = 30 dB.

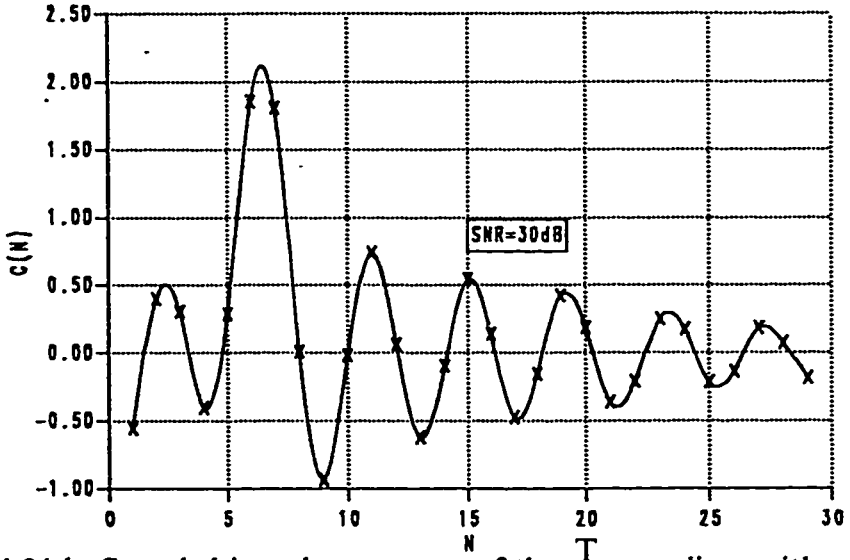

Figure 4.21.b: Sampled impulse response of the $\frac{T}{2}$ equalizer with main tap moved from main position and SNR = 30 dB.

and the $\frac{T}{2}$ equalizer, respectively. The MSE with respect to the number of iterations for both equalizers are shown in figures 4.22.a and 4.23.a. The same thing can be said here, as for those figures 4.20 and 4.21, when the main tap of the equalizer was moved to the begining of the sampled impulse response of the equalizer. But one can notice a difference when the main tap is at the end of the sampled impulse response of the equalizer, the value of the MSE is much greater than that when this last one is at the begining of the equalizer. This could be explained as follow, since the main tap is set at the end then equalization is not effective, whereas when it is at the begining equalization is more or less effective. Hence, perfect equalization is effective if and only if the main tap of the equalizer is at the center of the sampled impulse response of the equalizer for the channel considered here.

we can see from the above analysis that the $\frac{T}{2}$ equalizer in general outperforms the T equalizer. In all the cases studied whether the main tap was in the center of the impulse response, or at the begining of the impulse response, or at the end of the impulse response, the $\frac{T}{2}$ has exhibited its superiority over the synchronous equalizer. Above all, the $\frac{T}{2}$ equalizer outperforms the synchronous equalizer at low signal to noise ratio's, too. This is all to show that the $\frac{T}{2}$ equalizer is in fact the equalizer of the future. But one has to find a get away of its complexity.

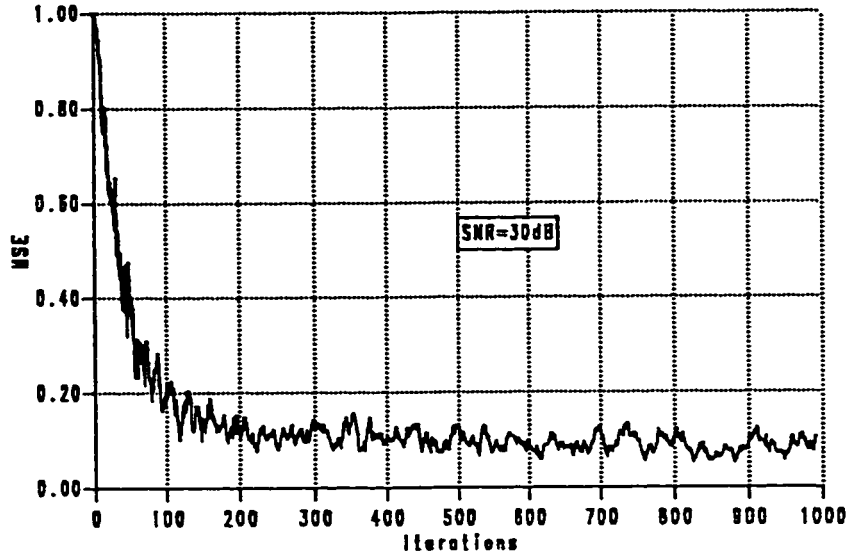

Figure 4.22.a: MSE using the LMS algorithm for the T equalizer with main tap moved from main position and SNR = 30 dB.

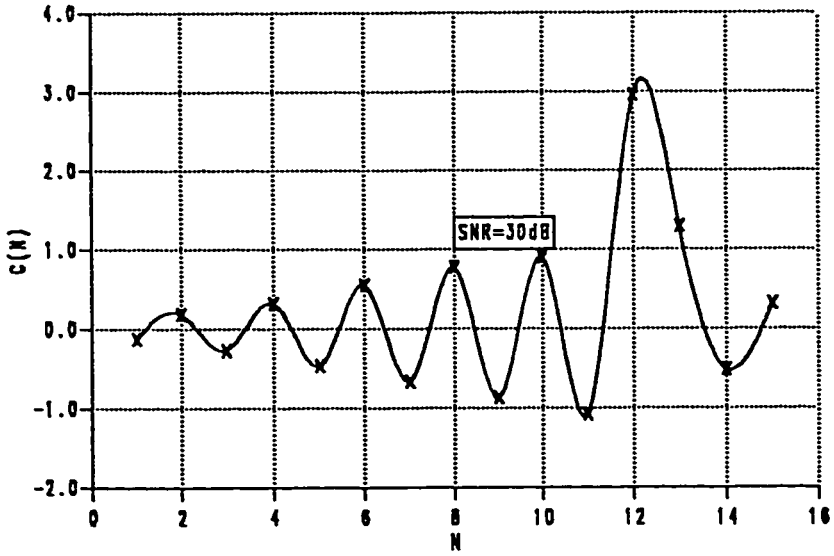

Figure 4.22.b: Sampled impulse response of the T equalizer with main tap moved from main position and SNR = 30 dB.

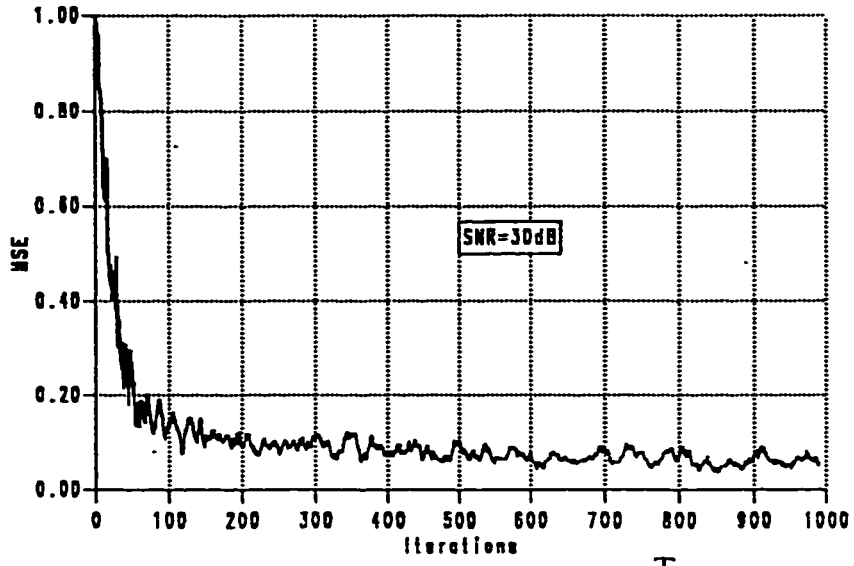

Figure 4.23.a: MSE using the LMS algorithm for the $\frac{T}{2}$ equalizer with main tap moved from main position and SNR = 30 dB.

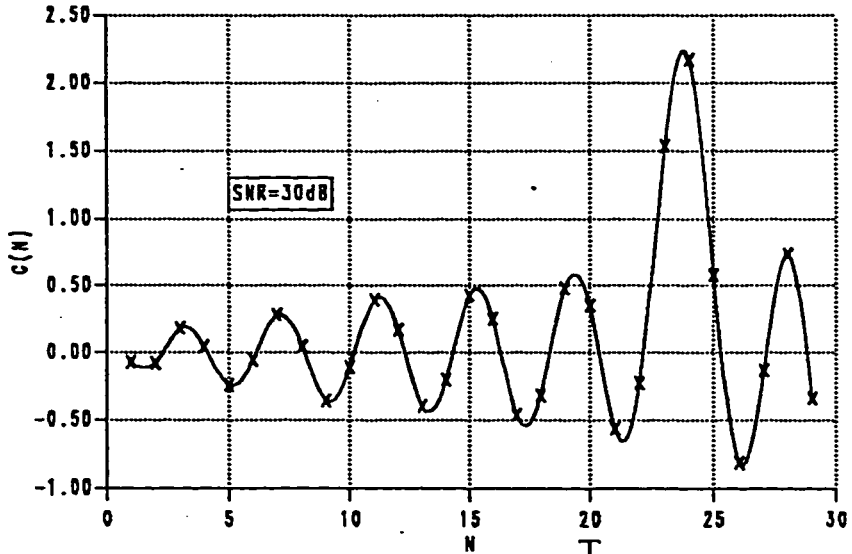

Figure 4.23.b: Sampled impulse response of the $\frac{T}{2}$ equalizer with main tap moved from main position and SNR = 30 dB.

A good characteristic achieved by a $\frac{T}{2}$ equalizer is that it is almost insensitive to the sampler phase, while the T equalizer lacks this feature. This could explained as follow; the fractionally-spaced equalizer acts directly on the sampled impulse response of the channel before aliasing, with respect to the sampling rate, takes place. Whereas the synchronous equalizer can only act to modify the aliased sampled impulse response of the channel, as opposed to directly modifying the sampled impulse response of the channel. Thus, the fractionally-spaced equalizer can compensate for any timing phase [2], [6], [17]. Hence, the sensitivity of the minimum MSE, achieved with an FSE with respect to the sampler phase, is typically smaller than that achieved with a synchronous equalizer [2]. The MSE versus delay for both equalizers is shown in figure 4.24. If an error is made in the sampler phase the $\frac{T}{2}$ equalizer can track that error.

As a conclusion we can say that the $\frac{T}{2}$ is more robust, in the sense that the MSE is almost non sensitive to the sampler phase, as compared to the T equalizer. On the other hand one has to choose between the degraded performance and the great complexity of the system. In this work, we introduce an idea where a compromise between performance and complexity, for both equalizers, is obtained. The results of this proposed method are the subject of the next section.

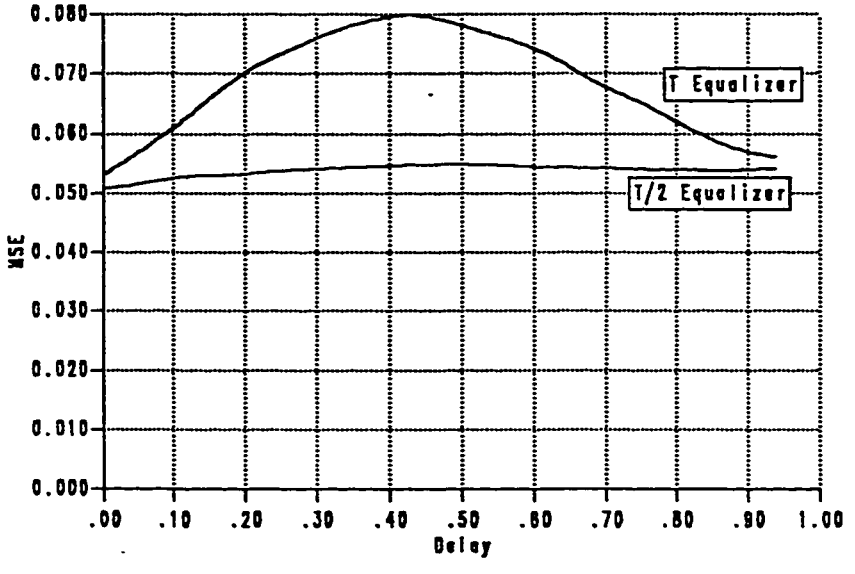

Figure 4.24: MSE as a function of the sampler phase for T equalizer and $\frac{T}{2}$ cqualizer.

This investigation has showed that the $\frac{T}{2}$ equalizer is really superior than the synchronous equalizer. All our aim, now, is that the proposed method will result in a behavior closer to that of the $\frac{T}{2}$ equalizer.

4.3 VARIOUS CONFIGURATIONS

The previous sections where only a proceeding to this section. The overall system was presented as well as a comparison between the T equalizer and the $\frac{T}{2}$ was made. Those results obtained for the two equalizers are of good help when results for this section are obtained. This will show the behavior of the proposed idea as far as the performance is concerned.

The results of the proposed configurations are given in this section. Some of the tap coefficients are set to zero and the MSE, which is a performance measure at the output of the equalizer, is obtained with respect to the number of iterations and as a function of the sampler phase. The later, i.e., the effect of the sampler phase on the MSE, will be of interest. Notice that the zero tap coefficients are not taken into account when calculating the output of the equalizer or when updating the tap coefficients of the equalizer. This figure will give us an idea how the new configuration behaves compared to the T spaced equalizer and the $\frac{T}{2}$ fractionally spaced

equalizer.

The study was done on the $\frac{T}{2}$ equalizer with some of its tap coefficients set to zero. The $\frac{T}{2}$ equalizer was designed with 29 tap coefficients.

Six different configurations have been chosen in the study of this proposed method. First, when tap coefficients 14 and 16 are set to zero, configuration 1 is obtained. In configuration 2 tap coefficients 12, 14, 16, and 18 are set to zero. In configuration 3 we have set only tap coefficients 2, 4, 26, and 28 to zero, while in configuration 4 tap coefficients 2, 4, 14, 16, 26, and 28 are set to zero. Configuration 5 is the result of setting tap coefficients 2, 4, 12, 14, 16, 18, 26, and 28 to zero. Finally, configuration 6 consisted of setting tap coefficients 1, 2, 28, and 29 to zero. Tap coefficients of the equalizer are numbered from 1 to 29.

In the simulation process, binary data $\{\pm 1\}$ generated by a PN sequence are sent through the channel given by Lucky [1], i.e., the same one used previously during the comparison of the T equalizer and the $\frac{T}{2}$ equalizer. Additive white Gaussian noise with zero mean and controllable variance is added to the samples at the output of the channel. A signal to noise ratio of 30 dB was chosen to all configurations under study. 50 simulation runs, each started at $n = 1$ and tap coefficients set to zero, are used in finding the MSE at the output of the equalizer. The LMS algorithm given by equation (2.21) is used during the adaptation of the tap

coefficients.

The MSE as a function of the number of iterations for each case is depicted in figures 4.25.a to 4.30.a, while the sampled impulse response of each one of them is shown in figures 4.25.b to 4.30.b, starting with configuration 1 to configuration 6, respectively. No noticeable differences can be said about the speed of convergence. They all approximately converge at the same speed. An observation is made on the behavior of each configuration from its sampled impulse response. Configuration 1, configuration 2, configuration 4, and configuration 5 have in more or less a close shape. Moreover, they are close to the shape of the T equalizer. Whereas the sampled impulse responses of configuration 3 and configuration 6 are different to the previous mentioned configurations. These last configurations, i.e., configurations 3 and 6, have a shape closer to the shape of the $\frac{T}{2}$ fractionally spaced equalizer.

Now, if one has to judge, his judgement would be on the MSE versus the sampler phase so that an affirmative statement would result. From figure 4.31.a which represents the MSE as a function of the sampler phase of configurations 1 through 6, one can observe that configurations 3 and 6 have a shape that is more acceptable than the other configurations. Now, if one has to choose a configuration among these configurations, configurations 3 and 6 would be the desirable ones. A comparision between these two configurations will be given later.

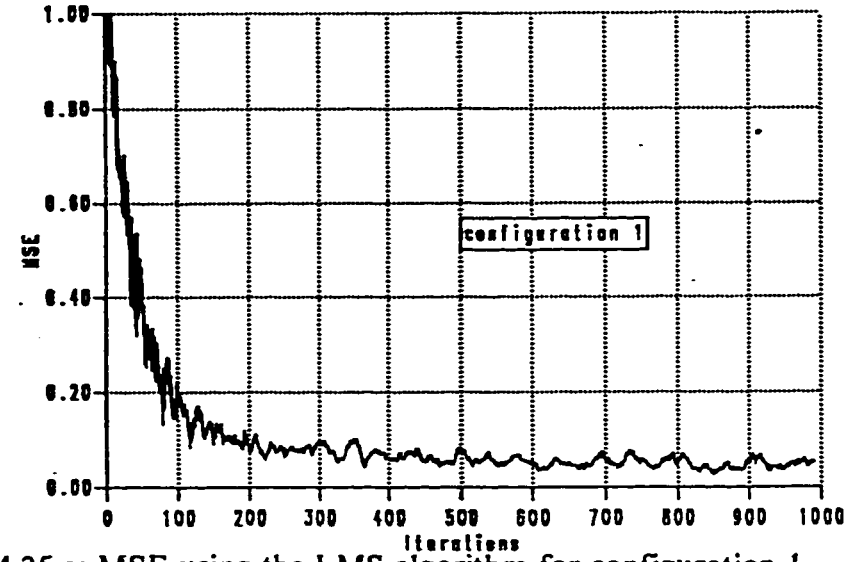

Figure 4.25.a: MSE using the LMS algorithm for configuration 1.

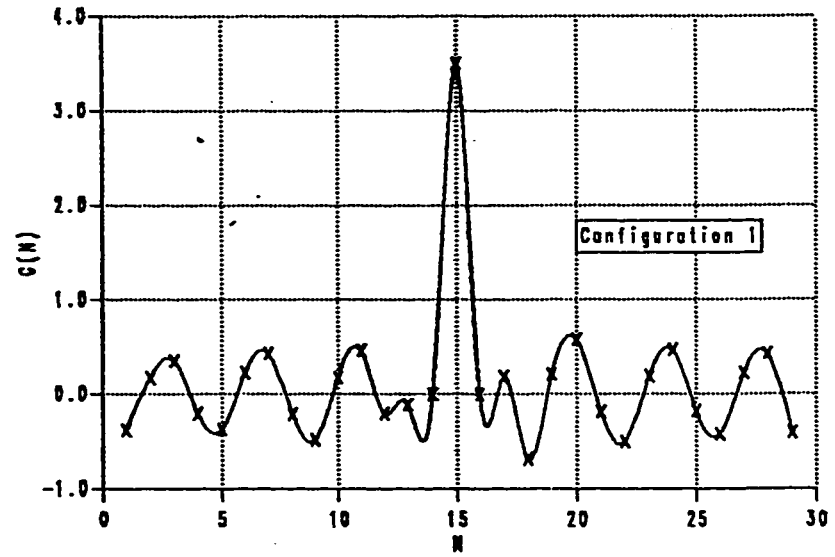

Figure 4.25.b: Sampled impulse response of configuration 1.

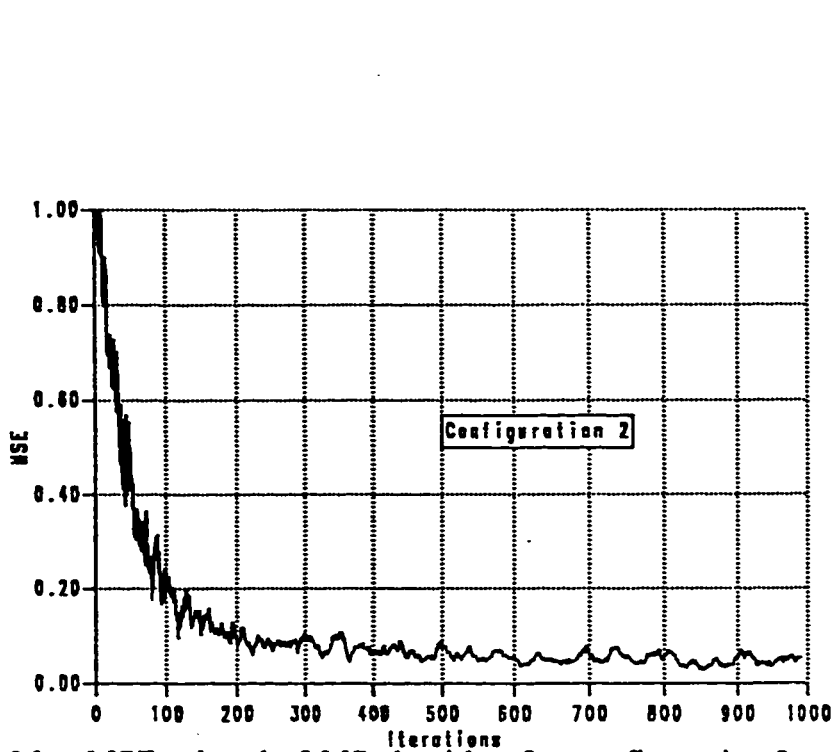

Figure 4.26.a: MSE using the LMS algorithm for configuration 2.

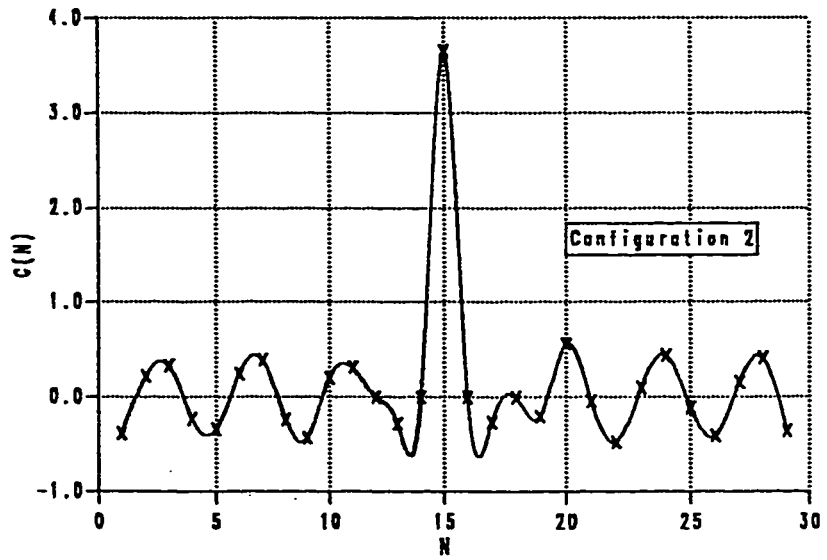

Figure 4.26.b: Sampled impulse response of configuration 2.

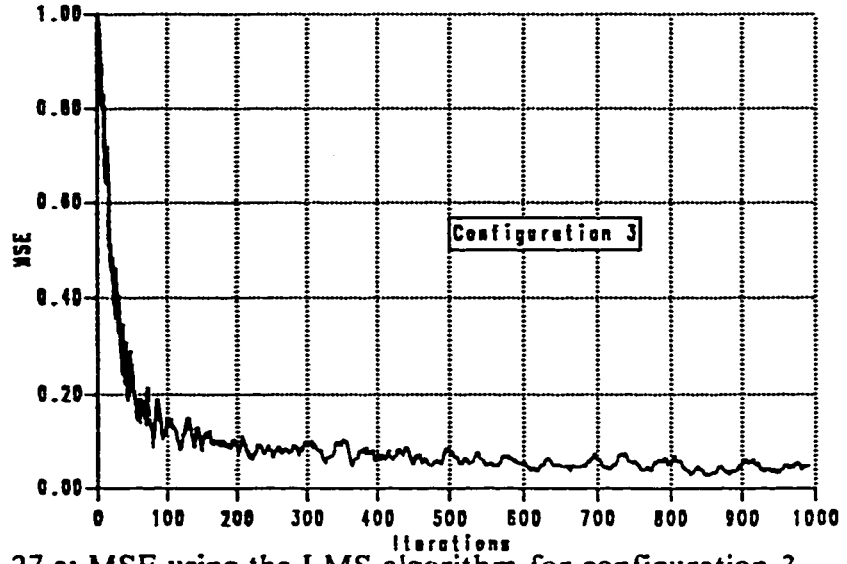

Figure 4.27.a: MSE using the LMS algorithm for configuration 3.

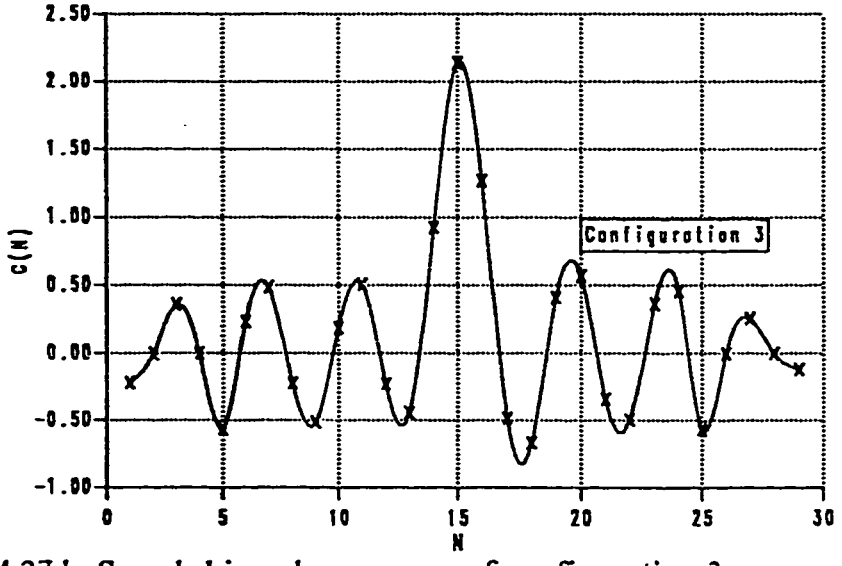

Figure 4.27.b: Sampled impulse response of configuration 3.

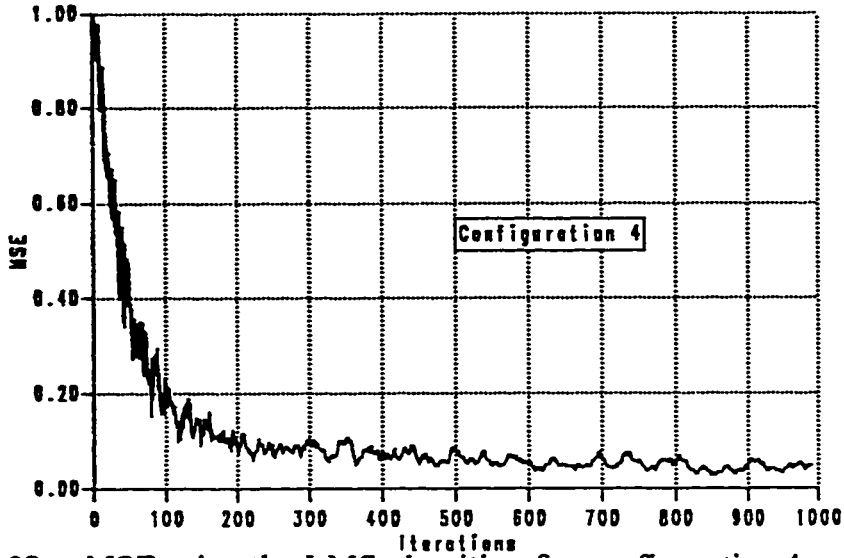

Figure 4.28.a: MSE using the LMS algorithm for configuration 4.

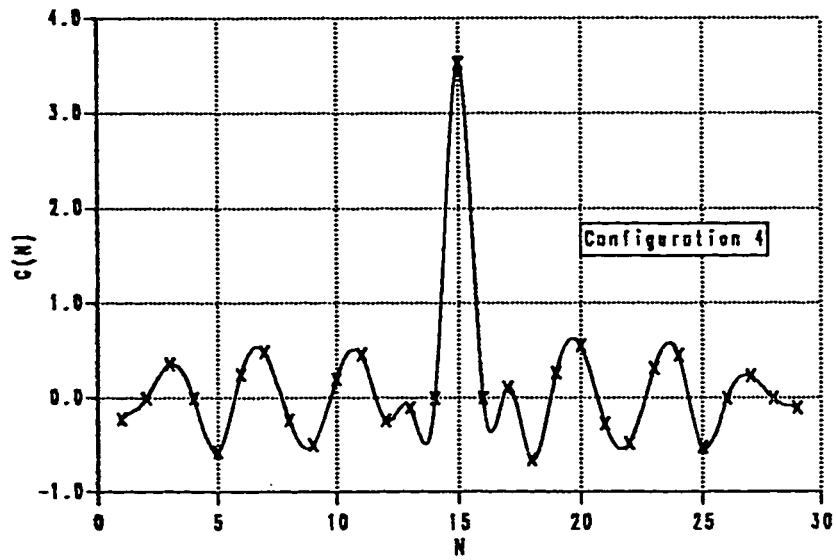

Figure 4.28.b: Sampled impulse response of configuration 4.

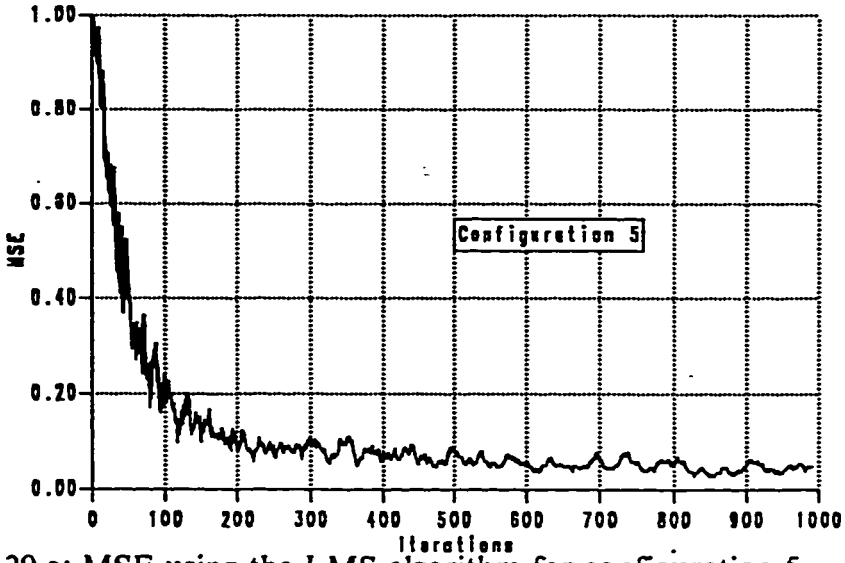

Figure 4.29.a: MSE using the LMS algorithm for configuration 5.

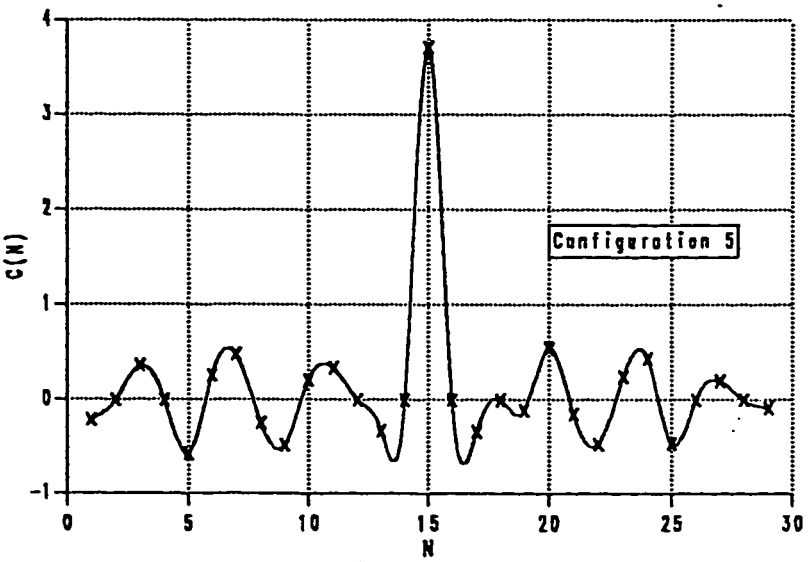

Figure 4.29.b: Sampled impulse response of configuration 5.

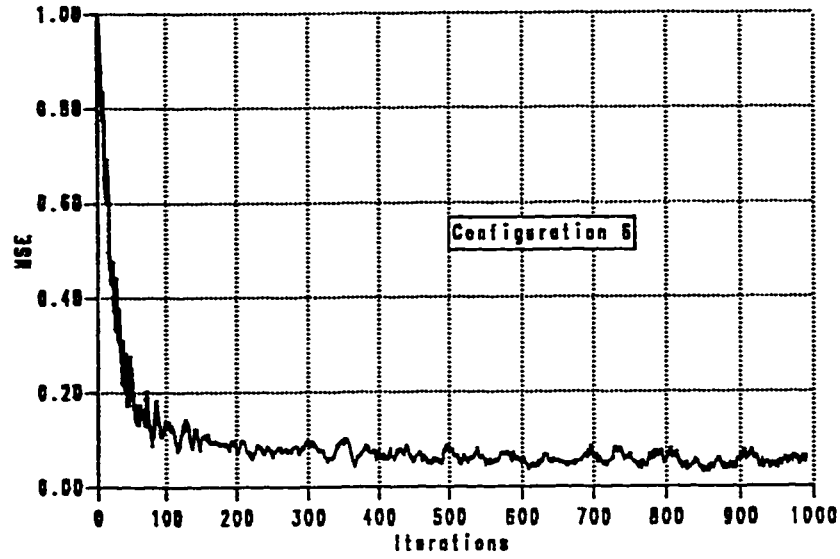

Figure 4.30.a: MSE using the LMS algorithm for configuration 6.

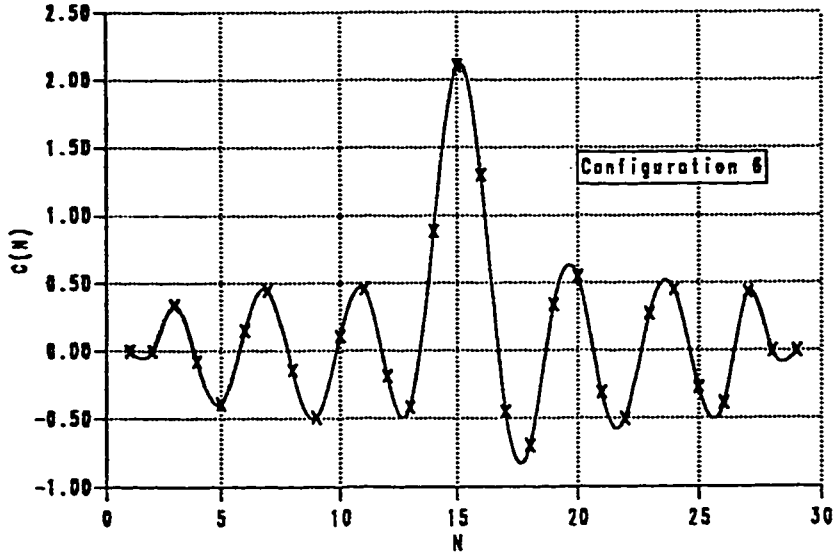

Figure 4.30.b: Sampled impulse response of configuration 6.

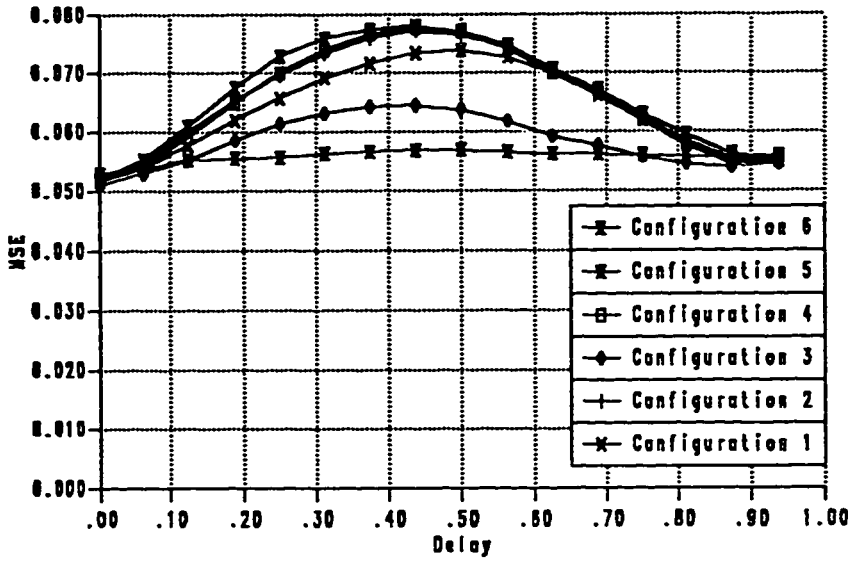

Figure 4.31.a: MSE as a function of the sampler phase for all configurations.

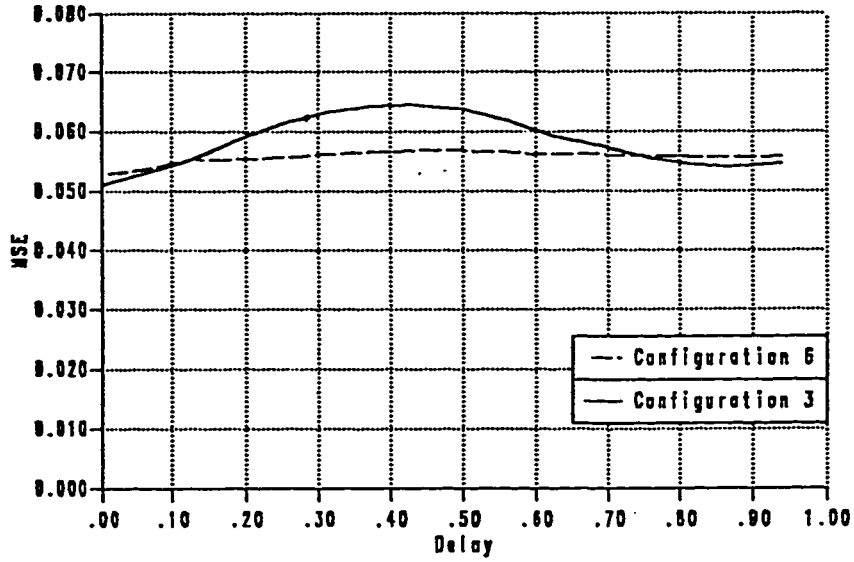

Figure 4.31.b: MSE as a function of the sampler phase for configurations 3 and 6.

From the point of view of complexity we see that the synchronous equalizer with (N) tap coefficients requires (N) arithmetic multiplications and (N-1) arithmetic additions to give one output. The tap coefficients for this equalizer will need (N) arithmetic additions and (2N) arithmetic multiplications each update. The fractionally-spaced equalizer with tap spacing $\frac{T}{2}$, however, with a total of (2N-1) tap coefficients constituting the equalizer, requires (2N-1) arithmetic multiplications and (2N-2) arithmetic additions operations to give one output. Besides, (2N-1) arithmetic additions and (2N-2) arithmetic multiplications are needed to update the tap coefficients every symbol period. Whereas, configuration 3 or configuration 6, with only (2N-5) tap coefficients, needs (2N-5) arithmetic multiplications and (2N-6) arithmetic additions to give one output. The tap coefficients for these two configurations need (2N-5) arithmetic additions and (4N-10) arithmetic multiplications for each update. In all configurations used, i.e., configurations 1 through 6, the tap coefficients which are set to zero are neither updated nor taken into account during the calculation of the output. We see from these numbers that a decrease in complexity of about 14%, between the FSE with tap spacing $\frac{T}{2}$ and either configuration 3 or configuration 6, has occured. And an increase of complexity of 67% between the synchronous equalizer and either configuration 3 or configuration 6 has showed up. This is as far as the complexity is concerned.

However, in the performance side, we see from figures 4.24 and 4.31,

that the MSE versus the sampler phase gave an acceptable result for configurations 3 and 6 compared to the synchronous equalizer. Configuration 3 gains 50% in performance over the synchronous equalizer, as far as the peak-to-peak deviation is concerned, and a gain of 14.29% in the average MSE, also. On the other hand, configuration 6 shows 81.34% and 17.96% gain over the synchronous equalizer in the peak-to-peak deviation and in the average MSE, respectively.

Table 4.2 summarizes the results of complexity and performance for the T equalizer, the $\frac{T}{2}$ equalizer, and configuration 3; whereas table 4.3 shows the details of complexity and performance for the T equalizer, the $\frac{T}{2}$ equalizer, and configuration 6. In these two tables the value of N is 15.

Now if one has to compare configuration 3 and configuration 6, it would be obvious that configuration 6 is better in two things. First, it is better for being regular in processing and calculations, and second it is insensitive to large sample phase difference as can be seen from figure 4.31.b. But these two differences could be overcome by specially tailored processor architecture, as far as the regularity of processing and calculations is concerned; and if timing error is small, the insensitivity of the MSE to the sampler phase is of no importance. However, configuration 3 is better than configuration 6 in that the MSE is close to the exact timing, which can not be obtained by configuration 6.

	Complexity of Computations				Performance	
	Output		Tap Coefficients		P.Pmax Deviation Delay	Average MSE
	+	x	+	x		
T	14	15	15	30	0.0268	0.0679
T/2	28	29	29	58	0.0041	0.0538
configuration 3	24	25	25	50	0.0134	0.0582
% Gain (+) or Loss (-) of configuration 3 with respect to T	-71.42%	-66.66%	-66.66%	-66.66%	+ 50%	+ 14.29%
% Gain (+) or Loss (-) of configuration 3 with respect to T/2	+ 14.29%	+ 13.79%	+ 13.79%	+ 13.79%	-69.40%	-8.17%

Table 4.2: Complexity and performance for the T equalizer, the T/2, and configuration 3 for a PAM system.

	Complexity of Computations				Performance	
	Output		Tap Coefficients		P.Pmax Deviation Delay	Average MSE
	+	x	+	x		
T	14	15	15	30	0.0268	0.0679
T/2	28	29	29	58	0.0041	0.0538
configuration 6	24	25	25	50	0.0050	0.0557
% Gain (+) or Loss (-) of configuration 6 with respect to T	-71.42%	-66.66%	-66.66%	-66.66%	+81.34%	+17.96%
% Gain (+) or Loss (-) of configuration 6 with respect to T/2	+14.29%	+13.79%	+13.79%	+13.79%	-21.95%	-3.53%

Table 4.3: Complexity and performance for the T equalizer, the T/2, and configuration 6 for a PAM system.

We can say that configuration 3 resulted in an acceptable performance. To see if this statement is right or wrong, let us apply this idea to a QAM system and see the result of it. In chapter 5 we will treat equalizers used in QAM systems and at the same time apply this new configuration to a QAM system.

Before we start chapter 5, let us see the effect of the timing jitter on the MSE for the synchronous equalizer, the fractionally-spaced equalizer with tap spacing $\frac{T}{2}$, and configuration 3. The results of this test are depicted in figures 4.32 through 4.34. The values obtained are as follow, the average MSE for the synchronous equalizer is 0.20, however, the FSE with tap spacing $\frac{T}{2}$ its average MSE is only 0.16, whereas the average MSE is only 0.17 for configuration 3. This still shows that configuration 3 is behaving closer to the FSE.

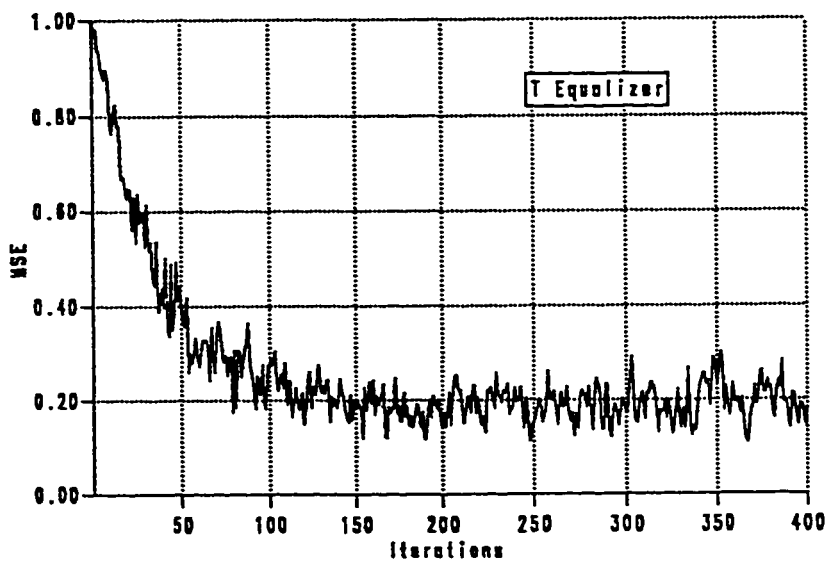

Figure 4.32: Timing jitter effect on the MSE for T equalizer.

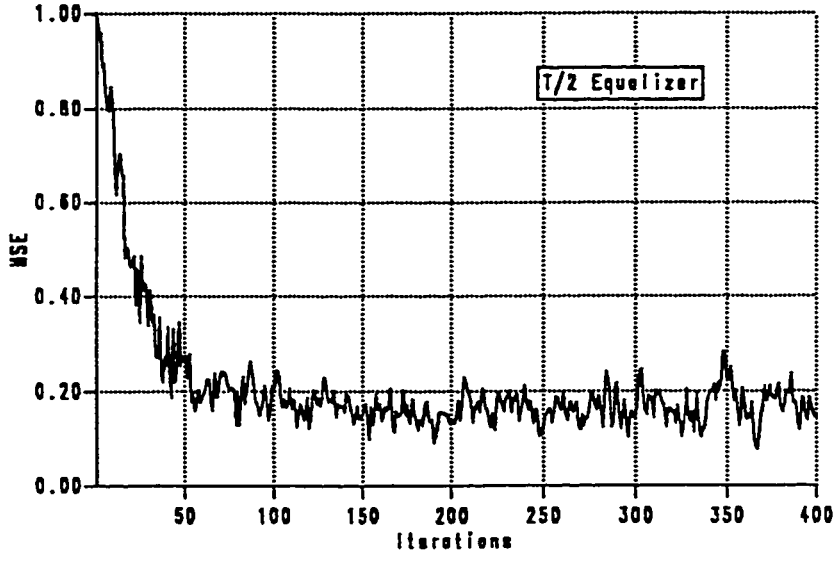

Figure 4.33: Timing jitter effect on the MSE for $\frac{T}{2}$ equalizer.

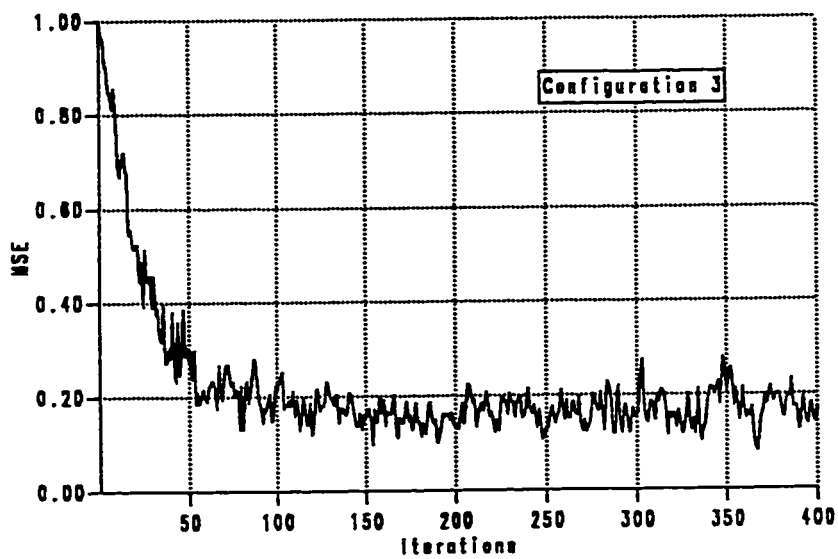

Figure 4.34: Timing jitter effect on the MSE for configuration 3.

CHAPTER V

EQUALIZATION IN QAM SYSTEMS

5.1 INTRODUCTION

So far we have dealt only with equalizers used in baseband PAM systems. There exists many types of modulation described in [3] used for transmitting informations at a rate of 9600 bits/sec. Among them is quadrature-amplitude modulation (QAM) scheme that represents a hybrid form of phase and amplitude modulation. QAM is as efficient in bits/second per Hz as vestigial or single-sideband modulation [2]. An M-QAM signal is an M-amplitude and M-phase signal which general form is given by

$$S_m(t) = A_m \cos 2\pi f_c t + B_m \sin 2\pi f_c t \quad , \quad m = 1,2,...,M \qquad (5.1)$$

As can be seen from (5.1), each pair of discrete amplitudes $\{A_m, B_m\}$ are modulating two phase-quadrature carriers. For simplicity we will index to the in-phase-part and the quadrature-part of the baseband signal by i and q, respectively. Figure 5.1 depicts an M-QAM signal constellation.

During its transmission through a channel, the signal issued is subject to all kind of distortions. Among them is the interference between the data

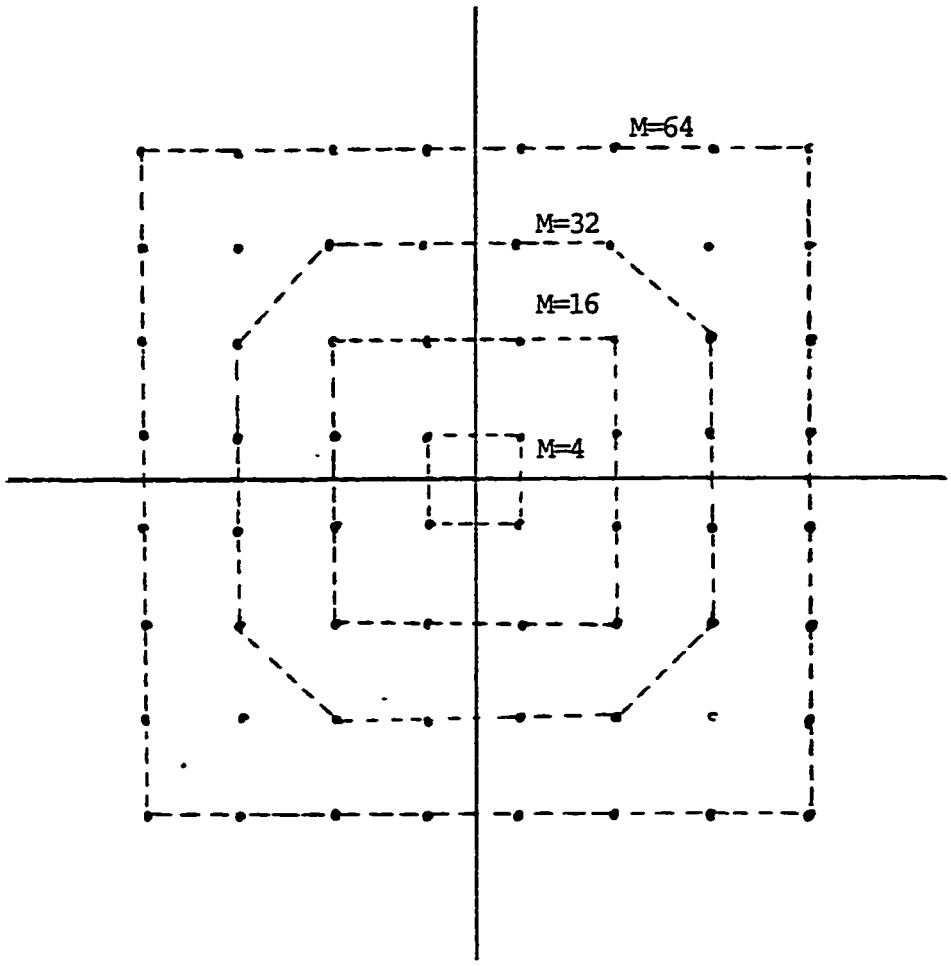

Figure 5.1: QAM signal constellation.

composing the emitted signal.

In the case of modulation by two carriers in quadrature, the channel distortions produce on the one hand interferences between symbols issued inside the same channel, on the other hand interferences between symbols issued through the in-phase and the quadrature channels (cross-terms) [22]. These interferences are cancelled by an adaptive equalizer. In the next section we will describe the structure of this equalizer used for modulations with carriers in quadrature.

5.2 STRUCTURE OF THE EQUALIZER

The main purpose of the equalizer, for modulations with carriers in quadrature, is to cancel the two types of interferences described previously.

Four elementary-equalizers EQ_{i1}, EQ_{q1}, EQ_{i2}, EQ_{q2}, and a decision device which, from the equalized signals y_i and y_q, restore the estimated values a_i and a_q issued through the channels in quadrature, constitute the equalizer.

The elementary equalizer EQ_{i1} compensates for the interferences between symbols in the in-phase channel, while the elementary equalizer EQ_{q1} compensates for cross-terms from the quadrature channel through the in-phase channel. The elementary-equalizers EQ_{i2} and EQ_{q2} have the same

functions for the quadrature channel as those described previously for the in-phase channel; that is the elementary equalizer EQ_{q2} compensates for the interferences between symbols in the quadrature channel, while the elementary equalizer EQ_{i2} compensates for cross-terms from the in-phase channel through the quadrature channel.

Taking into consideration the characteristics of the channels, the in-phase and the quadrature components, the elementary-equalizers EQ_{i1} and EQ_{i2} are identical and so are the elementary-equalizers EQ_{q1} and EQ_{q2}. We will note EQ_{i1} and EQ_{i2} as EQ_i and EQ_{q1} and EQ_{q2} as EQ_q. The structure of the equalizer is depicted in figure 5.2. Now, we have only to describe how the tap coefficients are updated when the LMS algorithm is used. This is the subject of the coming section.

5.3 UPDATE OF THE TAP COEFFICIENTS

For correcting and getting updated to the distortions caused by the channel, we have to use an updating scheme, from an error signal, to update the different coefficients of the equalizer. The updating scheme, which is considered for the equalizer, has the job to minimize the cost function J , here the MSE, is defined as follow

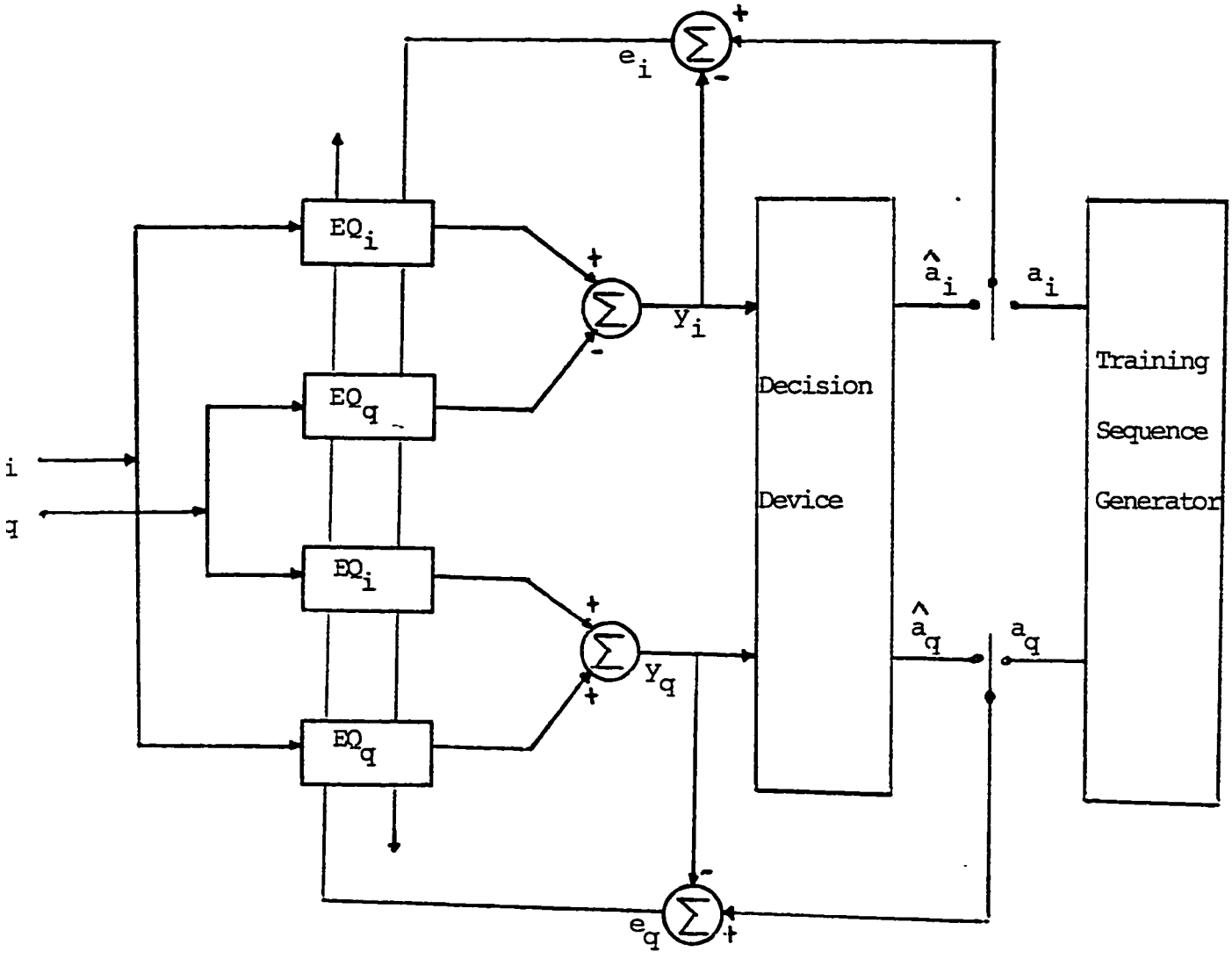

Figure 5.2: Adaptive Equalizer for QAM Systems

$$J = E\{e_i^2(n) + e_q^2(n)\} \tag{5.2}$$

where $e_i(n)$ and $e_q(n)$ are the in-phase error and the quadrature error at time nT, respectively, defined as

$$e_i(n) = y_i(n) - a_i(n) \tag{5.3.a}$$

$$e_q(n) = y_q(n) - a_q(n) \tag{5.3.b}$$

The minimization of J permits to minimize at the same time the degradations of the signal due to the noise and those due to the interferences.

Let us call the tap coefficients of the equalizer $C_i(k)$ and $C_q(k)$ for the in-phase part and the quadrature part, respectively; where $1 \le k \le N$, and N is the number of tap coefficients of the equalizer. The equalized signals $y_i(n)$ and $y_q(n)$ at time nT have the following expressions

$$y_i(n) = \sum_{k=1}^{N} C_i(k) r_i(n-k) - \sum_{k=1}^{N} C_q(k) r_q(n-k)$$

$$= \mathbf{R}_i^T \mathbf{C}_i - \mathbf{R}_q^T \mathbf{C}_q \tag{5.4.a}$$

$$y_q(n) = \sum_{k=1}^{N} C_i(k) r_q(n-k) + \sum_{k=1}^{N} C_q(k) r_i(n-k)$$

$$= \mathbf{R}_q^T \mathbf{C}_i + \mathbf{R}_i^T \mathbf{C}_q \qquad (5.4.b)$$

$r_i(n)$ and $r_q(n)$ are the in-phase and the quadrature components of the sampled received signal at time nT, respectively; and

$$\mathbf{R}_i = [r_i(n-1), r_i(n-2), \ldots, r_i(n-N)]^T \qquad (5.5.a)$$

and

$$\mathbf{R}_q = [r_q(n-1), r_q(n-2), \ldots, r_q(n-N)]^T \qquad (5.5.b)$$

The in-phase and the quadrature components of the tap coefficients are defined as follow

$$\mathbf{C}_i = [C_i(1), C_i(2), \ldots, C_i(N)]^T \qquad (5.6.a)$$

and

$$\mathbf{C}_q = [C_q(1), C_q(2), \ldots, C_q(N)]^T \qquad (5.6.b)$$

The coefficients are then updated every symbol period, according to the LMS algorithm given by [22]:

$$C_i^{n+1}(k) = C_i^n(k) + \Delta\{e_i(n)r_i(n-k) + e_q(n)r_q(n-k)\} \qquad (5.7.a)$$

$$C_q^{n+1}(k) = C_q^n(k) + \Delta\{e_q(n)r_i(n-k) - e_i(n)r_q(n-k)\} \qquad (5.7.b)$$

where Δ is the step size used in the LMS algorithm. Equations (5.7.a) and (5.7.b) read in complex form as

$$\mathbf{C}^{n+1} = \mathbf{C}^n + \Delta e^n \mathbf{R}^{*n} \qquad (5.8)$$

where $\mathbf{R}^*$ is the complex conjugate of $\mathbf{R}$, with $\mathbf{R} = \mathbf{R}_i + j\mathbf{R}_q$.

The convergence behavior of the LMS algorithm defined by equation (5.8) is governed by the choice of the step size, Δ. Fastest convergence is generally obtained by using the step size parameter

$$\Delta_{op} = \frac{1}{\text{Nx\{signal power\}}} \qquad (5.9)$$

And in general, for the LMS algorithm to converge, it is required that

$$0 \le \Delta \le \frac{2}{\text{Nx\{signal power\}}} \qquad (5.10)$$

The structure of the equalizer and the LMS algorithm have been described for QAM systems. Now, let us use these tools to simulate a synchronous equalizer, a fractionally-spaced equalizer with tap spacing $\frac{T}{2}$,

and the proposed method for QAM systems. The proposed method will consist of setting some of the tap coefficients of both the in-phase and the quadrature components of a $\frac{T}{2}$ fractionally-spaced equalizer to zero.

5.4 SIMULATION RESULTS

5.4.1 Results obtained for T and $\frac{T}{2}$ equalizers

In this section, simulation results are given for the QAM systems using a T equalizer and a $\frac{T}{2}$ equalizer, and this is by using the methods described in this chapter. The T equalizer is designed with 15 tap coefficients while 29 tap coefficients are used for the $\frac{T}{2}$ equalizer, which are updated using the LMS algorithm. Thus a total of 14T is the total time span for both equalizers, where T is the symbol period.

Binary random data were generated by a PN sequence generator and sent through the complex channel. This data consists of two components, the in-phase data and the quadrature data. The channel considered here is the one given by Ungerboeck [6]. The outputs, the in-phase and the quadrature components, of the channel are added to the in-phase and the quadrature components of the noise, respectively; where both components of the noise are assumed to be stationary with zero mean and controllable

variance to give the desired signal to noise ratio.

The output of the equalizer is compared then with the transmitted signal to give a complex error, the in-phase component and the quadrature component, according to equations (5.3.a) and (5.3.b). This error is used along the LMS algorithm to update the tap coefficients. Notice that every output from the equalizer and each update is done at every symbol period T, whether a synchronous equalizer or an FSE is used. This error is used, too, in obtaining the MSE at the output of the equalizer.

The MSE obtained is the result of 50 simulation runs. Each run started at $n = 1$ and the tap coefficients are set to zero. The graphs of each MSE corresponding to the T equalizer and to the $\frac{T}{2}$ equalizer are depicted in figures 5.3.a and 5.4.a, respectively. An SNR of 27 dB is used in the simulation process. Where the SNR is defined, here, as the average power of the transmitted signal to the average power of the noise. The step size chosen for the T equalizer is 0.0133 , whereas the one for the $\frac{T}{2}$ equalizer is 0.0069. These two values are in accordance with equation (5.10). As can be seen from these graphs both equalizers converge at approximately the same speed. We see that the $\frac{T}{2}$ FSE gains about 2 dB over the synchronous equalizer. The corresponding sampled impulse responses for the T equalizer and the $\frac{T}{2}$ equalizer are shown in figures 5.3.b and 5.4.b, respectively. We

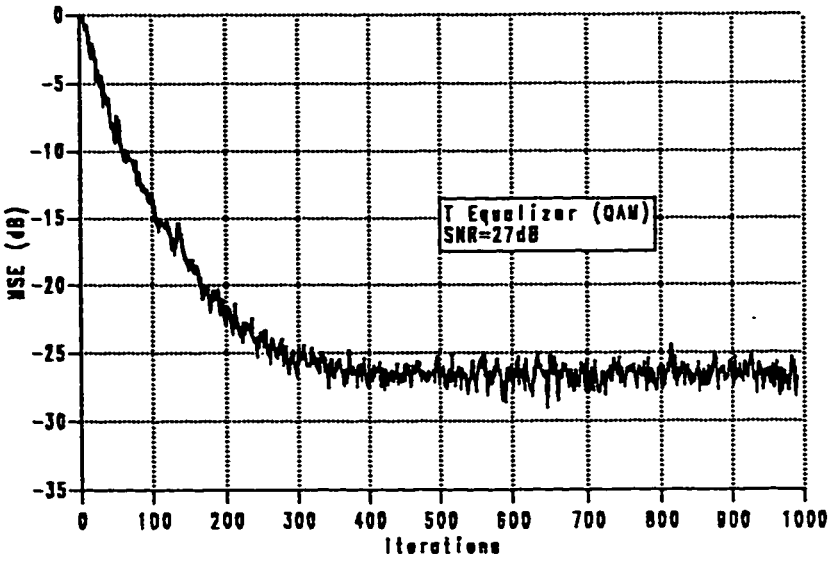

Figure 5.3.a: MSE using the LMS algorithm for the T equalizer with SNR = 27 dB.

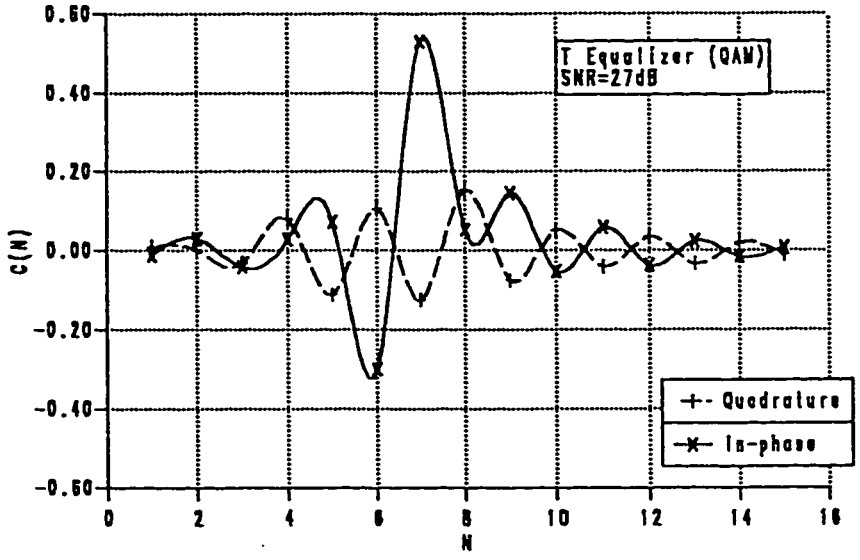

Figure 5.3.b: Sampled impulse response of the T equalizer with SNR = 27 dB.

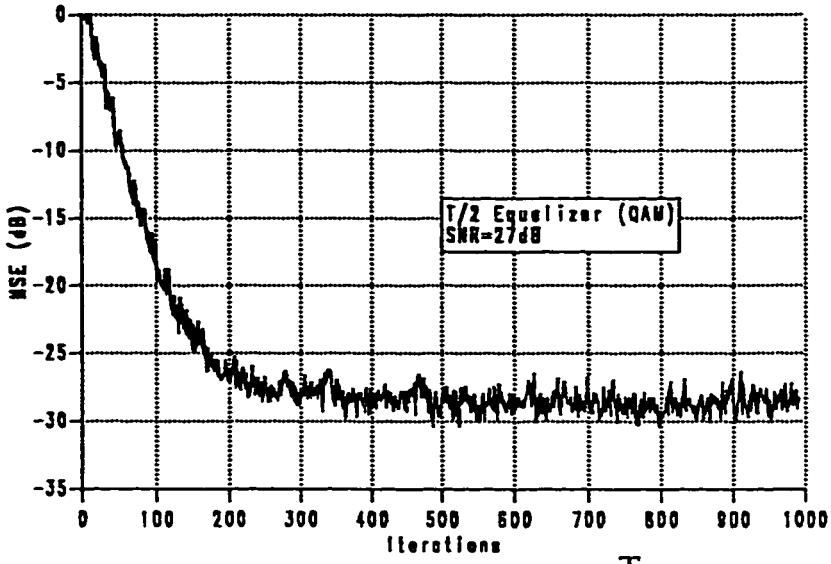

Figure 5.4.a: MSE using the LMS algorithm for the $\frac{T}{2}$ equalizer with SNR = 27 dB.

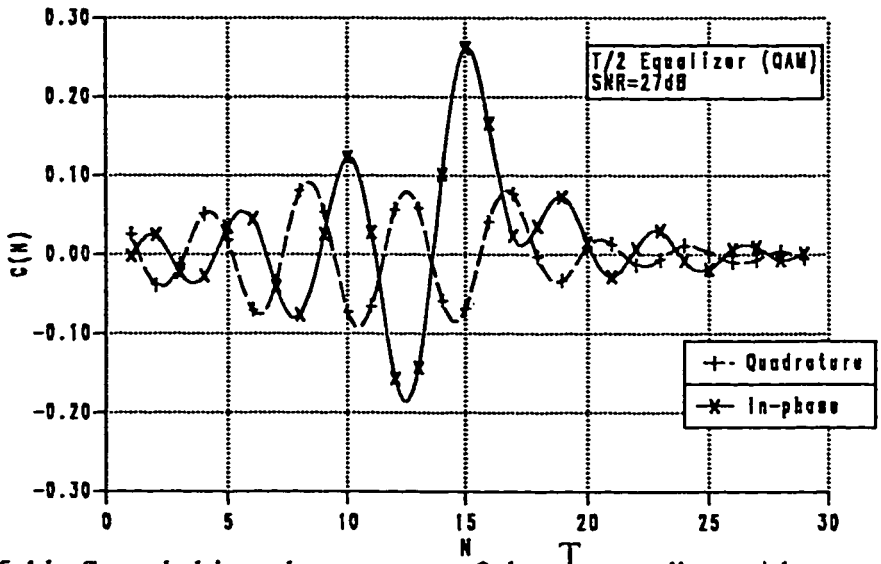

Figure 5.4.b: Sampled impulse response of the $\frac{T}{2}$ equalizer with SNR = 27 dB.

can notice from these graphs that the main tap of the synchronous equalizer is twice as much as that of the $\frac{T}{2}$ equalizer.

Other values of signal-to-noise ratios were used too. Figures 5.5.a and 5.6.a depict the MSE of the T equalizer and the $\frac{T}{2}$ equalizer, respectively, when an SNR of 20 is used. The corresponding sampled impulse responses of the T equalizer and the $\frac{T}{2}$ equalizer are shown in figures 5.5.b and 5.6.b, respectively. Figures 5.7 and 5.8 show the same thing but for an SNR of 10 dB. The same observations can be made here from these figures, where in the case when the SNR is 20 dB, the MSE of the fractionally-spaced equalizer gains 2 dB difference over that of the synchronous equalizer, whereas in the case when the SNR is 10 dB, here, a 2 dB difference is observed, too.

Finally, the MSE for both equalizers was evaluated as a function of the sampler phase. This is depicted in figure 5.9, were both curves corresponding to the T equalizer and the $\frac{T}{2}$ equalizer are shown.

The two curves differ remarkably and show that the MSE of the T equalizer depends critically on the choice of the sampler phase, whereas the MSE of the $\frac{T}{2}$ equalizer is almost independent of the sampler phase within this range of values. Moreover, in this simulation the $\frac{T}{2}$ equalizer gains

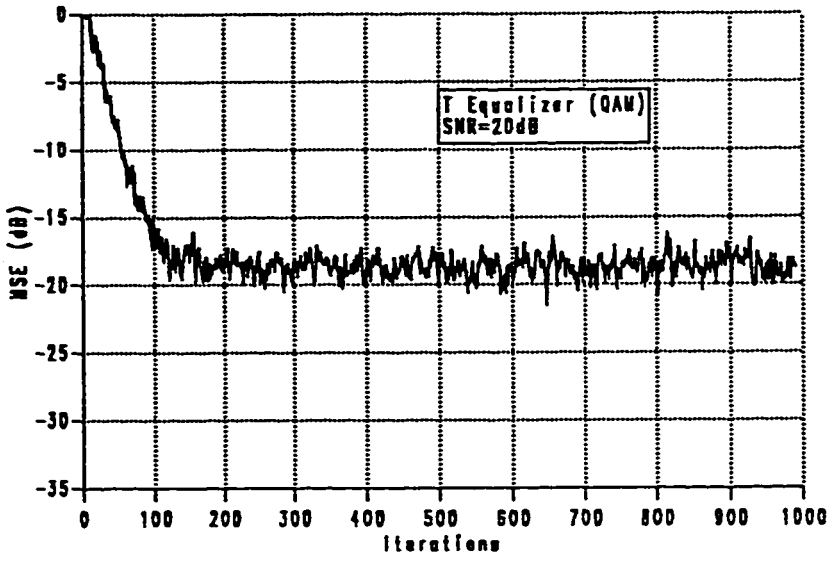

Figure 5.5.a: MSE using the LMS algorithm for the T equalizer with SNR = 20 dB.

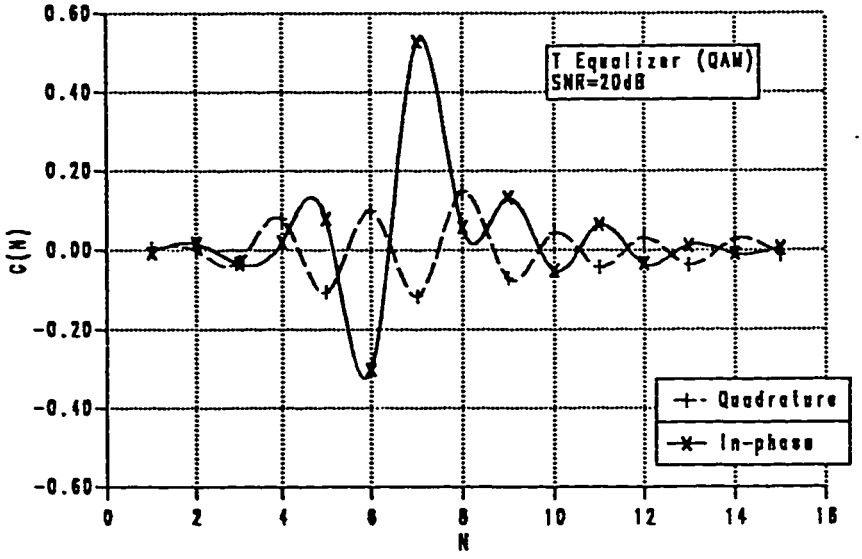

Figure 5.5.b: Sampled impulse response of the T equalizer with SNR = 20 dB.

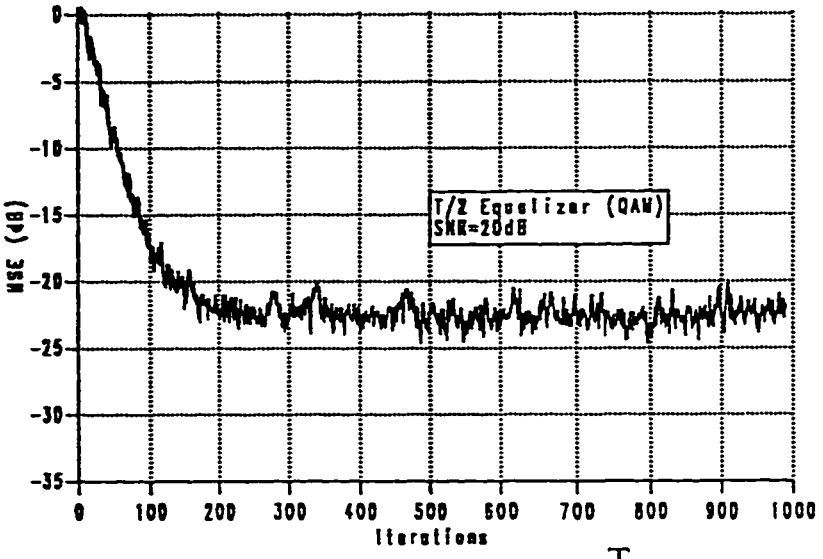

Figure 5.6.a: MSE using the LMS algorithm for the $\frac{T}{2}$ equalizer with SNR = 20 dB.

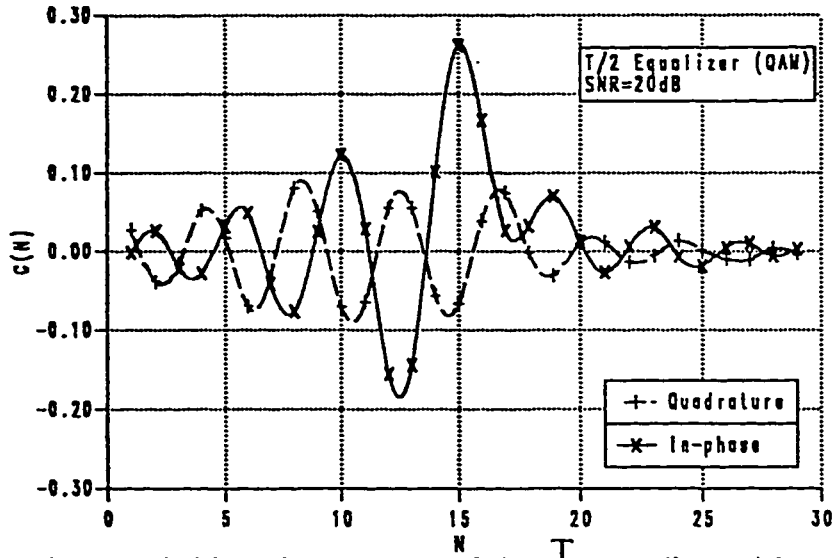

Figure 5.6.b: Sampled impulse response of the $\frac{T}{2}$ equalizer with SNR = 20 dB.

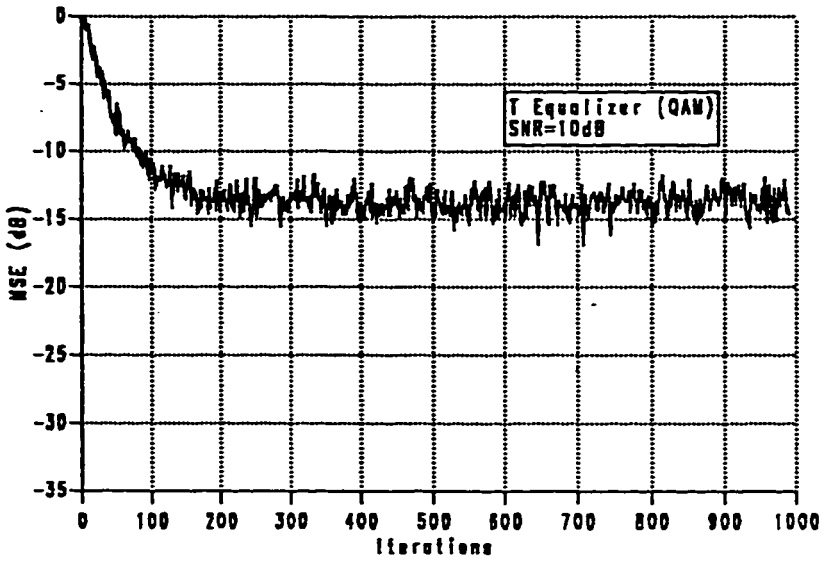

Figure 5.7.a: MSE using the LMS algorithm for the T equalizer with SNR = 10 dB.

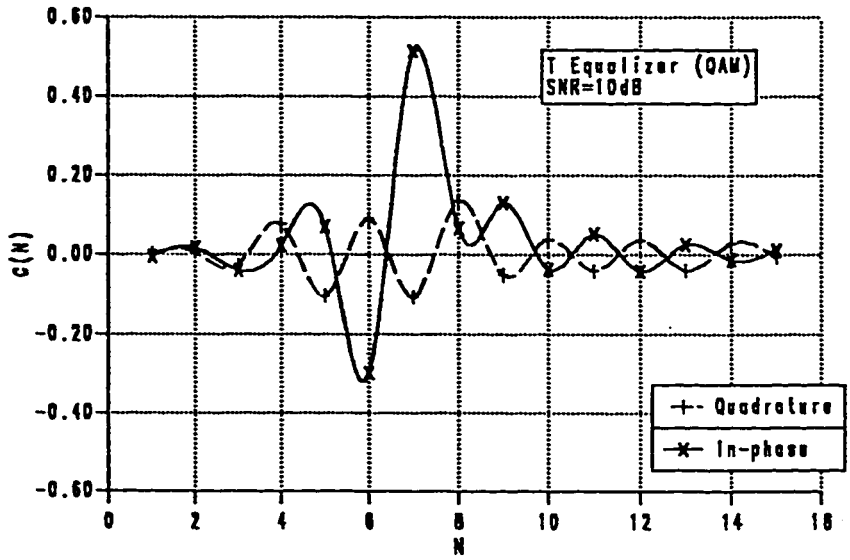

Figure 5.7.b: Sampled impulse response of the T equalizer with SNR = 10 dB.

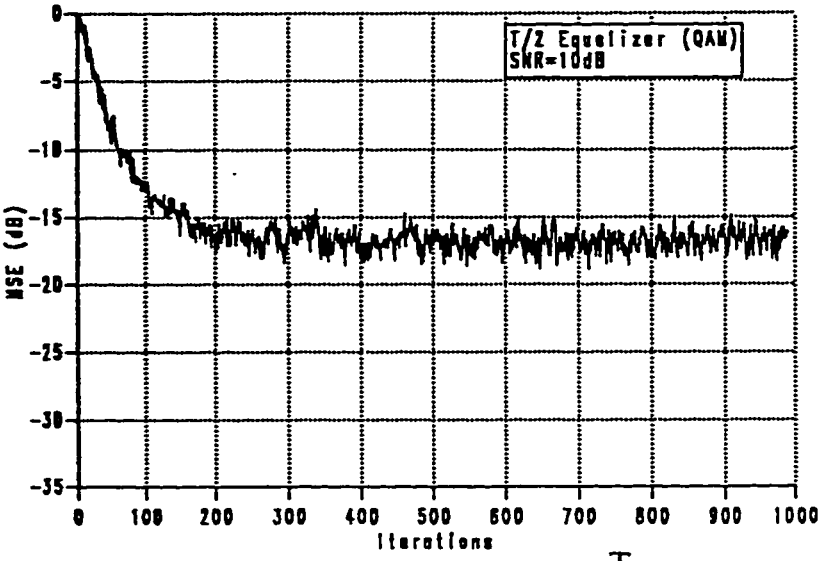

Figure 5.8.a: MSE using the LMS algorithm for the $\frac{T}{2}$ equalizer with SNR = 10 dB.

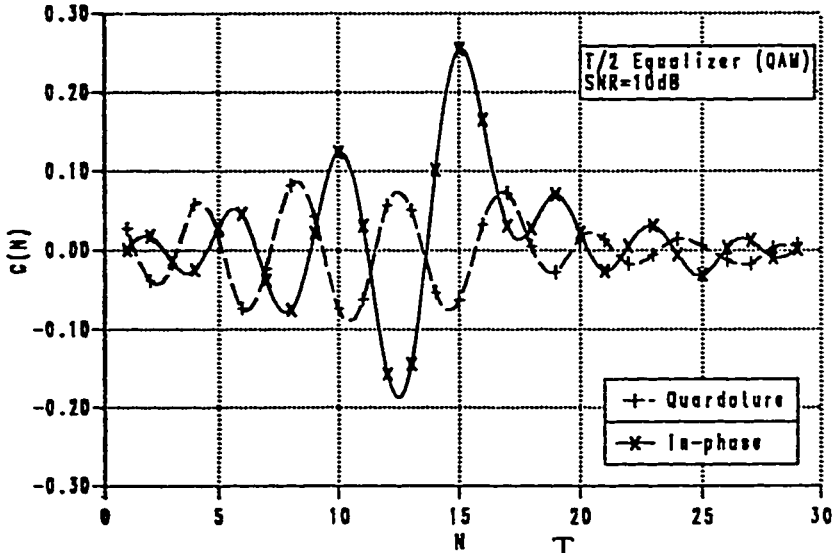

Figure 5.8.b: Sampled impulse response of the $\frac{T}{2}$ equalizer with SNR = 10 dB.

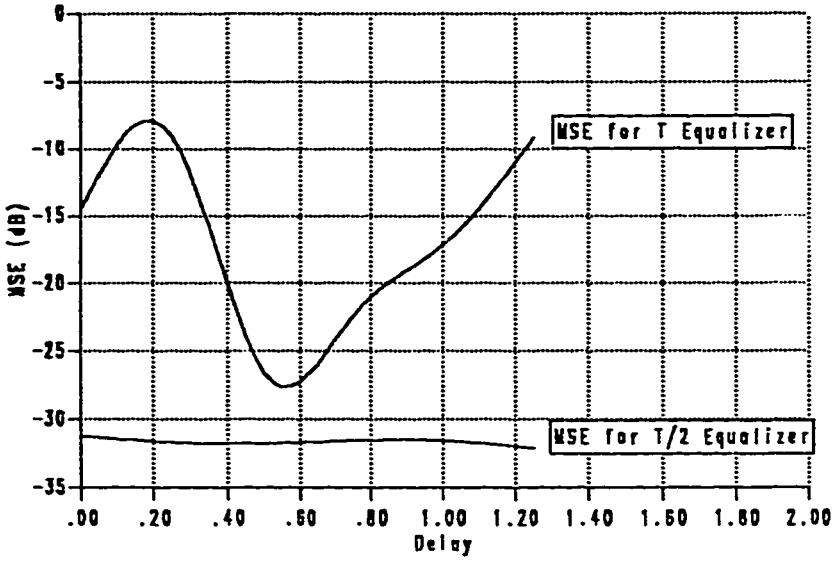

Figure 5.9: MSE as a function of the sampler phase.

about 6 dB in its MSE over the T equalizer, which is due partly to the larger number of tap coefficients available for equalization.

Given all these results, we can assert really the superiority of the $\frac{T}{2}$ equalizer over the synchronous equalizer. However, the only thing that lacks this type of equalizer, i.e., the $\frac{T}{2}$ equalizer, or in general any fractionally-spaced equalizer, is the great complexity associated with it. Many more tap coefficients are associated with any FSE than those associated with a synchronous equalizer. Hence, too many computations are needed at every symbol period to update these tap coefficients for an FSE, while a small number of computations are used in the case of a synchronous equalizer.

The results obtained in this section are of good help when the proposed method will be evaluated. Thus, the coming section will be totally devoted to the proposed method. In particular, we have chosen only the configuration that gave an acceptable result during the previous chapter, in the case of baseband PAM system. And this is only to ascertain if this idea will work for the case of a QAM system.

5.4.2 Results of the proposed method

Here, in this section we will try to give the results of the simulation for the proposed method. The acceptable results obtained from configuration 3

during the previous chapter has made us to do two things. The first thing is to learn more about equalizers used in QAM systems, and the second thing is to test this configuration for these systems. Hence, only configuration 3 is the one to be under test, which is defined here by setting tap coefficients 2, 4, 26, and 28 of the in-phase and the quadrature components of the $\frac{T}{2}$ fractionally-spaced equalizer to zero.

As usual, during our simulation, the LMS algorithm for QAM systems defined by equation (5.8) is used for updating the tap coefficients of this newly proposed idea at each symbol period. There is a total of 25 tap coefficients for the in-phase and the quadrature components of the equalizer, respectively, to be updated each symbol period. The other zero-taps are neither updated nor entered in the calculation process.

An SNR of 27 dB is chosen, so that a comparison between this configuration and the results obtained during the previous section for the synchronous equalizer and the $\frac{T}{2}$ equalizer can be made.

Figure 5.10.a shows the behaviour of the MSE as a function of the number of iterations, where it is shown that this MSE converges approximately on the same speed as that of the $\frac{T}{2}$ FSE depicted in figure 5.4.a. The sampled impulse response of this new configuration is shown in figure 5.10.b.

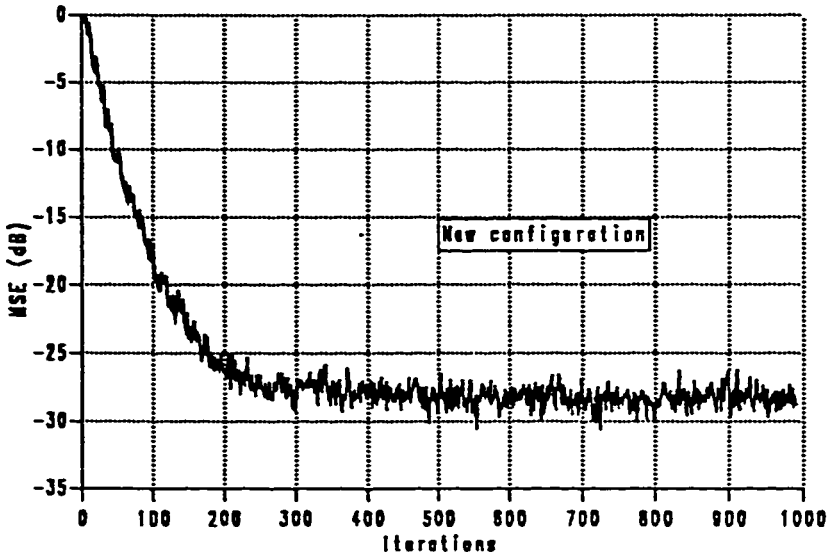

Figure 5.10.a: MSE using the LMS algorithm for new configuration.

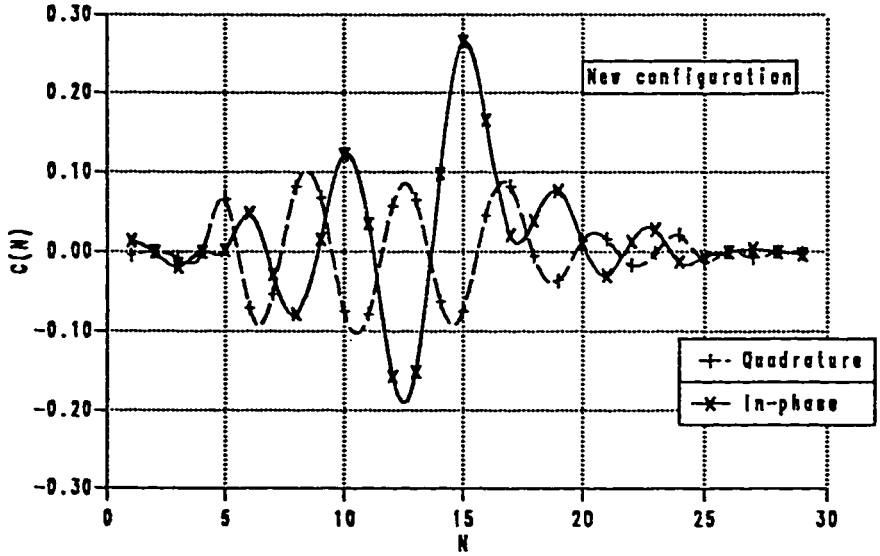

Figure 5.10.b: Sampled impulse response of new configuration.

The MSE versus the sampling phase, for this configuration, is depicted in figure 5.11, where, truly, this configuration has made it here, too. we see from this figure that the small variations in the MSE versus the delay are low to those of the synchronous equalizer. Before we end this section, let us weight the performance and the reduction in complexity gained for this configuration over the synchronous equalizer and the FSE with tap spacing $\frac{T}{2}$, respectively.

In general, the synchronous equalizer with N tap coefficients, for both the in-phase and the quadrature components of the equalizer, will need (4N-2) arithmetic additions and (4N) arithmetic multiplications to compute both outputs, the in-phase output and the quadrature output. The tap coefficients, at each update, will need (4N) arithmetic additions and (6N) arithmetic multiplications. However, the FSE with tap spacing $\frac{T}{2}$, (2N-1) tap coefficients constitute both the in-phase and the quadrature components of the equalizer will need (8N-6) arithmetic additions and (8N-4) arithmetic multiplications to compute the in-phase output and the quadrature output. Also, (8N-4) arithmetic additions and (12N-6) arithmetic multiplications are needed to update the tap coefficients of the $\frac{T}{2}$ FSE. While only (8N-22) arithmetic additions and (8N-20) arithmetic multiplications are needed to compute the in-phase output and the quadrature output of the proposed equalizer with (2N-5) tap coefficients. The tap coefficients of this new configuration will need (8N-20) arithmetic additions and (12N-30)

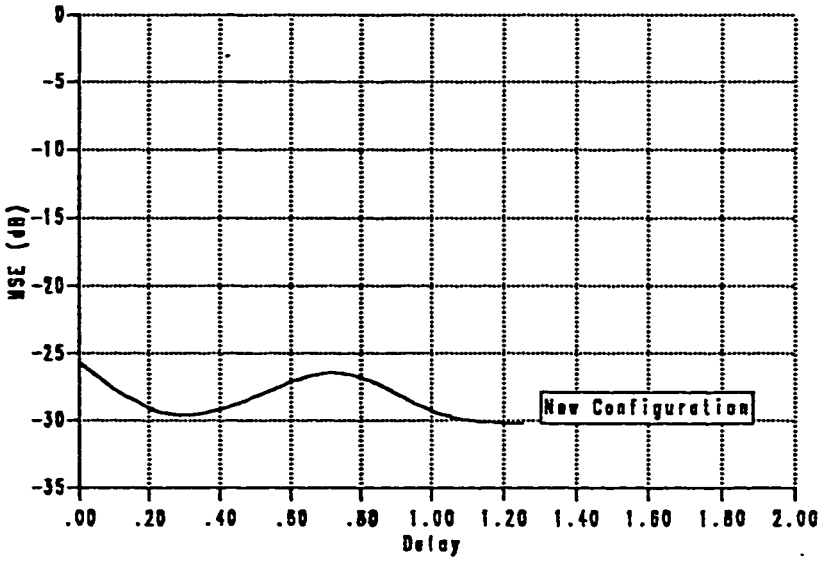

Figure 5.11: MSE as a function of the sampler phase.

arithmetic multiplications at each update. Thus, we can see that a reduction in the computational complexity of about 14% has occured between the $\frac{T}{2}$ FSE and the proposed method, and an increase in complexity of about 67% is shown between the synchronous equalizer and the proposed equalizer.

Table 5.1 summarizes complexity and performance of the three equalizers. Where here complexity is evaluated as being the number of arithmetic additions and arithmetic multiplications needed to compute the output and to update the tap coefficients at every symbol period, T. The performance, however, is shown to be as the average MSE and the peak-to-peak deviation in the MSE versus the sampler phase.

We can see from this table 5.1 that the new configuration has gained about 73.69% over the synchronous equalizer, and has lost about 79.43% over the $\frac{T}{2}$ FSE in the peak-to-peak deviation. However, it has lost only 10.89% over $\frac{T}{2}$ FSE and gained 41.57% over the synchronous equalizer in the average MSE.

Finally, we can say that this configuration has given acceptable results. The final decision should be left to the user when economical considerations are taken into account.

	Complexity of Computations				Performance	
	Output		Tap Coefficients		P.Pmax Deviation Delay(dB)	Average MSE(dB)
	+	x	+	x		
T	58	60	60	90	17.56	-16.47
T/2	114	116	116	174	0.95	-31.62
New configuration	98	100	100	150	4.62	-28.19
% Gain (+) or Loss (-) of New configuration with respect to T	-68.96%	-66.66%	-66.66%	-66.66%	+ 73.69%	+ 41.57%
% Gain (+) or Loss (-) of New configuration with respect to T/2	+ 14.04%	+ 13.79%	+ 13.79%	+ 13.79%	-79.43%	-10.84%

Table 5.1: Complexity and performance for the T equalizer, the T/2, and New configuration for a QAM system.

CHAPTER VI

CONCLUSION AND SUGGESTIONS FOR FUTURE WORK

An equalizer placed in the path of the received signal will cancel the effect of the ISI and noise terms as much as possible so that the probability of error will be minimum. These It is used in general for channels whose impulse responses are unknown to the receiver. Equalizers are in general adaptive elements, where a tapped-delay line filter, with an automatically adjustable gain at each tap, is the essential element for them.

The tap gains are usually adapted using a main cost function. The MSE is becoming a standard performance at the equalizer output, and the LMS algorithm is one of the most used algorithm in updating the tap coefficients.

The synchronous equalizer and the FSE are among the types of equalizers used in building these adaptive elements. But, for each one of these equalizers is associated with it some problems. The synchronous equalizer suffers from aliasing problems and the MSE is function of the sampler phase. Although the FSE does not suffer from aliasing and the

MSE is almost not a function of the sampler phase, however it suffers from the number of computations needed to update the tap coefficients every symbol period. Hence, we have proposed a new idea where some of the tap coefficients of the FSE have been set to zero.

The study of this proposed method was done for both a baseband PAM system and a baseband QAM system. The main parameter that was used in the evaluation process is the effect of the sampler phase on the MSE. Other factors were studied, too, like the convergence rate of the MSE at the output of the equalizer with respect to the number of iterations. But, the sign to the performance behavior was the MSE versus the sampler phase.

This proposed method consists of setting some of the tap coefficients of the FSE with tap spacing $\frac{T}{2}$ to zero. These coefficients, i.e., the zero coefficients are neither updated nor entered in the calculation process; thus, giving a simplified algorithm. Six configurations were studied in the PAM system. Among these configurations, only one configuration gave an acceptable performance. This configuration consisted of setting some of the tap coefficients of the FSE with tap spacing $\frac{T}{2}$ to zero, at the begining and at the end of the sampled impulse response of the equalizer in a symmetrical way. Then, this last configuration undertook the same test, but for a QAM system. The result was an acceptable one. The implementation of this configuration is left to the application, where economic issues are balanced. As far as the performance is taken into account, this configuration did show

an acceptable performance.

Other factors were studied too, but only for the case of the synchronous equalizer and fractionally-spaced equalizer with tap spacing $\frac{T}{2}$ in the baseband PAM system, which are the effect of the position of the main tap of the equalizer on the MSE, and the behavior of the MSE when different signal to noise ratios are used. The analysis showed that as long as the main tap of the equalizer is in the center of the sampled impulse response of the equalizer, right equalization is achieved.

In the QAM system, the effect of the signal to noise ratio on the MSE was studied too, for both equalizers, the synchronous equalizer and the fractionally-spaced $\frac{T}{2}$ equalizer.

During these studies the fractionally-spaced equalizer with tap spacing $\frac{T}{2}$ demonstrated its superiority over the synchronous equalizer.

From the quantitative point of view we saw that in the case of the baseband PAM system, configuration 3 showed a decrease in complexity of about 14%, and an increase in complexity of 67% between the $\frac{T}{2}$ FSE and the synchronous equalizer, respectively. However, a gain of 50% and 14.29% over the synchronous equalizer in performance (peak-to-peak deviation) and in the average MSE, respectively.

For the case of the baseband QAM system, however, the proposed configuration has gained 73.69% over the synchronous equalizer, and has lost about 79.43% over the $\frac{T}{2}$ FSE in the peak-to-peak deviation. Whereas in the average MSE it has lost only 10.89% over $\frac{T}{2}$ FSE and gained 41.57% over the synchronous equalizer.

Finally, outlined are some suggestions for future work.

SUGGESTIONS FOR FUTURE WORK

1. Use two-stage equalization, where a combination of synchronous and fractionally-spaced equalizer is used. Here, an updating scheme must be developed for the update of the tap coefficients of each different equalizer constituting the overall equalizer.
2. Apply the new configuration to a fading channel and see if it can track the variations of the channel.

APPENDIX

Since the MSE is a quadratic form in **C** which reaches its minimum value when **C** equals $\mathbf{C}_{op}$, one might expect that it could be expressed as

$$J = J_{min} + (\mathbf{C} - \mathbf{C}_{op})^T \mathbf{A} (\mathbf{C} - \mathbf{C}_{op}) \tag{A1}$$

We demonstrate that this expression is valid in the following manner. Noting that in general

$$(\mathbf{X} - \mathbf{Y})^T = \mathbf{X}^T - \mathbf{Y}^T \tag{A2}$$

we expand (A1) to obtain

$$J = J_{min} + \mathbf{C}_{op}^T \mathbf{A} \mathbf{C}_{op} + \mathbf{C}^T \mathbf{A} \mathbf{C} - \mathbf{C}^T \mathbf{A} \mathbf{C}_{op} - \mathbf{C}_{op}^T \mathbf{A} \mathbf{C} \tag{A3}$$

Each term in (A3) is a scalar and therefore equal to its transpose. Thus the last two terms are equal. We now combine these and also substitute (2.16) for J_{min} in (A3), and get

$$J = E[d_k^2] - \mathbf{b}^T \mathbf{C}_{op} + \mathbf{C}_{op}^T \mathbf{A} \mathbf{C}_{op} + \mathbf{C}^T \mathbf{A} \mathbf{C} - 2\mathbf{C}^T \mathbf{A} \mathbf{C}_{op} \tag{A4}$$

Next, substituting (2.15) for $\mathbf{C}_{op}$ and recalling again that $\mathbf{A}$ is symmetric, we get

$$J = E[d_k^2] - \mathbf{b}^T\mathbf{A}^{-1}\mathbf{b} + \mathbf{b}^T\mathbf{A}^{-1}\mathbf{A}\mathbf{A}^{-1}\mathbf{b} + \mathbf{C}^T\mathbf{A}\mathbf{C} - 2\mathbf{C}^T\mathbf{A}\mathbf{A}^{-1}\mathbf{b}$$

$$= E[d_k^2] + \mathbf{C}^T\mathbf{A}\mathbf{C} - 2\mathbf{C}^T\mathbf{b}$$

$$= E[d_k^2] - 2\mathbf{C}^T\mathbf{b} + \mathbf{C}^T\mathbf{A}\mathbf{C} \qquad \text{(A.5)}$$

This result corresponds with (2.12) and thus validates (A1), that is (2.17).

REFERENCES

[1] R. W. Lucky,"Automatic Equalization for digital Communication," B.S.T.J., 44, No. 4, part 1 (April 1965), pp. 547-588.

[2] S. Qureshi,"Adaptive Equalization," IEEE Communications magazine, March 1982, pp. 9-16.

[3] R. W. Lucky, J. Salz, and E. J. Weldon, Jr., Principles of data Communication, New York: McGraw-Hill, 1968.

[4] J. Proakis, Digital Communications. New york: McGraw-hill, 1983.

[5] J. Proakis and J. H. Miller,"An adaptive receiver for digital signaling through channels with intersymbol interference," IEEE Trans. Inform. Theory, Vol. IT-15, pp.484-497, July 1969.

[6] G. Ungerboeck,"Fractional tap-spacing Equalizer and consequences for clock recovery in data modems," IEEE trans. Commun., August 1976, pp. 856-864.

[7] M. S. Mueller,"Least-Squares Algorithms for Adaptive Equalizers," B.S.T.J., 60, No. 8, (October 1981), pp. 1905-1925.

[8] D. Preis and C. Bunks,"Three Algorithms for the Design of Transversal-Filter Equalizers," IEEE International Symposium on Circuits and systems 1981, pp. 536-539.

[9] R. W. Chang,"A New Equalizer Structure for Fast Start-Up Digital Communication," B.S.T.J., 50, No. 6, (July-August 1971), pp. 1969-2014.

[10] M. S. Mueller,"On the Rapid Initial convergence of Least-Squares Equalizer Adjustment Algorithms," B.S.T.J., 60, No. 10, (December 1981), pp. 2345-2358.

[11] J. Speidel,"An Automatic Decision Feedback Equalizer with Variable optimum size," IEEE International Symposium on Circuits and Systems 1981, pp. 653-657.

[12] A. Gersho,"Adaptive Equalization of Highly Dispersive Channels for Data Transmission," B.S.T.J., 48, No. 1, (January 1969), pp. 55-70.

[13] R. D. Gitlin and S. B. Weinstein,"On the required tap weight precision for Digitally-Implemented adaptive Equalizers," B.S.T.J, 58, No. 2 (February 1979), pp. 301-321.

[14] R. D. Gitlin, J. E. Mazo, and M. G. Taylor,"On the Design Algorithms for Digitally Implemented Adaptive Filters," IEEE Trans. Circuit Theory, Vol. CT-20, March 1973, pp. 125-136.

[15] S. Haykin, Introduction to adaptive filters, NewYork: MacMillan Publishing company, 1984.

[16] B. Widrow and S. D. Stearns, Adaptive Signal Processing, Englewood Cliffs, N.J: Prentice-Hall,1985.

[17] R. D. Gitlin and S. B. Weinstein,"Fractionally-Spaced Equalization An improved digital transversal Equalizer," B.S.T.J, 60, No. 2, (February 1981), pp. 275-296.

[18] S. U. Qureshi and G. D. Forney, Jr.,"Performance and propreties of T/2 Equalizer;" NTC Record, December 1977.

[19] V.32

[20] S. Haykin, Communication Systems. Second editon. New York: Wiley,1983.

[21] L. B. Jackson, Digital Filters and Signal Processing. Third Printing. Norwell, MA: Kluwer Academic Publishers,1986.

[22] L. Guidoux, "Egaliseur Autoadaptif a Double Echantillonnage," L'Onde Electrique, vol. 55, pp. 9-13, January 1975.